HITACHI

GE Hitachi Nuclear Energy

Richard E. Kingston
Vice President, ESBWR Licensing

P.O. Box 780
3901 Castle Hayne Road, M/C A-55
Wilmington, NC 28402 USA

T 910.819.6192
F 910.362.6192
rick.kingston@ge.com

Security Notice
This letter forwards Security-Related information in accordance with 10CFR2.390. Upon removal of Enclosure 1, the balance of this letter may be considered non-Security-Related.

MFN 06-191
Supplement 10

Docket No. 52-010

December 4, 2008

U.S. Nuclear Regulatory Commission
Document Control Desk
Washington, D.C. 20555-0001

Subject: **Response to Portion of NRC RAI Letter No. 228 Related to ESBWR Design Certification Application – DCD Tier 2 Section 3.8 – Seismic Category I Structures; RAI Number 3.8-41 S06**

The purpose of this letter is to submit the GE Hitachi Nuclear Energy (GEH) response to the U.S. Nuclear Regulatory Commission (NRC) Request for Additional Information (RAI) letter number 228 sent by NRC letter dated August 6, 2008 (Reference 1).

The original RAI was received via NRC Request for Additional Information letter number 38 (Reference 6). Previous GEH responses were provided via References 2 through 5. RAI Number 3.8-41 S06 is addressed in Enclosure 1.

Enclosure 1 contains Security-Related information identified by the designation "{{{Security-Related Information - Withhold Under 10 CFR 2.390}}}." GE hereby requests this information be withheld from public disclosure in accordance with the provisions of 10 CFR 2.390. A public version is contained in Enclosure 2.

If you have any questions or require additional information, please contact me.

Sincerely,

Lee F. Dougherty for

Richard E. Kingston
Vice President, ESBWR Licensing

D068
NRO

References:

1. MFN 08-623, Letter from U.S. Nuclear Regulatory Commission to Robert E. Brown, GEH, *Request For Additional Information Letter No. 228 Related to ESBWR Design Certification Application*, dated August 6, 2008

2. MFN 06-191, Supplement 6, Letter from James C. Kinsey to U.S. Nuclear Regulatory Commission, *Response to Portion of NRC Request for Additional Information Letter No. 38 Related to ESBWR Design Certification Application - Structural Analysis - RAIs 3.8-25 S04, 3.8-41 S04, 3.8-91 S04*, dated December 12, 2007

3. MFN 06-191, Supplement 3, Letter from David Hinds to U.S. Nuclear Regulatory Commission, *Response to Portion of RAI Letter No. 38 Related to ESBWR Design Certification Application - Seismic Category I Structures - RAI Numbers 3.8-3 S03, 3.8-6 S02, 3.8-13 S03, 3.8-14 S02, 3.8-18 S02, 3-8-20 S01, 3.8-25 S03, 3.8-26 S01, 3.8-27 S02, 3.8-41 S03, 3.8-46 S02, 3.8-48 S03, 3.8-51 S03, 3.8-56 S01, 3.8-64 S03, 3.8-87 S02, 3.8-90 S02, 3.8-91 S03 & 3.8-100 S02 - Supplement 3*, dated January 24, 2007

4. MFN 06-191, Supplement 2, Letter from David Hinds to U.S. Nuclear Regulatory Commission, *Response to Portion of RAI Letter No. 38 Related to ESBWR Design Certification Application - Seismic Category I Structures - RAI Numbers 3.8-3, 3-8-13, 3.8-25, 3.8-41, 3.8-48, 3.8-51, 3.8-64, and 3.8-91 - Supplement 2*, dated November 7, 2006

5. MFN 06-191, Letter from David Hinds to U.S. Nuclear Regulatory Commission, *Response to Portion of NRC Request for Additional Information Letter No. 38 Related to ESBWR Design Certification Application - Structural Analysis - RAI Numbers 3.8-3, 3.8-6, 3.8-13, 3.8-14, 3.8-18, 3.8-19, 3.8-20, 3.8-23, 3.8-25, 3.8-26, 3.8-27, 3.8-40, 3.8-41, 3.8-46, 3.8-47, 3.8-48, 3.8-49, 3.8-51, 3.8-56, 3.8-63, 3.8-64, 3.8-82, 3.8-83, 3.8-87, 3.8-90, 3.8-91, 3.8-100, 3.8-104, 3.8-105 and 3.8-106*, dated June 28, 2006

6. MFN 06-197, Letter from U.S. Nuclear Regulatory Commission to David H. Hinds, *Request for Additional Information Letter No. 38 Related to ESBWR Design Certification Application*, dated June 23, 2006

Enclosures:

1. Response to Portion of NRC RAI Letter No. 228 Related to ESBWR Design Certification Application - DCD Tier 2 Section 3.8 – Seismic Category I Structures; RAI Number 3.8-41 S06 –Security Related Version

2. Response to Portion of NRC RAI Letter No. 228 Related to ESBWR Design Certification Application - DCD Tier 2 Section 3.8 – Seismic Category I Structures; RAI Number 3.8-41 S06 - Public Version

cc:	AE Cubbage	USNRC (with enclosures)
	RE Brown	GEH/Wilmington (with enclosures)
	DH Hinds	GEH/Wilmington (with enclosures)
	eDRF Section	0000-0092-2852 (RAI 3.8-41 S06)

ENCLOSURE 2

MFN 06-191
Supplement 10

Response to Portion of NRC RAI Letter No. 228
Related to ESBWR Design Certification Application

DCD Tier 2 Section 3.8 – Seismic Category I Structures

RAI Number 3.8-41 S06

Public Version

For historical purposes, the text and GEH response of RAI 3.8-41 and supplements 1 thorough 5 are included. The attachments (if any) are not included from the previous responses to avoid confusion.

NRC RAI 3.8-41

DCD Sections 3.8.3.1.1 and 3.8.3.1.4 indicate that the diaphragm floor (DF) and vent wall (VW) are constructed from steel plates filled with concrete. Section 3G.1.4.1 of Appendix 3G indicates that the infill concrete is conservatively neglected in the analysis model. Neglecting the mass and stiffness of the concrete may not be conservative. Therefore, provide more information which explains how the infill concrete is considered in the analysis and design of these structures. Describe how the mass, stiffness, and strength are considered when analyzing the DF and VW structures for each applicable loading condition. For analysis of thermal transients, how was the infill concrete modeled in heat transfer analyses, and how was the constraint to thermal growth/contraction of the steel plates considered in the thermal stress analyses?

Include this information in DCD Section 3.8.3 and/or Appendix 3G. In addition, (1) identify the applicable detailed report/calculation (number, title, revision and date, and brief description of content) that will be available for audit by the staff, and (2) reference this report/calculation in the DCD.

GE Response

Concrete strength and stiffness are conservatively neglected in both the structural analysis model and the seismic analysis model. The mass of concrete is considered in the seismic analysis model and in the structural analysis model.

For the linear thermal analysis, concrete strength and stiffness are neglected and thus the constraint to thermal expansion or contraction of the steel plates from the infill concrete is not considered. However, for the non linear analyses, the infill concrete in VW and DF is explicitly included as brick elements with strain compatibility between the steel and concrete interfaces and using the respective values for the coefficient of thermal expansion for concrete and steel. This modeling includes the effect of the constraint to thermal expansion or contraction to both the concrete and steel components. Note that concrete cracking is also included, and this would relieve some of the thermal induced stress. The effect of this infill concrete on thermal constraint from the nonlinear model is then transferred to the linear thermal-stress design model through scaling via thermal ratios. Concrete cracking effects due to thermal loads are obtained by a nonlinear, concrete cracking analysis using ABAQUS/ANACAP program as described in DCD Appendix 3C.

Thermal transients in the heat transfer analysis done to determine temperature distribution, the heat transfer coefficient of concrete is neglected in the DF and WW for the linear analysis but concrete is included in the non-linear model. Through the use of the thermal ratios to account for the thermal stresses, the effect of infill concrete on the heat transfer is implicitly addressed in the linear analysis.

the thermal ratios to account for the thermal stresses, the effect of infill concrete on the heat transfer is implicitly addressed in the linear analysis.

Therefore, for the non-thermal and non-seismic loads, neglecting the strength of the infill concrete in the design of the VW and DF structures is conservative, because the steel sections must then resist all these type of loads (under the bending of the VW or DF, the concrete could resist significant load in compression, if not neglected). For seismic load, neglecting the strength and stiffness of the concrete but including the mass is conservative because the mass can add significant dynamic load without the benefit of any stiffness or strength to resist this load. For the thermal loads, the stiffness, strength, and associated constraint due to thermal expansion or contraction of the infill concrete is included in the nonlinear modeling. In addition, concrete cracking due to thermal induced stress and the associated reduction and redistribution of thermal load is also included. The effect of concrete expansion or contraction and cracking of the infill concrete in the steel composite structures (VW, DF) associated with thermal loads is incorporated into the design through the use of thermal ratios that scale results of the design basis model that use linear thermal stress analysis neglecting the infill concrete.

(1) The applicable detailed report/calculation that will be available for NRC audit is 26A6625, Cracking Analysis of Containment Structure for DBA Thermal Loads, Revision 1, October 2005. This report documents the non-linear analyses for the thermal loads taking into account of concrete cracking and the redistribution of section forces due to concrete cracking.

(2) Since this information exists as part of GE internal tracking system, it is not necessary to add it to the DCD submittal to the NRC.

DCD Impact

No DCD change was made in response to this RAI.

NRC RAI 3.8-41, Supplement 1

Additional topics discussed at audit

None.

GE Response

None.

No DCD change was made in response to this RAI Supplement.

NRC RAI 3.8-41, Supplement 2

GE Additional Post Audit Action

Since concrete properties were not used in the stick model for the VW and DF, indicate what is the effect on frequency shift when considering concrete, even if cracked, in the spectrum curves generated for equipment and piping design.

GE Response

To address the effect of in-fill concrete on the frequency shift for the VW and DF, the stiffness properties of the two structures in the seismic model were adjusted to include contribution of concrete stiffness. Since the in-fill concrete is unreinforced, it would likely to crack under SSE. An effective concrete stiffness equal to 50% of the nominal uncracked stiffness was thus assumed. The resulting fundamental frequency was found to be 113% higher for the VW and 26% higher for the DF than that of the base model without consideration of the in-fill concrete stiffness. (See Table 3.8-41(1))

The effect of frequency shift on the floor response spectra was evaluated by additional parametric SSI analysis for generic uniform sites with single envelope ground motion input. The results were compared with the enveloping results obtained from Report SER-ESB-033, *Parametric Evaluation of Effects on SSI Response, Rev. 0,* submitted to NRC as Enclosure 2 to MFN 06-274. As shown in Figs. 3.8-41(1) through 3.8-41(25) for spectra comparison at selected locations, the existing site-envelope spectra without the in-fill concrete stiffness consideration do not completely bound. (In these figures, U-3 means the case without concrete stiffness (base model), and U-5 means with 50% concrete stiffness.) In view of this comparison, the results of the in-fill concrete stiffness parametric evaluation will be included in the site-envelope seismic design loads.

It should be noted that additional parametric seismic analysis is being performed to address the effect of containment LOCA flooding (see response to NRC RAI 3.8-8) and the effect of updated modeling properties of containment internal structures for more consistency with the design configuration.

Table 3.8-41(1) Effect of concrete rigidity for natural frequencies for VW and DF

Structure		Modulus of elasticity of concrete	
		0% (E=0MPa)	50% (E=13900MPa)
Vent Wall	Frequency (Hz)	21.6	46.0
	Ratio	1	2.13
Diaphragm Floor	Frequency (Hz)	13.5	17.0
	Ratio	1	1.26

Material properties:

(1) Concrete
Modulus of elasticity: E=13900MPa (50%)
Poison's ratio : ν=0.17

(2) Steel
Modulus of elasticity: E=200000MPa
Poison's ratio : ν=0.3

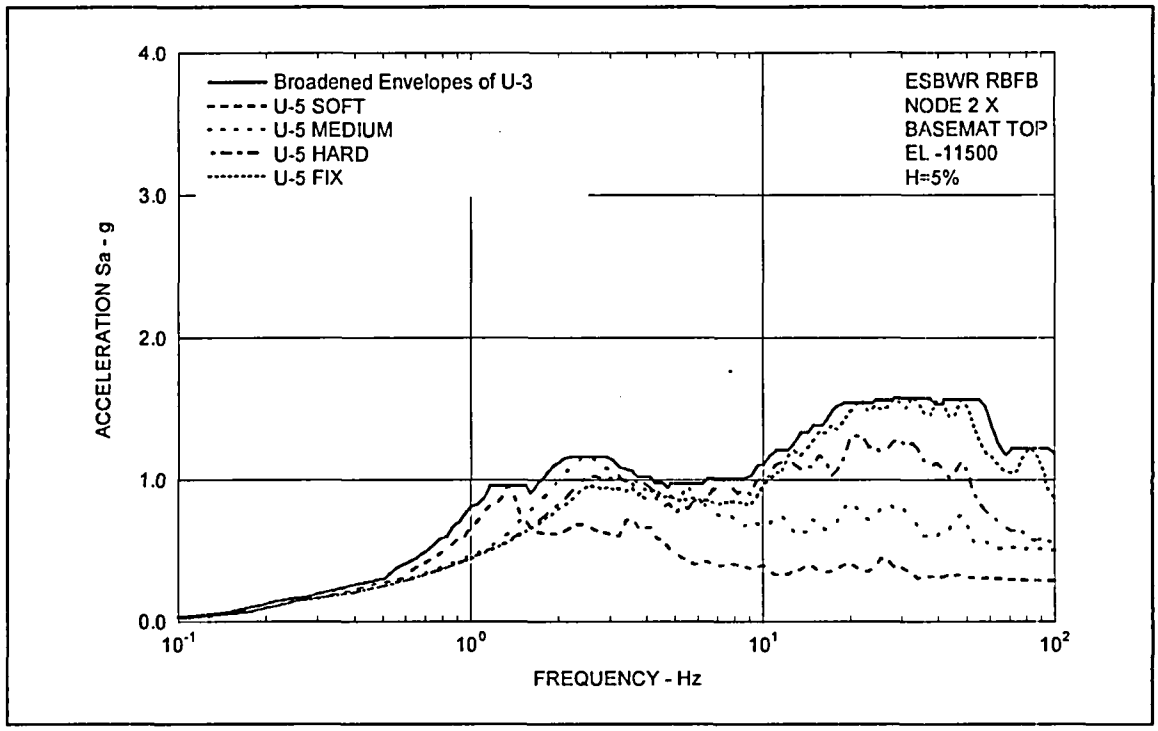

Figure 3.8-41(1) Floor Response Spectra - RBFB Basemat X

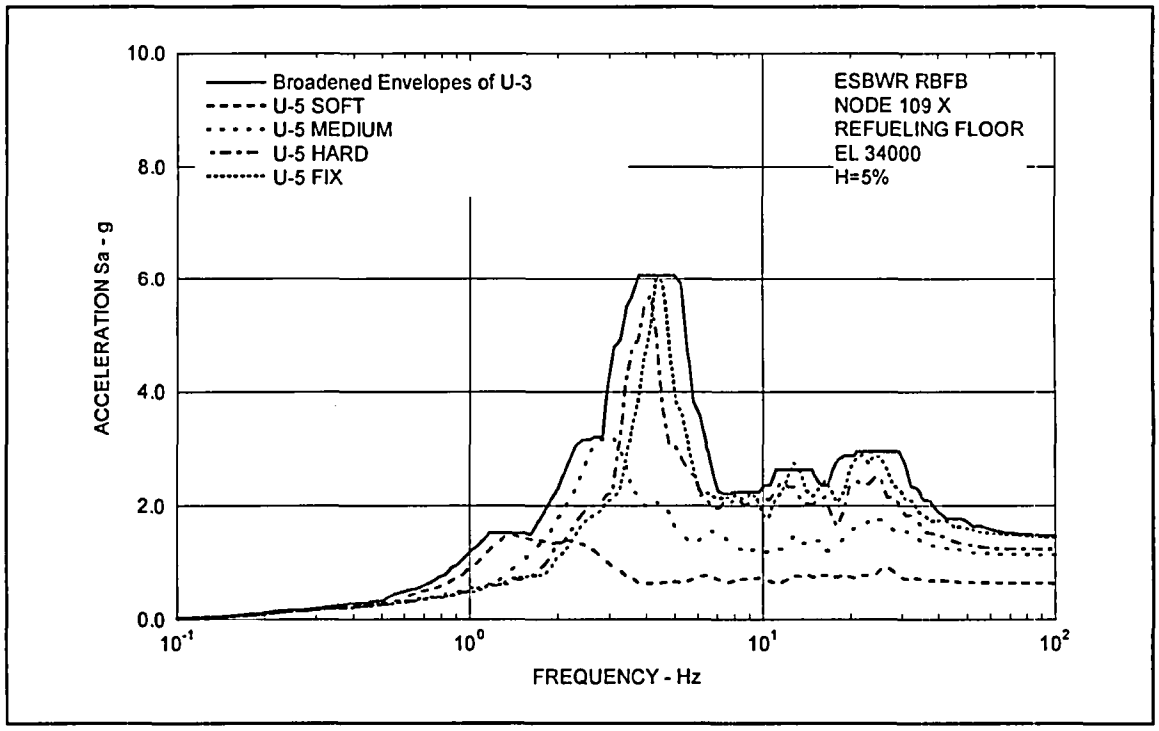

Figure 3.8-41(2) Floor Response Spectra - RBFB Refueling Floor X

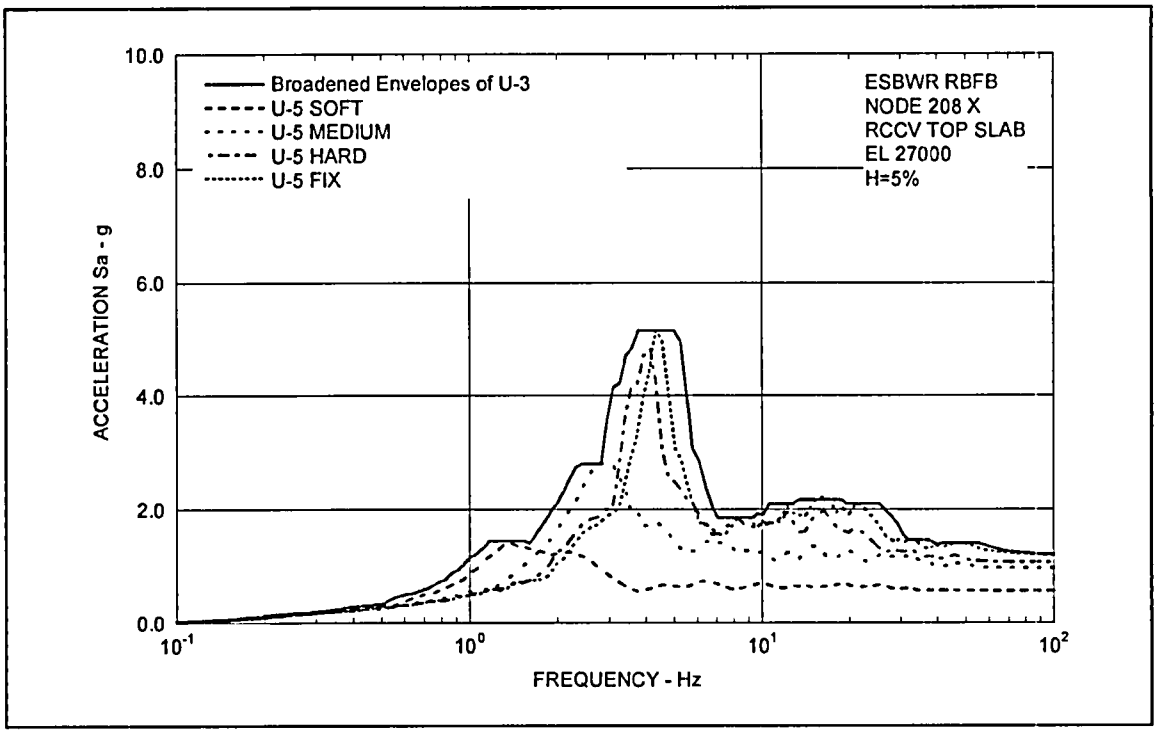

Figure 3.8-41(3) Floor Response Spectra - RCCV Top Slab X

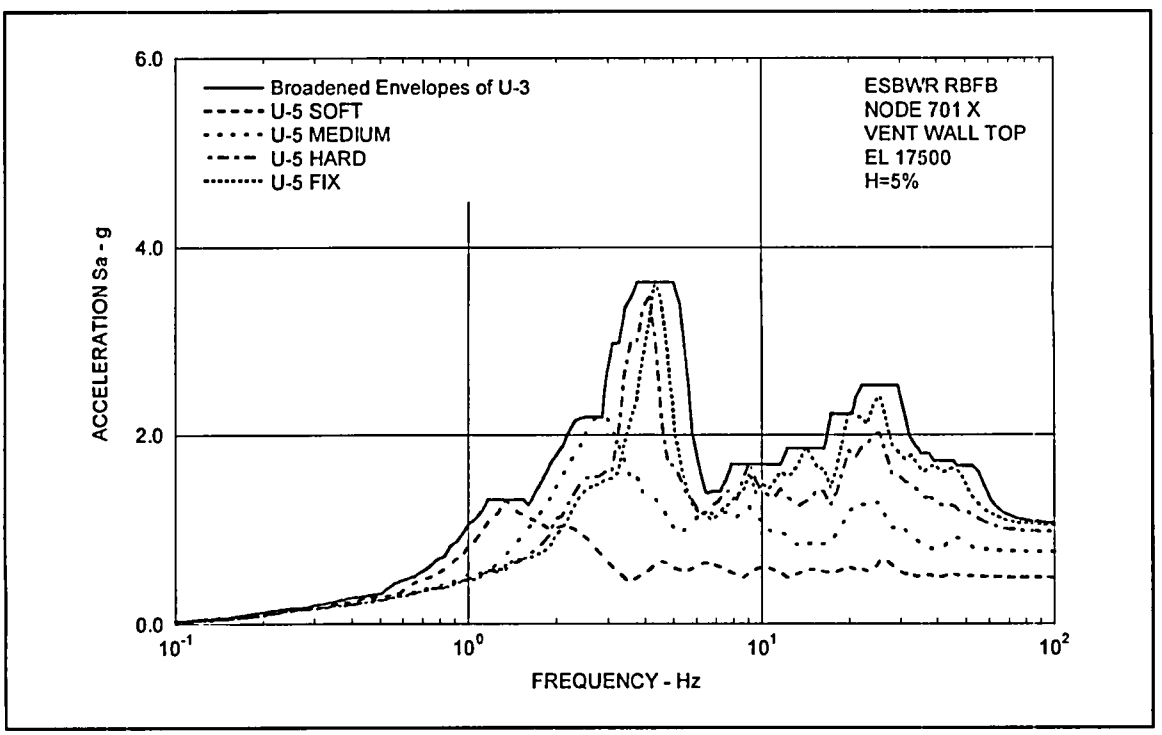

Figure 3.8-41(4) Floor Response Spectra - Vent Wall Top X

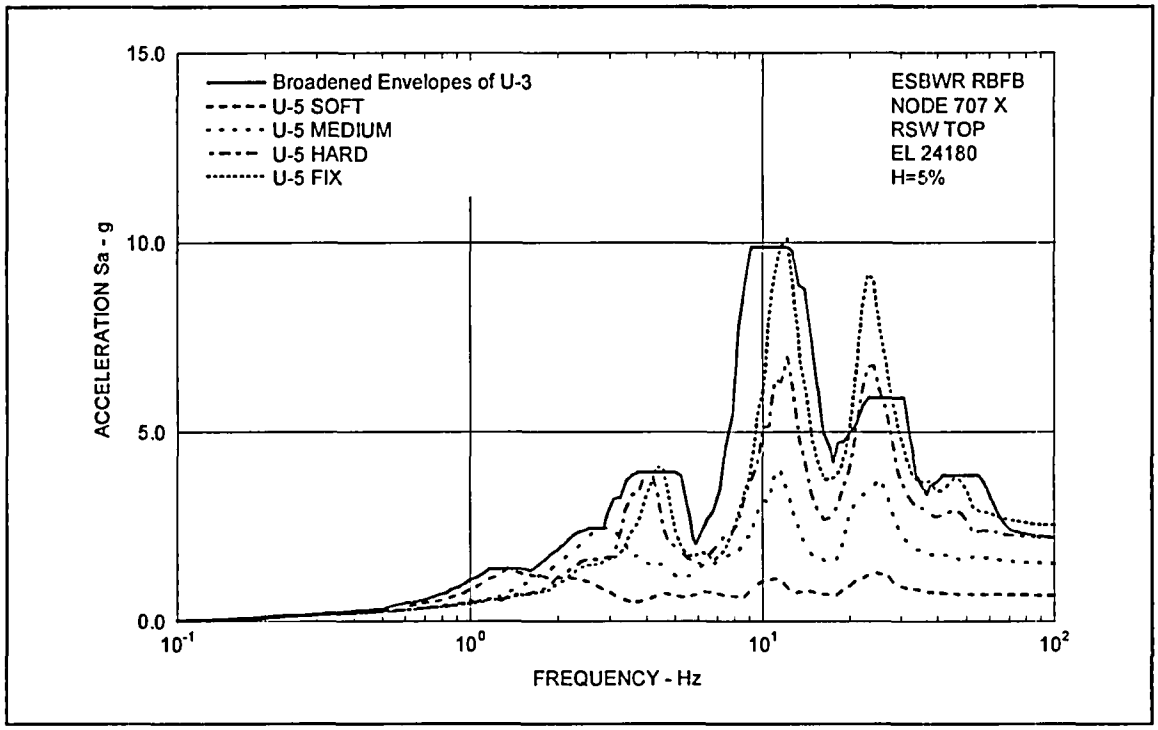

Figure 3.8-41(5) Floor Response Spectra - RSW Top X

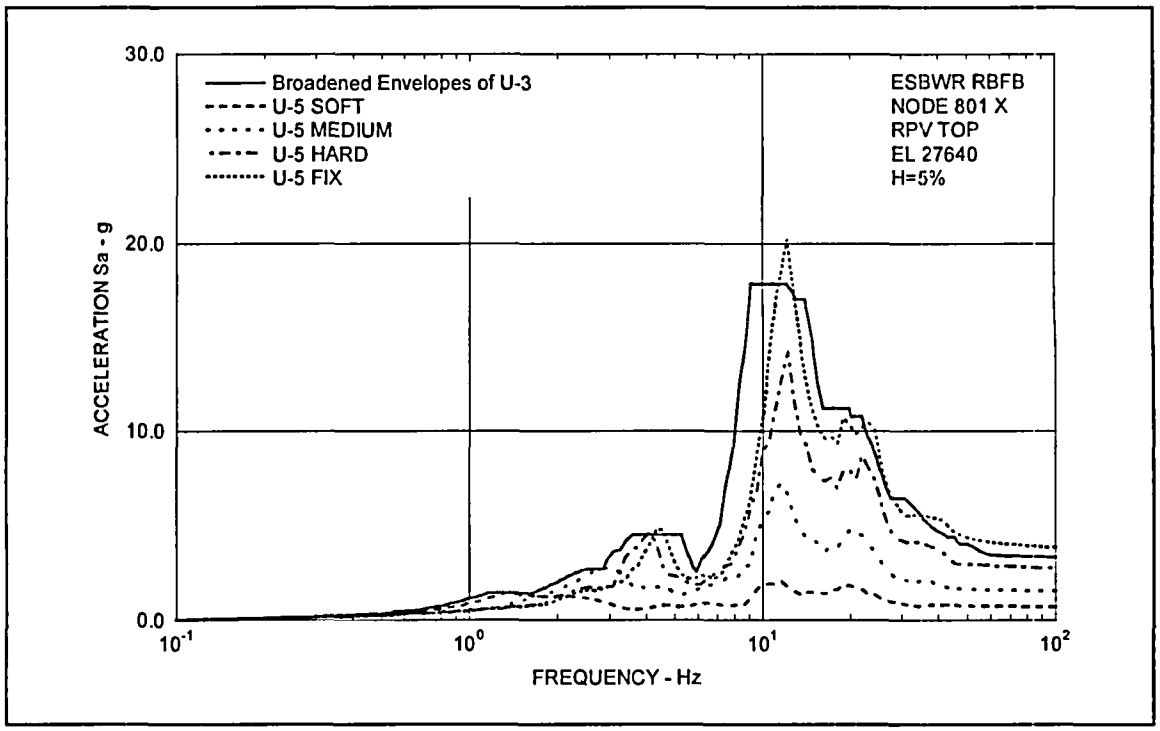

Figure 3.8-41(6) Floor Response Spectra - RPV Top X

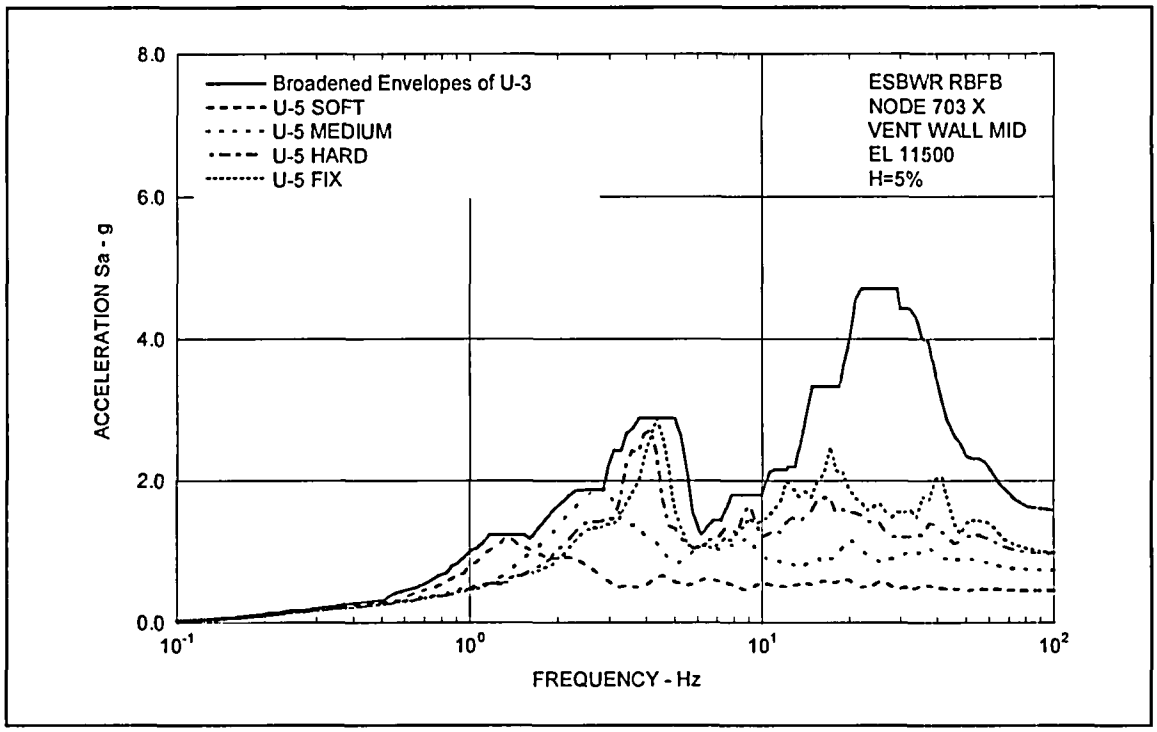

Figure 3.8-41(7) Floor Response Spectra - Vent Wall Middle X

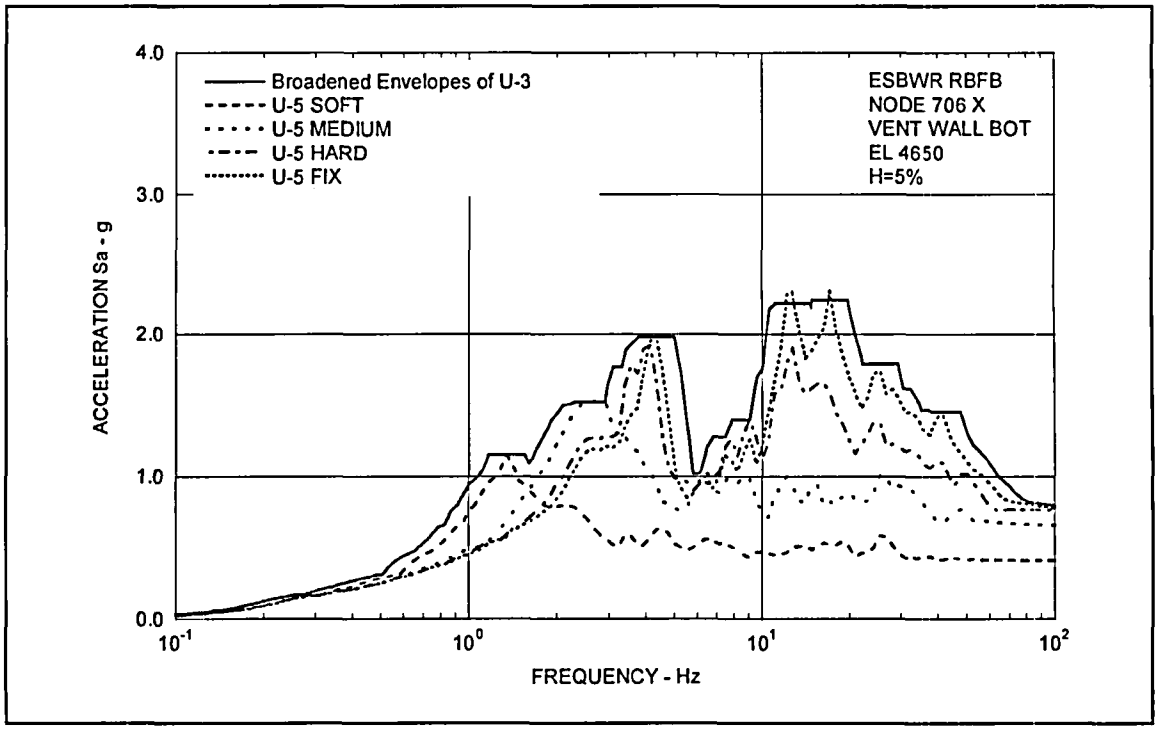

Figure 3.8-41(8) Floor Response Spectra - Vent Wall Bottom X

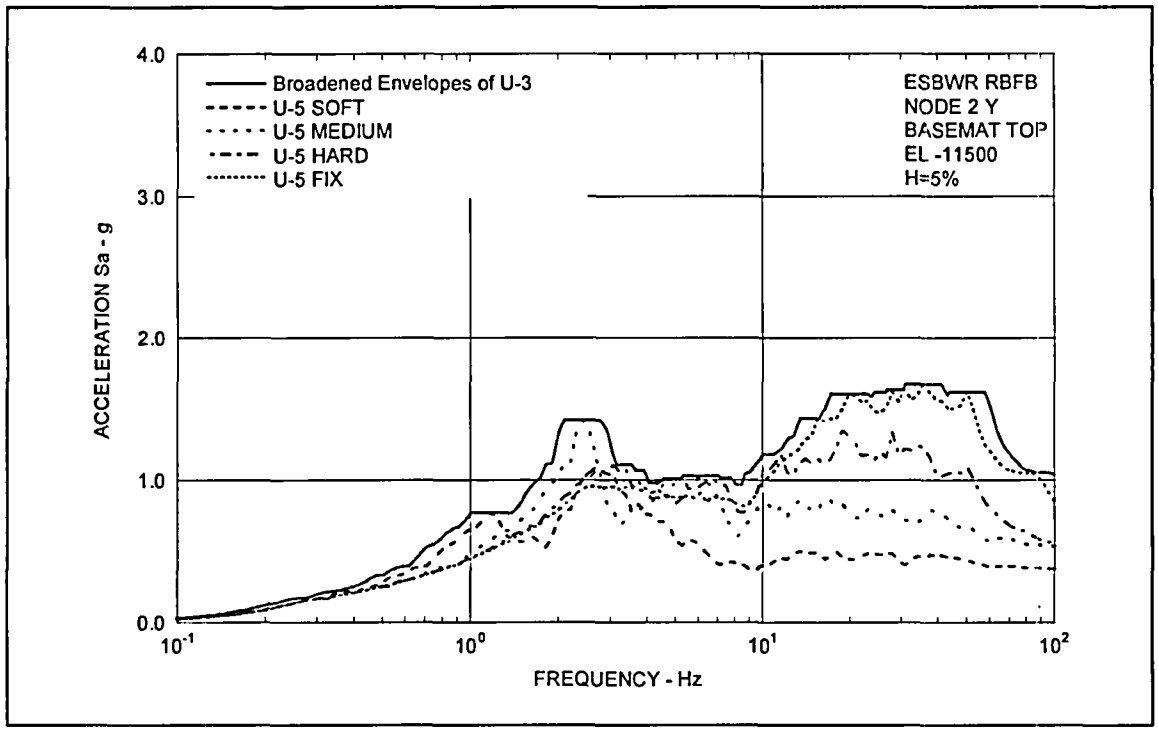

Figure 3.8-41(9) Floor Response Spectra - RBFB Basemat Y

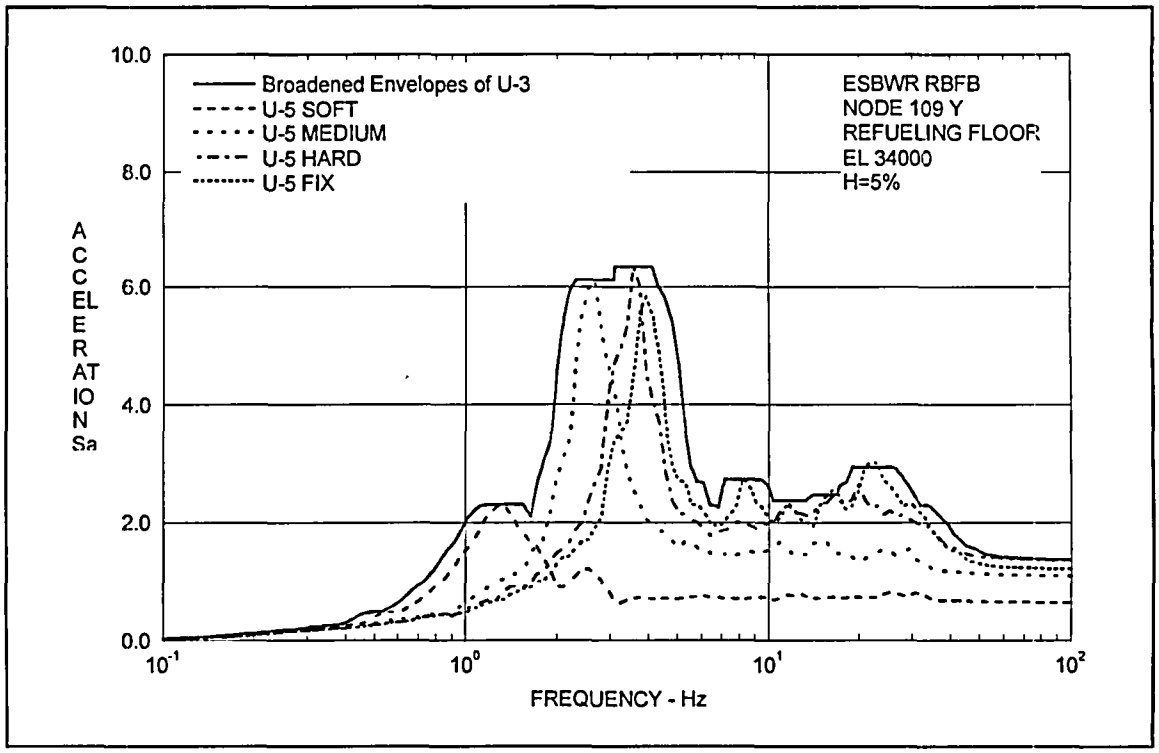

Figure 3.8-41(10) Floor Response Spectra - RBFB Refueling Floor Y

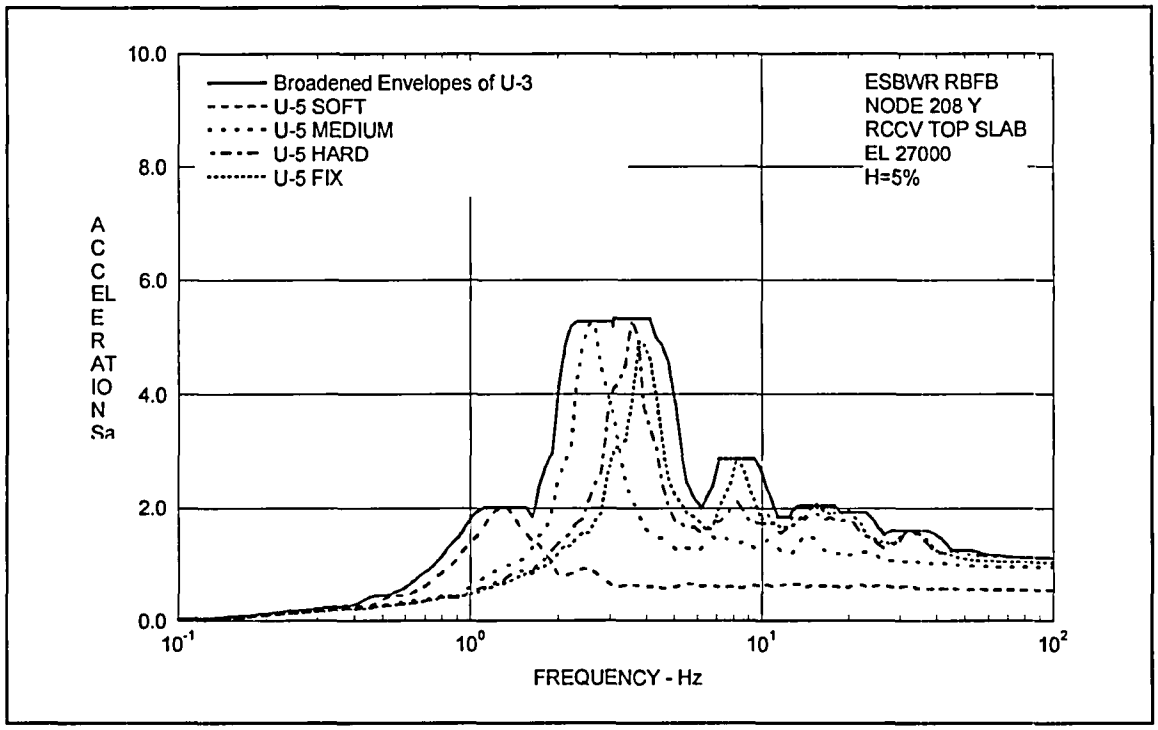

Figure 3.8-41(11) Floor Response Spectra - RCCV Top Slab Y

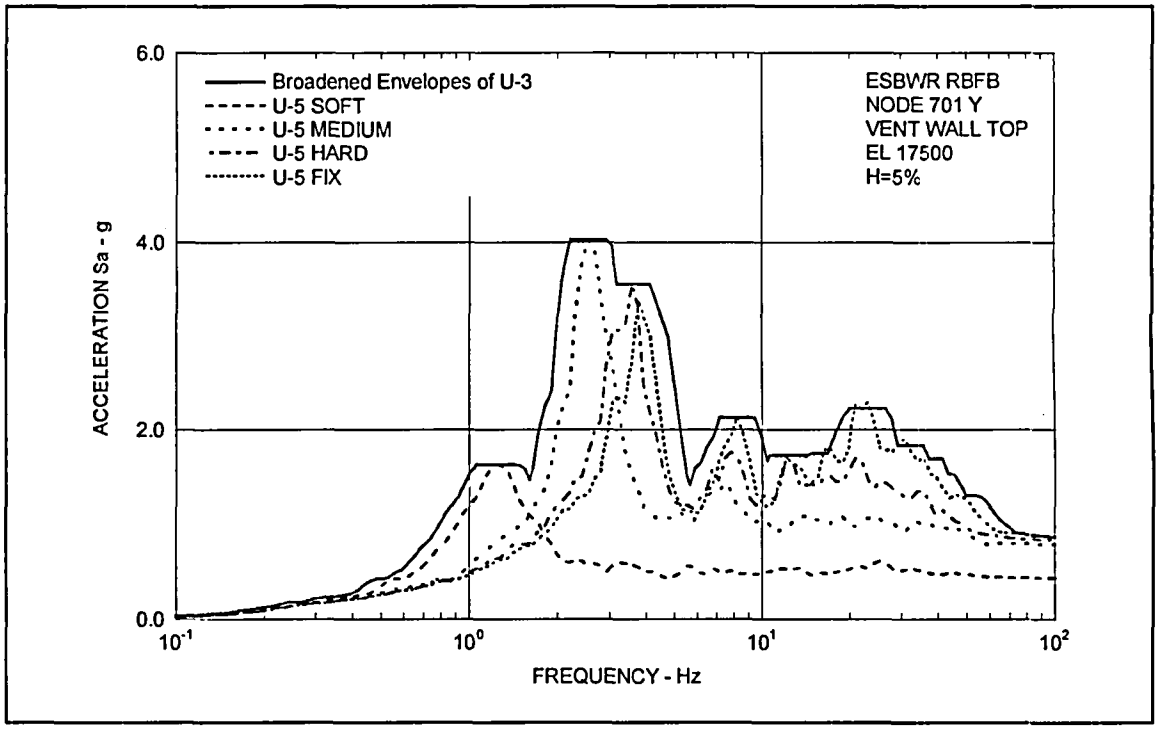

Figure 3.8-41(12) Floor Response Spectra - Vent Wall Top Y

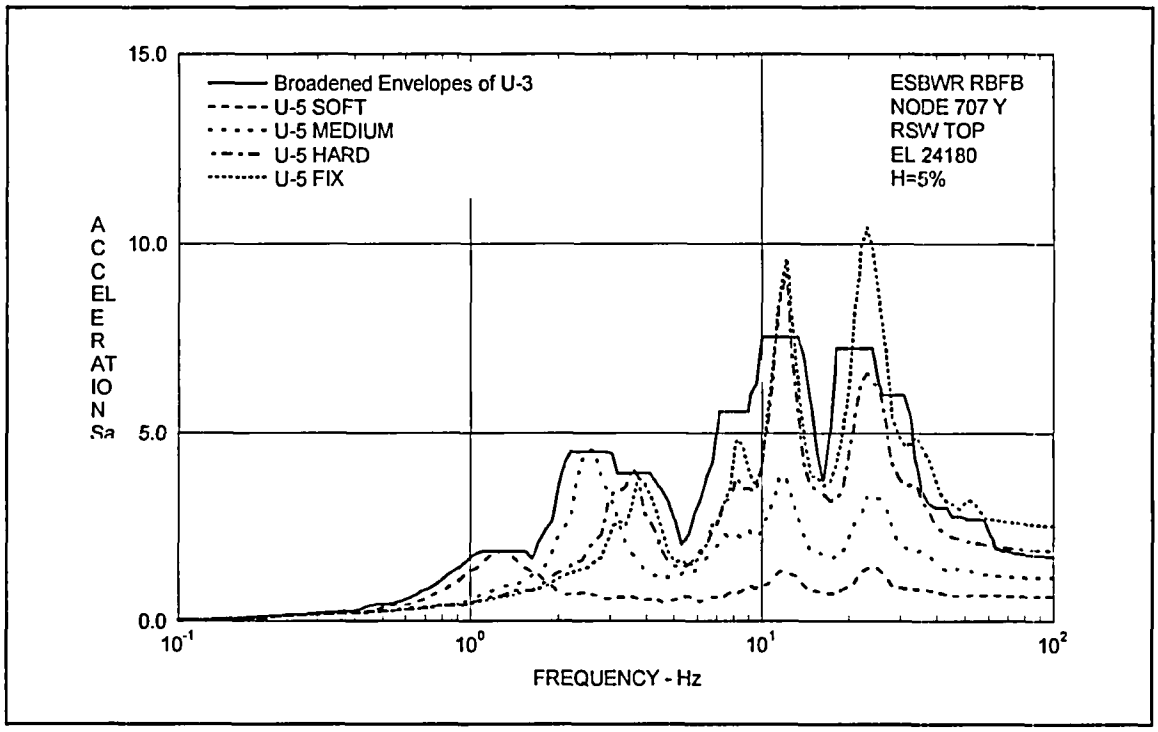

Figure 3.8-41(13) Floor Response Spectra - RSW Top Y

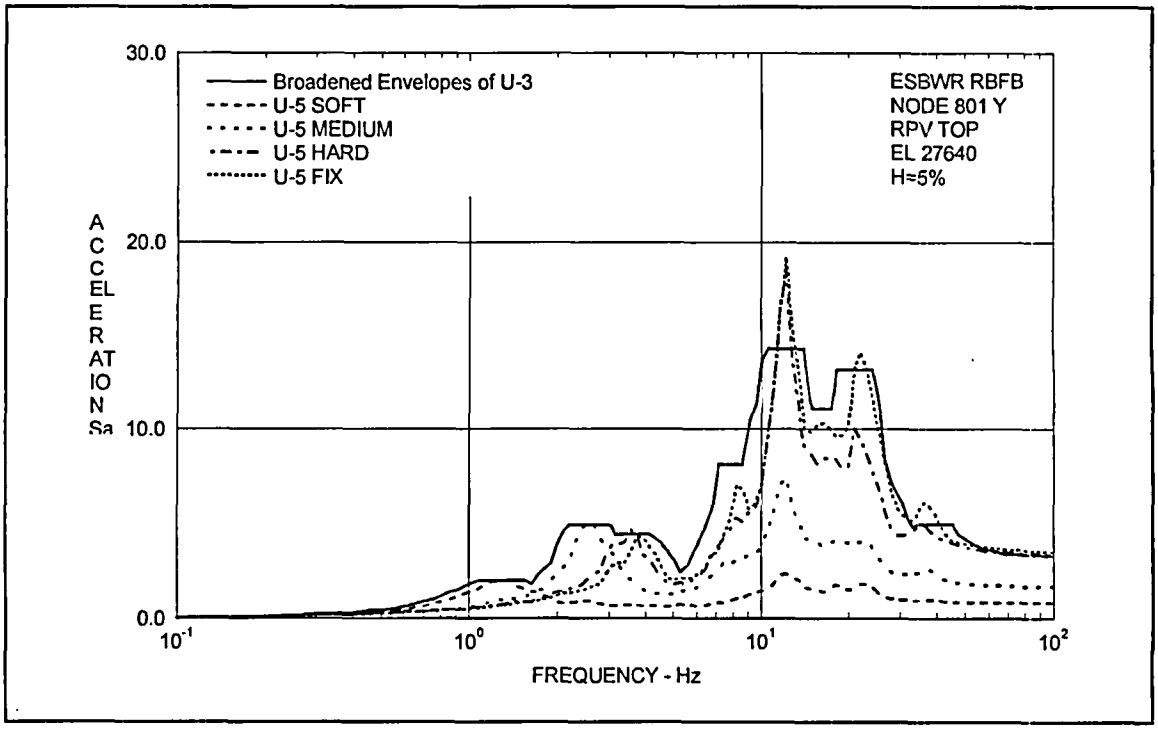

Figure 3.8-41(14) Floor Response Spectra - RPV Top Y

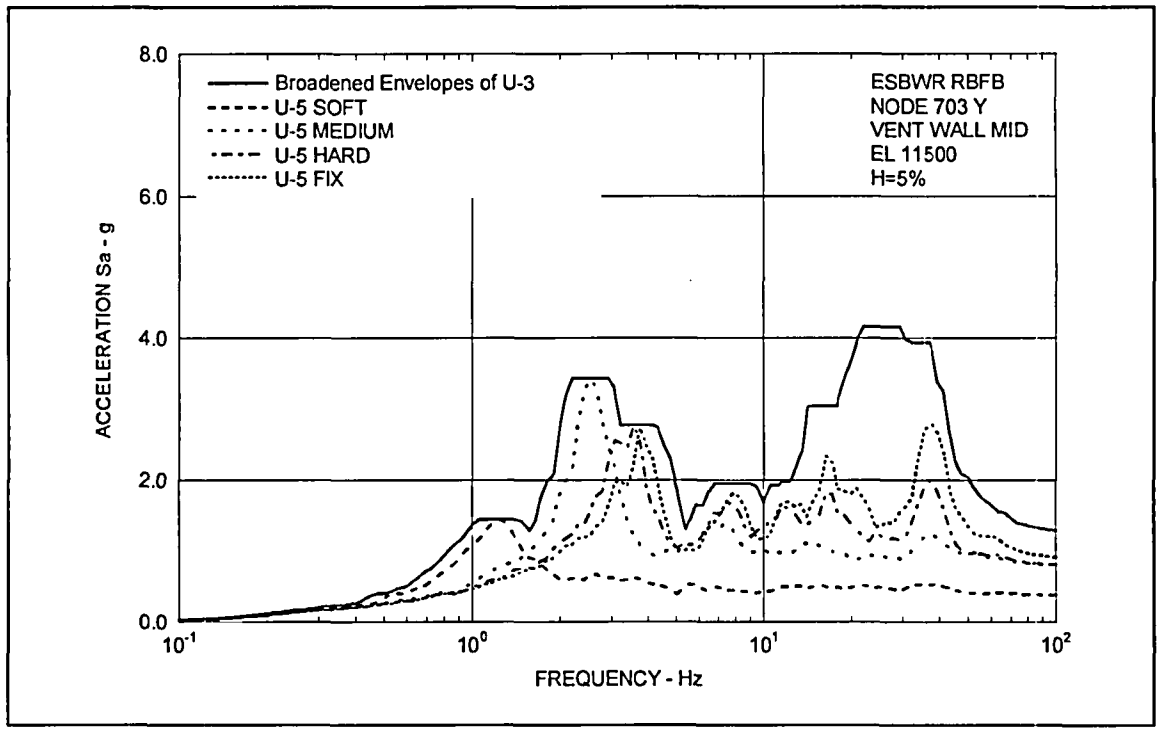

Figure 3.8-41(15) Floor Response Spectra - Vent Wall Middle Y

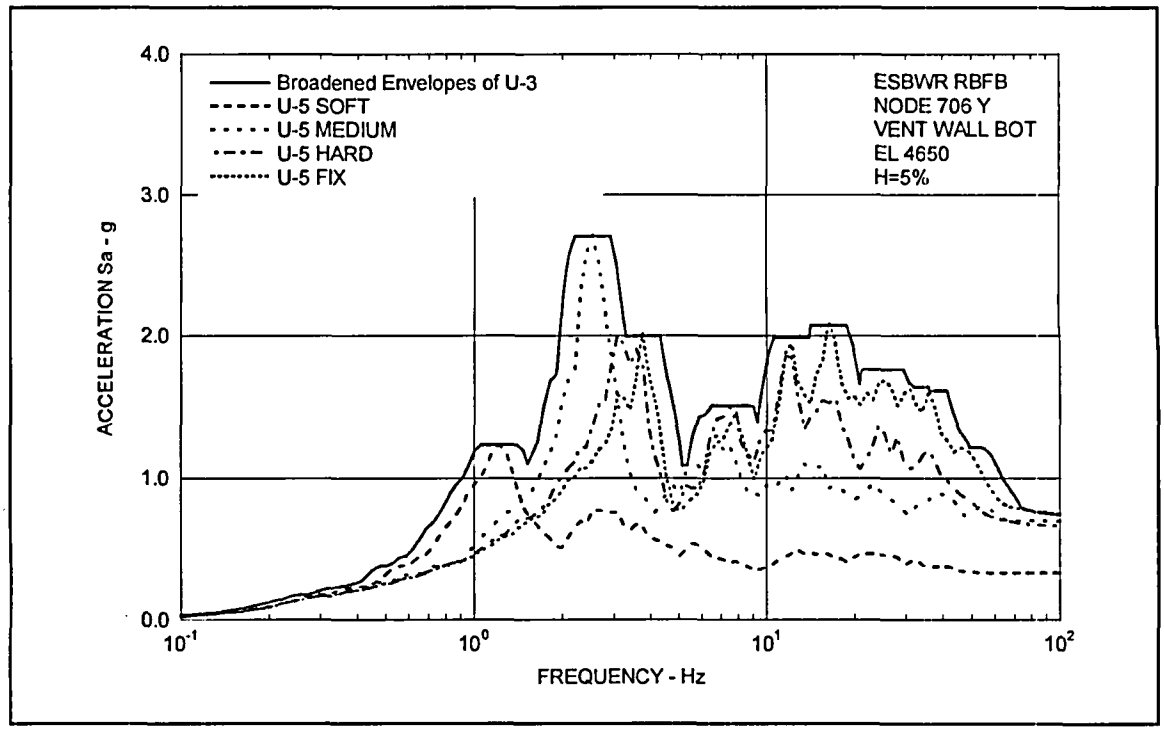

Figure 3.8-41(16) Floor Response Spectra - Vent Wall Bottom Y

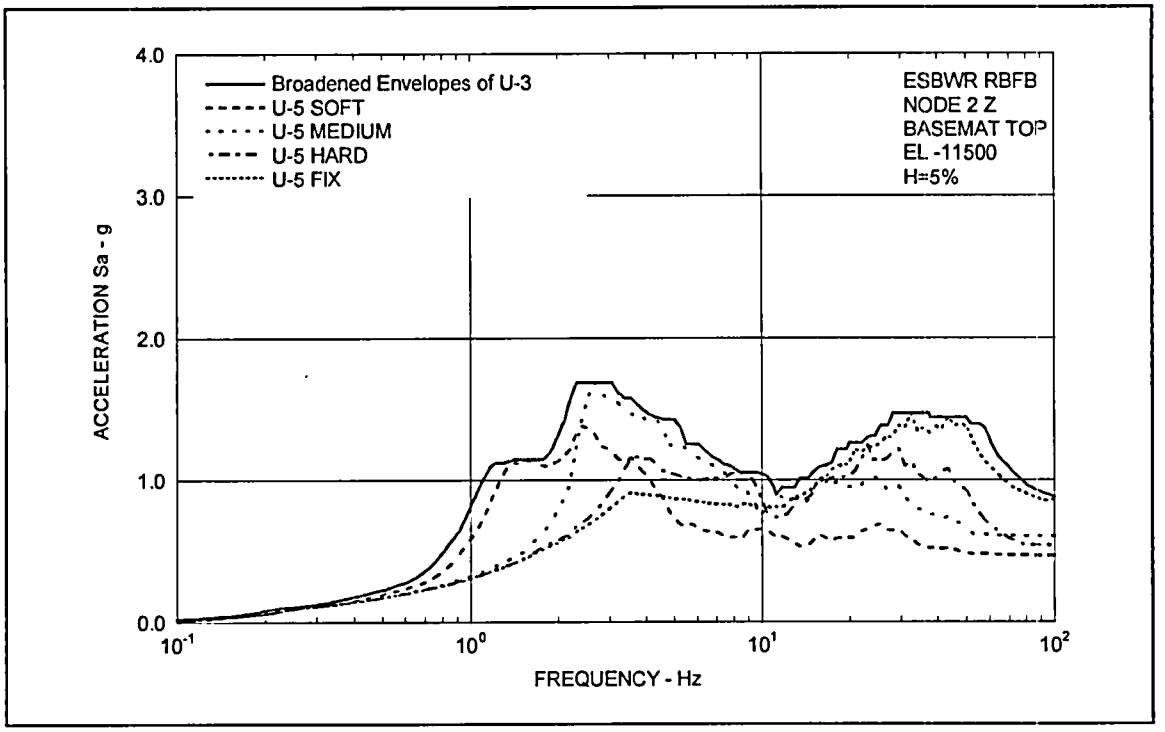

Figure 3.8-41(17) Floor Response Spectra - RBFB Basemat Z

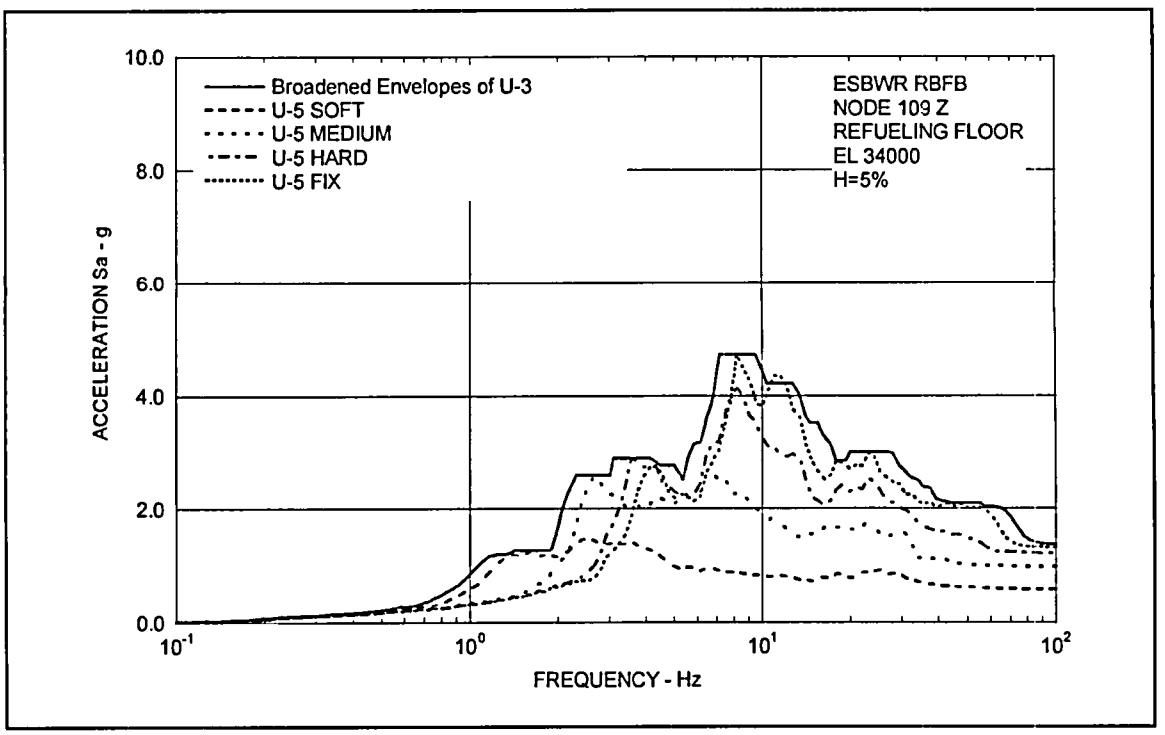

Figure 3.8-41(18) Floor Response Spectra - RBFB Refueling Floor Z

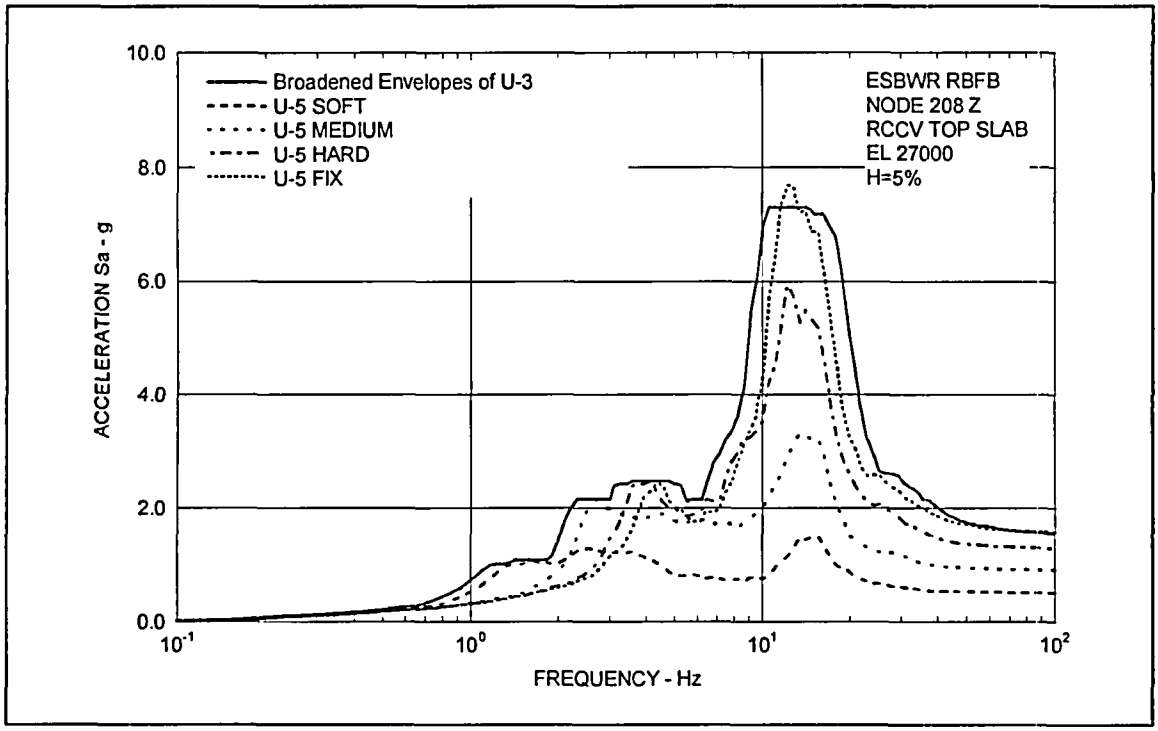

Figure 3.8-41(19) Floor Response Spectra - RCCV Top Slab Z

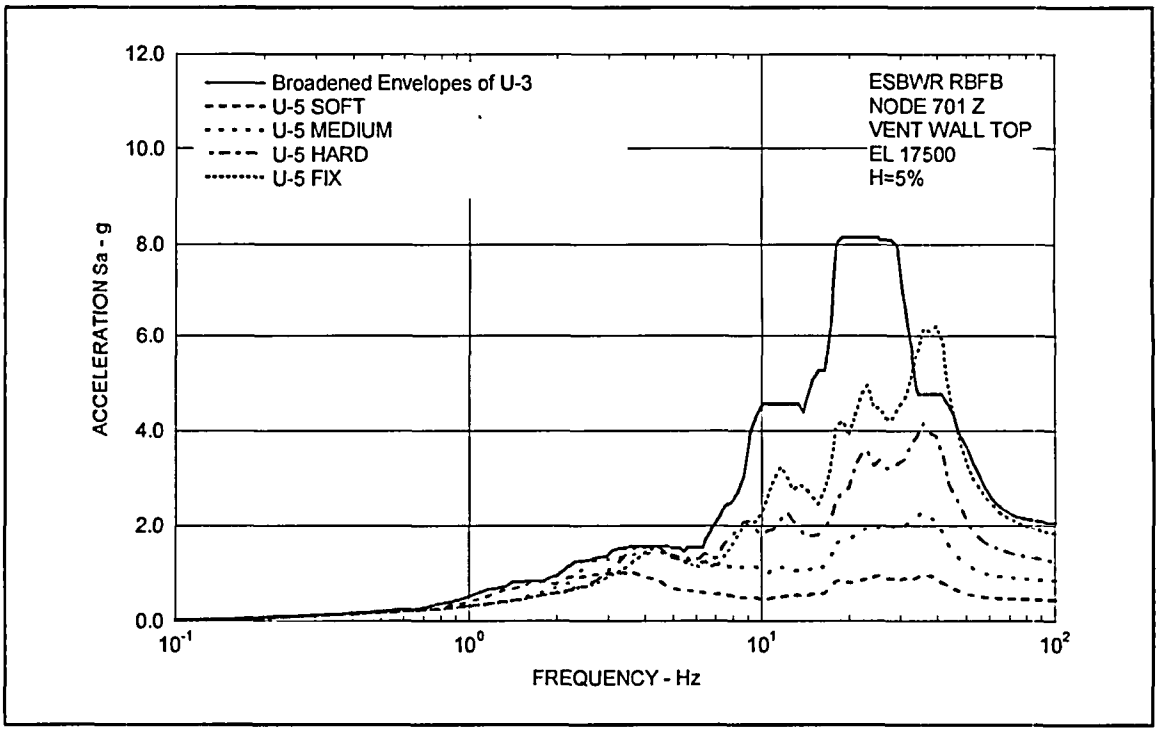

Figure 3.8-41(20) Floor Response Spectra - Vent Wall Top Z

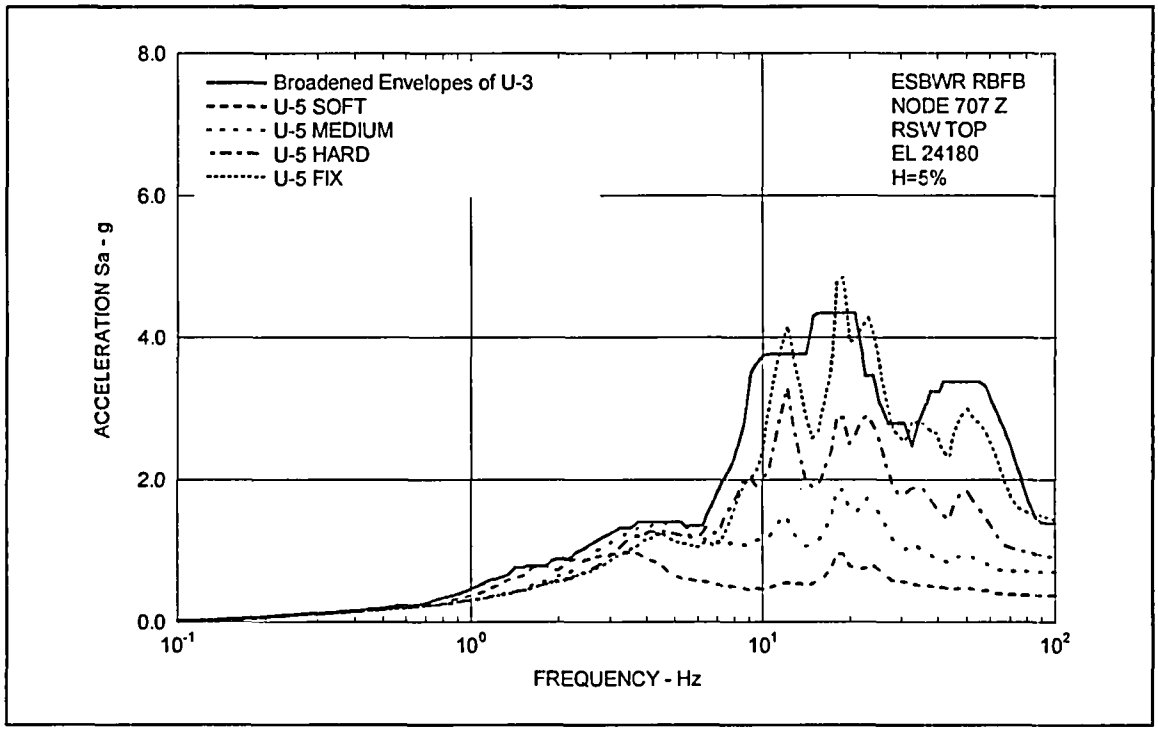

Figure 3.8-41(21) Floor Response Spectra - RSW Top Z

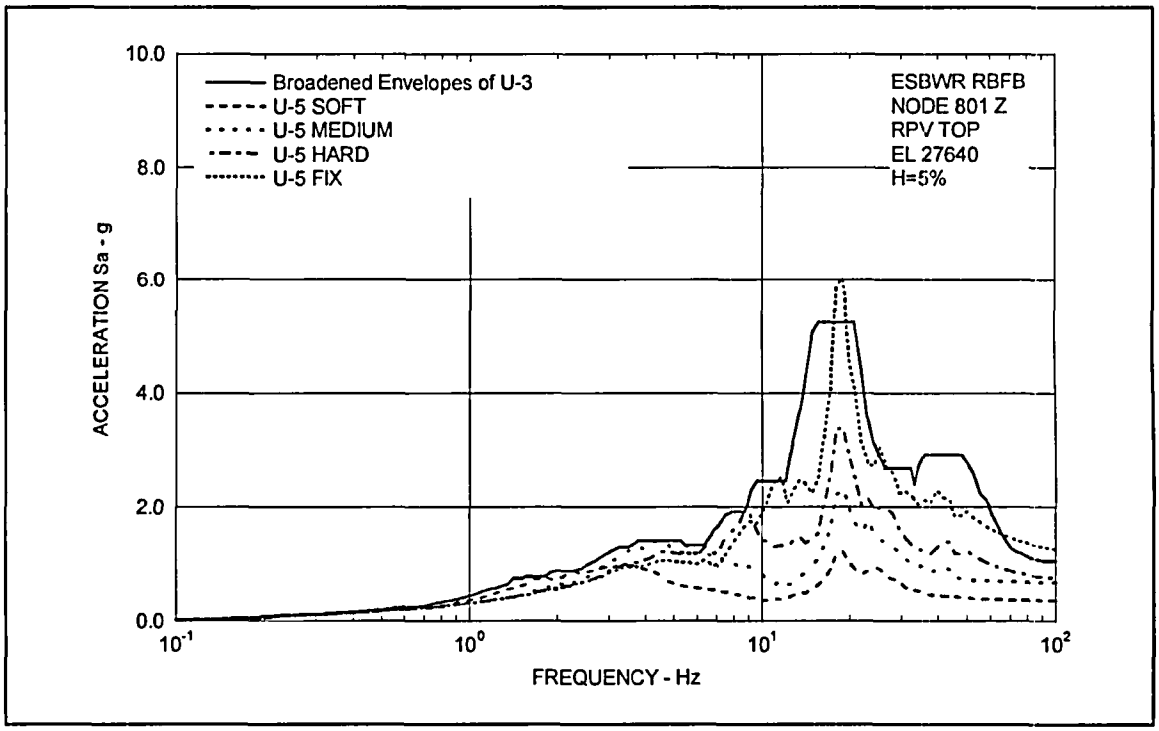

Figure 3.8-41(22) Floor Response Spectra - RPV Top Z

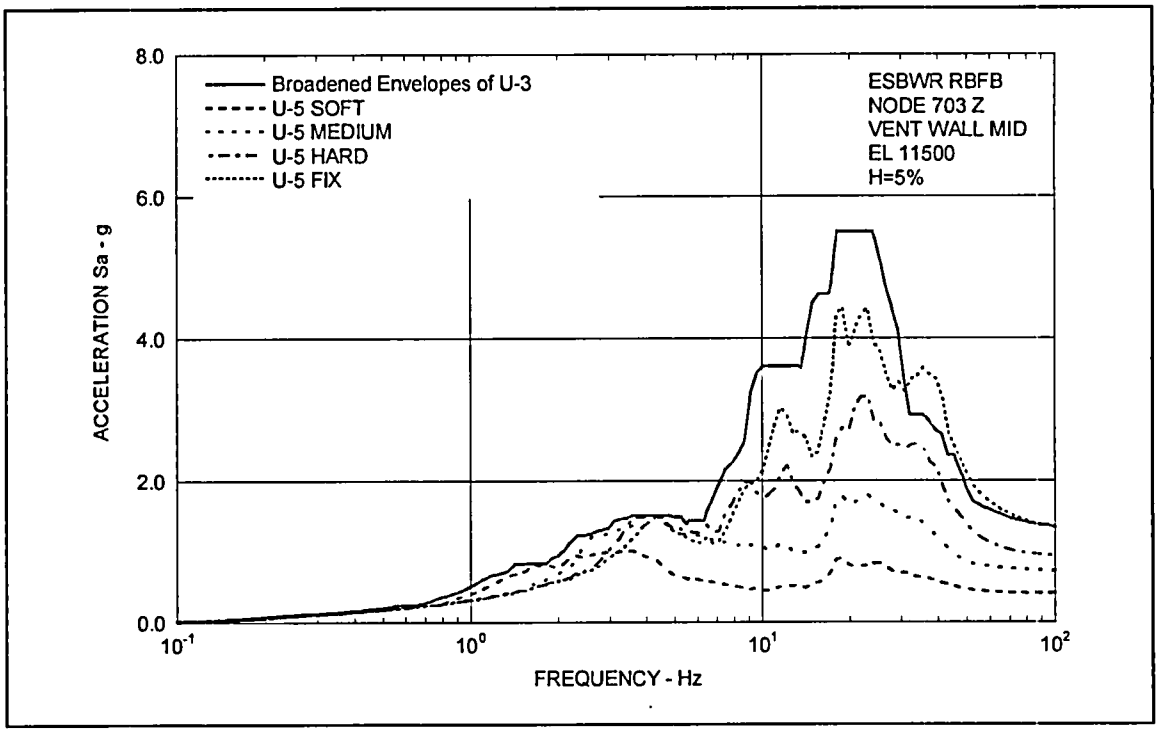

Figure 3.8-41(23) Floor Response Spectra - Vent Wall Middle Z

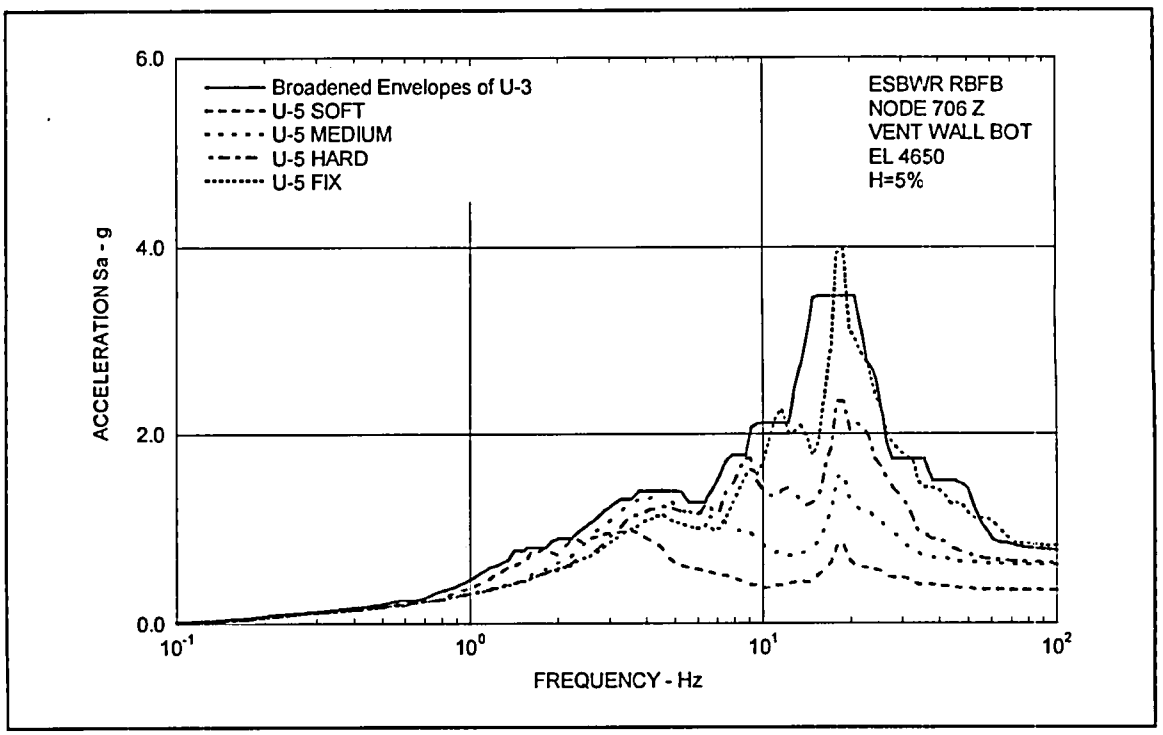

Figure 3.8-41(24) Floor Response Spectra - Vent Wall Bottom Z

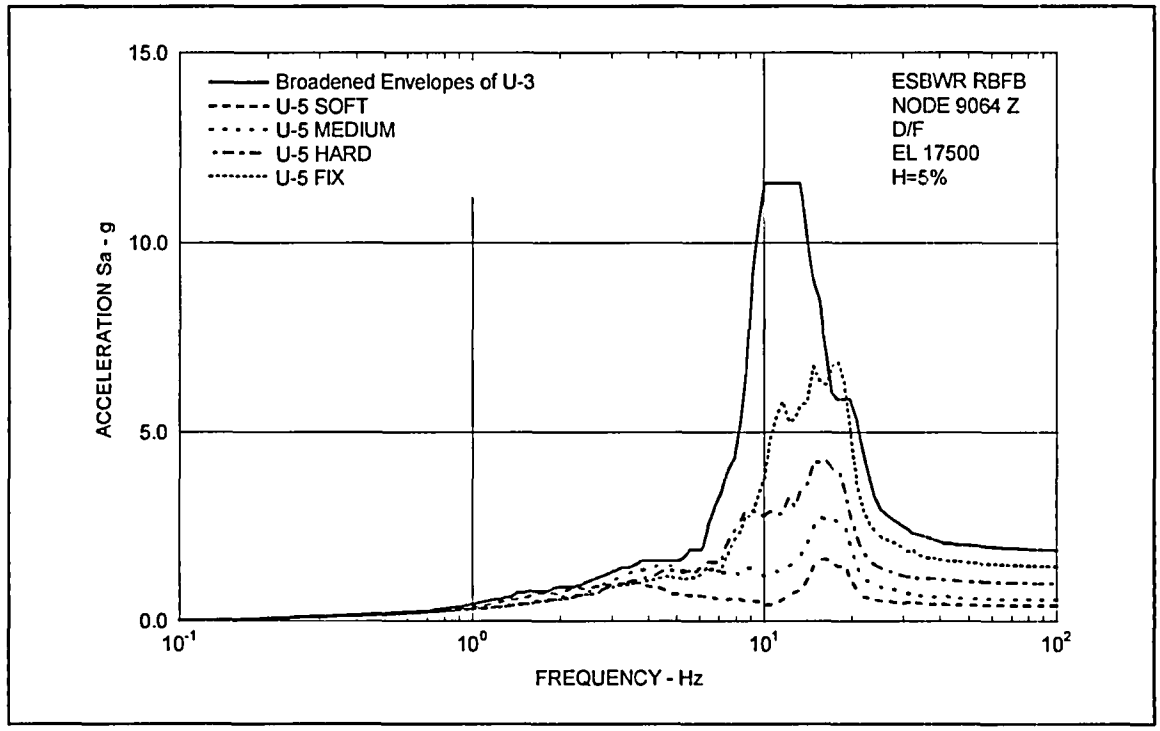

Figure 3.8-41(25) Floor Response Spectra - D/F Oscillator

DCD Impact

Final seismic loads were to be documented in next update of DCD Appendix 3A.

NRC RAI 3.8-41, Supplement 3

NRC Assessment Following the December 14, 2006 Audit

The results presented raise a concern whether 50% of the uncracked concrete stiffness is the appropriate assumption. If 75% or 100% of the uncracked concrete stiffness had been used, then the frequency increase would be greater. GE needs to provide its technical basis for the 50% assumption, for the confined unreinforced in-fill concrete. The response only discussed seismic loading; GE needs to provide an assessment of the effect of the in-fill concrete on response spectra generated from hydrodynamic loads (SRV & LOCA). GE also needs to confirm that all thermal loading conditions analyzed using NASTRAN (including normal operating conditions) have been adjusted to account for the presence of the concrete infill, using thermal ratios obtained from ABAQUS/ANACAP thermal stress analyses.

During the audit, GE provided a draft supplemental response to address the above items. The NRC needs to review this response.

GE Response

As shown in Table 3.8-41(2), the frequency change is insignificant as the stiffness increases from 50 to 100% and the frequency shift (10% for VW and 8% for DF) is well within the 15% spectral broadening. Therefore, the consideration of 50% effective stiffness is sufficient.

Table 3.8-41(2) Effect of Concrete Rigidity for Natural Frequencies for VW and DF

Structure		Seismic Model			
		Original	Update	Update+50% Concrete Stiffness	Update+100% Concrete Stiffness
Vent Wall	Frequency (Hz)	25.4	26.8	46.7	51.3
	Ratio	1.0	1.06	1.84 (1.0)	2.02 (1.10)
Diaphragm Floor	Frequency (Hz)	13.5	12.7	17.0	18.3
	Ratio	1.0	0.94	1.26 (1.0)	1.36 (1.08)

Material property
(1) Concrete
Modulus of elasticity: E=13900MPa (50%)

E=27800Mpa (100%)
Poison's ratio : ν=0.17
(2) Steel
Modulus of elasticity: E=200000MPa
Poison's ratio: ν=0.3

The effect of in-fill concrete stiffness on hydrodynamic response has been evaluated for the same two conditions, no concrete stiffness and 50% concrete stiffness, as considered in the seismic analysis. The results indicate that the response spectra are mostly affected at the vent wall and diaphragm floor locations. The representative response spectra from the reanalysis are shown in Figure 3.8-41(26) through 3.8-41(31) for various hydrodynamic loads.

The Design Basis Accident (DBA) thermal loading conditions analyzed using NASTRAN have been adjusted to account for the presence of the concrete infill in the vent wall and diaphragm floor, using thermal ratios obtained from ABAQUS/ANACAP thermal stress analyses. Normal operating temperature is much lower than DBA and no thermal ratios were considered for normal operating conditions, which is conservative.

In ABAQUS/ANACAP DBA thermal analyses, separate models are used for both a linear solution and a cracking analysis solution as a basis for developing the thermal ratios for the redistribution of internal section forces due to concrete cracking under the DBA thermal loads. The only difference in the modeling between the linear analysis and the cracking analysis is in the treatment of the infill concrete in the vent wall and diaphragm floor. The structural design of these components is based on assuming that the steel will carry all the loads, that is, no credit is taken for the loads that will be carried by the infill concrete. Thus, the design-based NASTRAN models ignore the infill concrete in the linear analyses for section stresses under the required combination of loads. However, since the cracking analyses are intended to provide the actual internal section force distributions under the thermal loads, these models must include the effect of the infill concrete. Thus, for this ABAQUS/ANACAP study, the linear analysis model does not include the infill concrete. In the cracking analysis model, this infill concrete is included and modeled with 20-node brick elements with strain-compatibility enforced at the connections of the plate bending elements used for the steel plates in the vent wall and diaphragm floor.

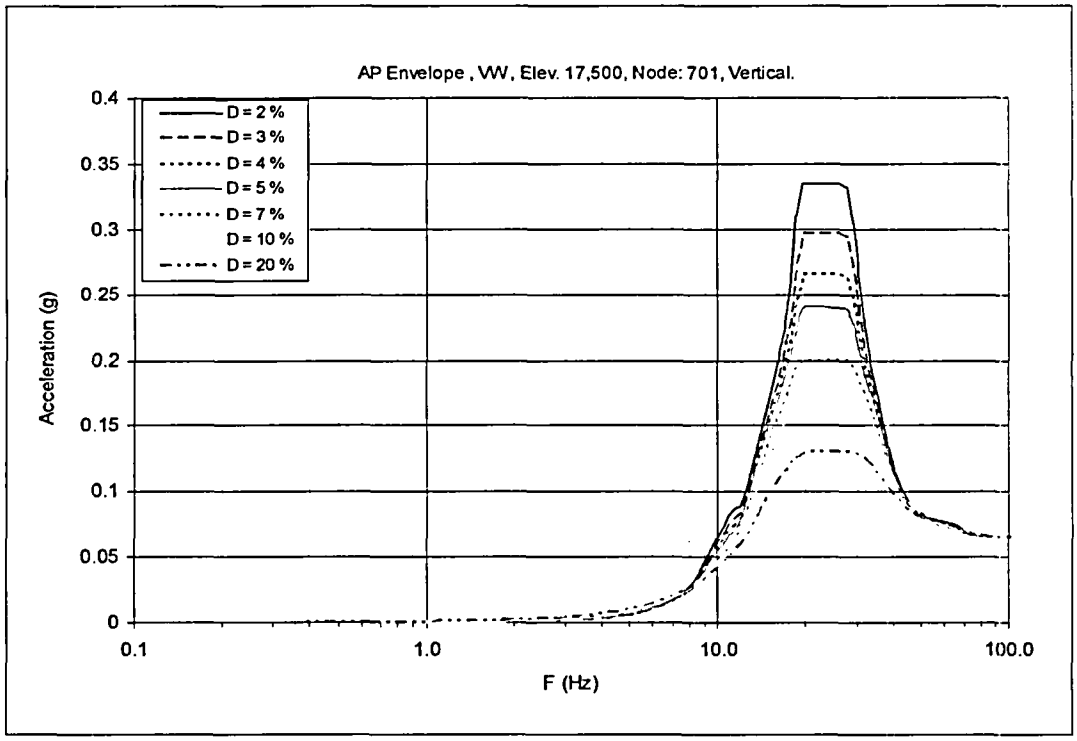

Figure 3.8-41(26). Floor Response Spectrum—AP Envelope, Node: 701 Vertical

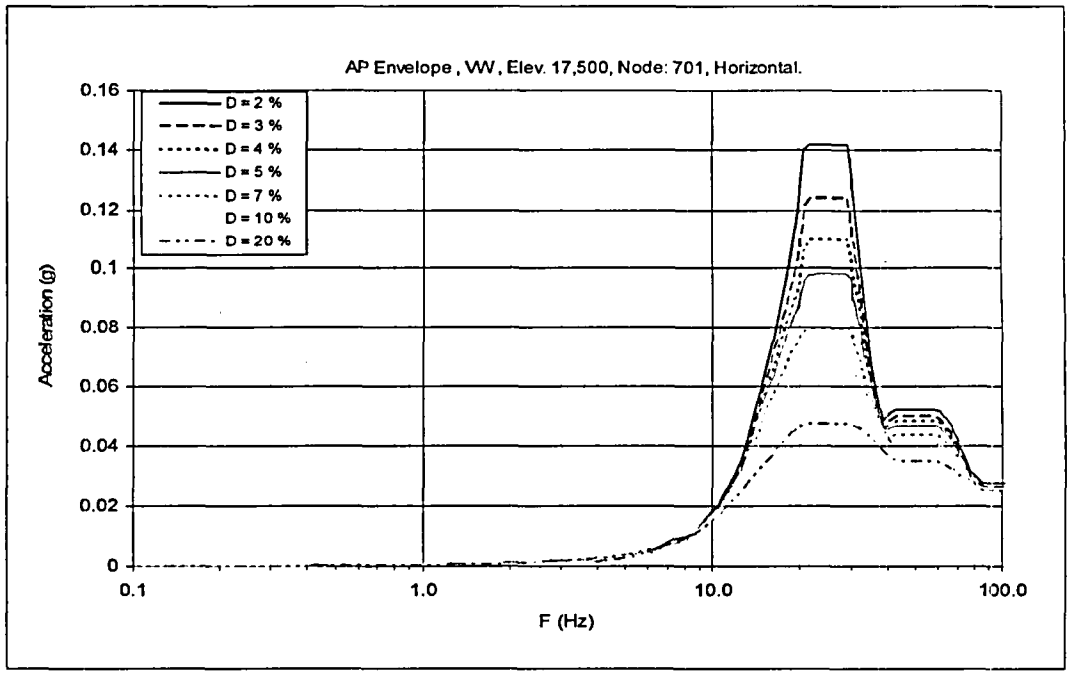

Figure 3.8-41(27). Floor Response Spectrum—AP Envelope, Node: 701 Horizontal

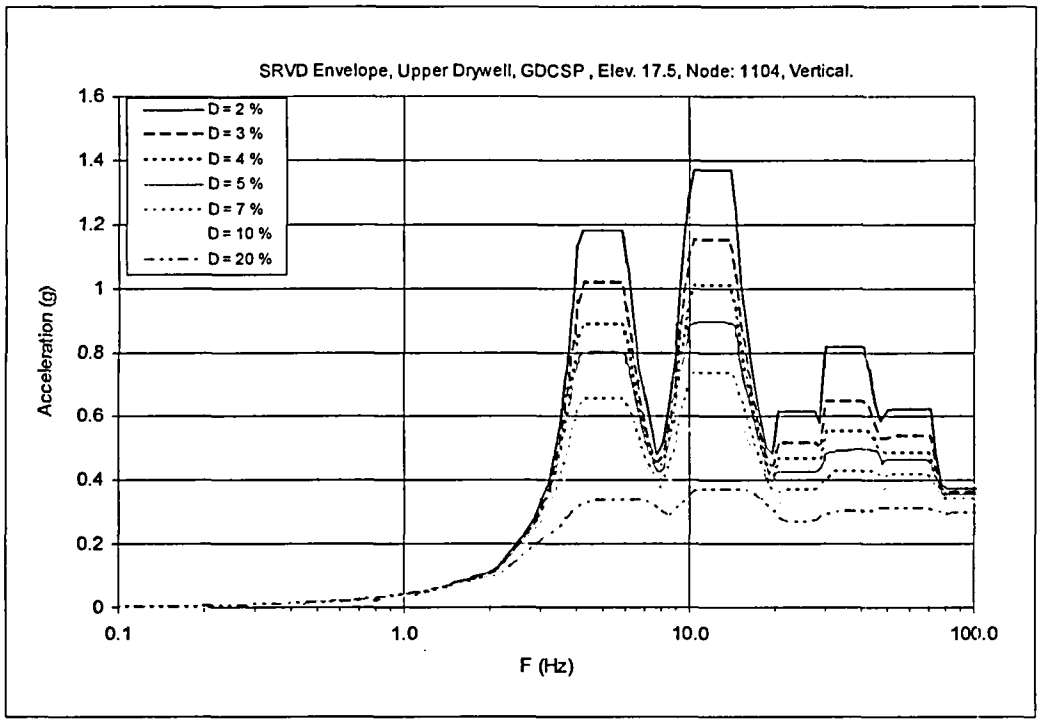

Figure 3.8-41(28). Floor Response Spectrum—SRV Envelope , Node: 1104, Vertical

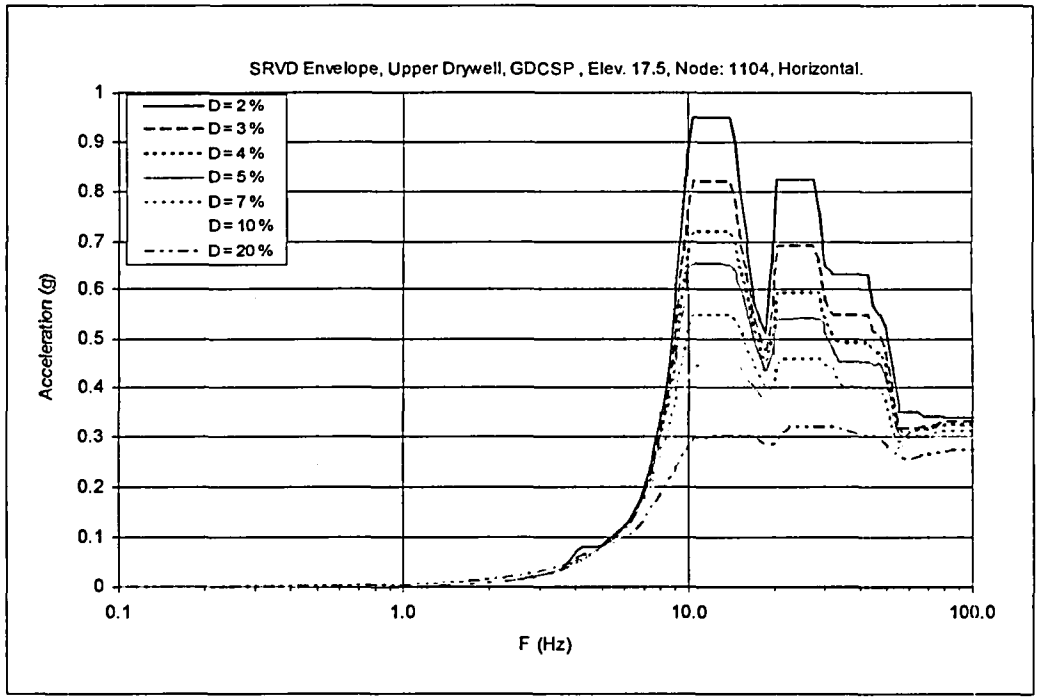

Figure 3.8-41(29) Floor Response Spectrum—SRV Envelope , Node: 1104, Horizontal

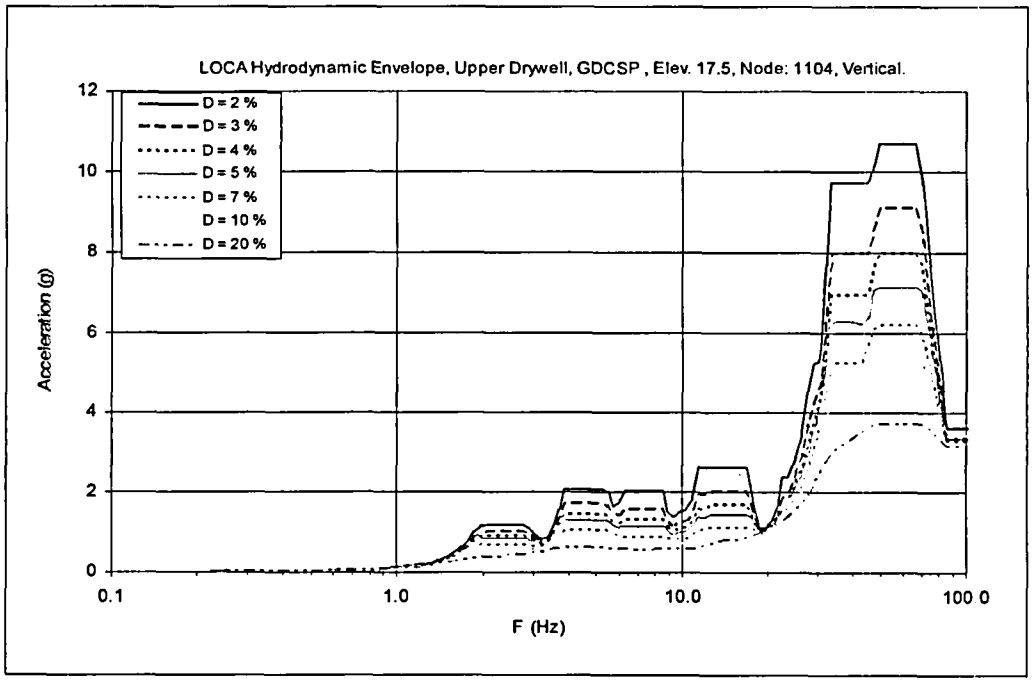

Figure 3.8-41(30). Floor Response Spectrum—CH & CO Envelope, Node: 1104, Vertical

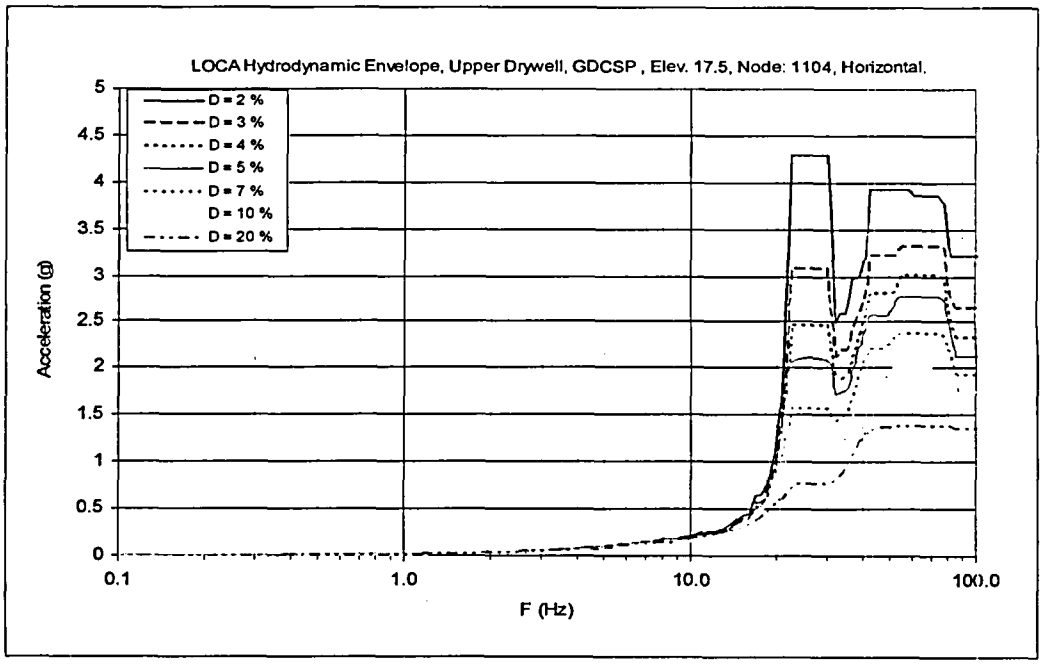

Figure 3.8-41(31). Floor Response Spectrum—CH & CO Envelope, Node: 1104, Horizontal

DCD Impact

DCD Tier 2 Appendix 3F was revised in the next update.

NRC RAI 3.8-41, Supplement 4

NRC Assessment from Chandu Patel E-mail Dated May 24, 2007

Based on its review of the latest response, the staff requests the applicant to address the following:

(1) When 50% of the concrete stiffness was considered, the natural frequencies of the vent wall and the diaphragm wall increased 84% and 26%, respectively, compared to the original values. When 100% of the concrete stiffness was considered, the natural frequencies only increased an additional 8 to 10%. Based on the results obtained from considering 50% of the concrete stiffness, GE needs to explain how the natural frequencies could rise only 8 to 10% when 100% of the concrete stiffness values were utilized. For seismic loadings, GE indicated that differences were noted in the floor response spectra at certain locations when 50% of the concrete stiffness values were included. Therefore, GE stated that the results of the infill concrete stiffness parametric evaluation will be included in the site-envelope seismic design loads. In addition, GE indicated that additional parametric seismic analysis is being performed to address containment Loss of Coolant Accident flooding and the effect of updated modeling properties of the containment internal structures. From a review of DCD Rev. 3, it is not clear whether the enveloping and updates of the modeling properties discussed above have been incorporated for the seismic loading.

(2) For evaluating the effects of the infill concrete on hydrodynamic response spectra generation, spectra were provided at representative locations for annulus pressurization, safety relief valve, chugging, and condensation oscillation loadings. However, there was no comparison to show how the spectra for the 50% infill concrete case differ from the original (no infill concrete) case, as was done for the seismic case.

(3) In addition to the effect of the infill concrete on the generation of floor response spectra, GE still has not confirmed whether the member design loads (for seismic and hydrodynamic loads) for the vent wall and diaphragm walls are affected by a shift in the natural frequencies of these two structures (i.e., could the accelerations increase due to a shift in frequency).

(4) For the thermal loading condition, GE indicated that the normal operating temperature is much lower than design bases accident (DBA) and no thermal ratios were used for normal operating conditions, which is conservative. Does this imply that the DBA thermal loading is used for all load combinations, even those that specify the normal operating condition? If not, then GE needs to explain why neglecting the thermal ratios is conservative..

GEH Response

(1) The vent wall is supported by the RPV pedestal at the base and laterally constrained by the diaphragm floor at the top. Natural frequencies of the vent wall were calculated by an integrated stick model shown in Figure 3.8-41(32), which is consistent with the RBFB complex seismic model in DCD Tier 2 Figure 3A.7-4. Because of the coupled configuration, the stiffer vent wall

with 100% concrete stiffness does not alter its natural frequencies significantly as the system frequencies are controlled by the more flexible supporting structures.

Natural frequencies of the diaphragm floor were calculated by a 3D FEM model shown in Figure 3.8-41(33).

The effect of concrete stiffness on natural frequencies is further examined by comparing the overall stiffness summarized in Table 3.8-41(3). As shown in this table, the increment of diaphragm floor stiffness ratio from 0 to 50% concrete stiffness is larger than that from 50% to 100% concrete stiffness. This is because the diaphragm floor has girders under the bottom plate, which also contributes to overall stiffness. The neutral axis of the section is below the bottom plate if concrete stiffness is ignored. When concrete stiffness is added between the top and bottom plates, the neutral axis of the section moves upward. As the concrete stiffness becomes larger, the neutral axis moves up further. Because of the neutral axis shift, the total stiffness of the section with 100% concrete stiffness is only 15% higher than that with 50% concrete stiffness. Since natural frequency is proportional to the square root of stiffness, the frequency ratio is only 1.07 when the concrete stiffness is increased from 50% to 100%.

Seismic analyses regarding the effect of in-fill concrete stiffness of the VW and DF and the effect of LOCA flooding are described in DCD Tier 2 Subsections 3A.8.4 and 3A.8.5, respectively. Site-envelope seismic design loads summarized in DCD Tier 2 Subsection 3A.9.1 are determined by enveloping the above analysis results.

(2) The hydrodynamic floor response spectra between the 50% infill concrete case (labeled U-5) and the no infill concrete case (labeled U-3) are compared in Figures 3.8-41(34) through 3.8-41(39) at the same locations as those in Figures 3.8-41(26) through 3.8-41(31) contained in NRC RAI 3.8-41, Supplement 3. The load cases considered are the Safety Relief Valve Discharge (SRVD) envelope, Chugging (CH) and Condensation (CO) envelope and Annulus Pressurization (AP) envelope.

(3) The member design loads for seismic and hydrodynamic loads for the vent wall and diaphragm floor have considered the effect of natural frequency shift on the response analysis results for these two structures. A shift in natural frequencies does not always result in acceleration increase for structural members.

(4) For the load combinations involving the normal operating temperature conditions, the contribution to section forces and moments due to thermal load is calculated by applying the normal operating temperature distributions to the structure and assuming linear properties and linear behavior. These thermal induced section forces and moments are then combined, without factoring from thermal ratios, with the forces and moments from mechanical loads for the load combination. This is conservative because the section forces and moments from the thermal loads will be reduced if cracking is considered.

Table 3.8-41(3) Evaluation of Diaphragm Floor Stiffness due to Concrete

Infill Concrete Stiffness	0%	50%	100%
Calculation Model	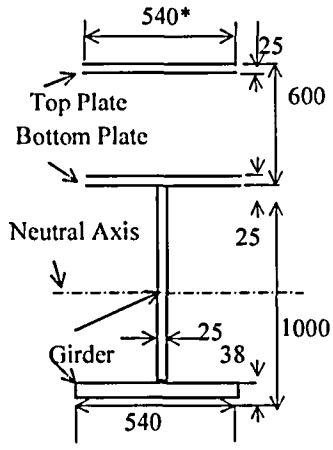	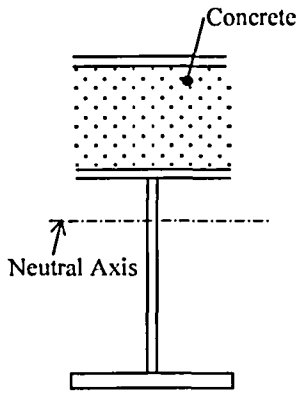	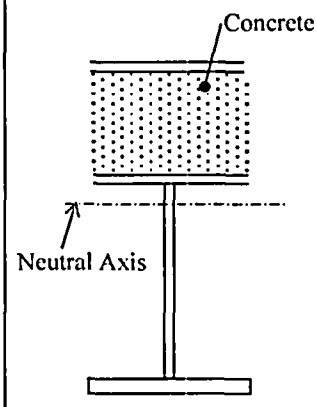
Stiffness Ratio	1.0 -	1.29 (1.0)	1.48 (1.15)
Square Root of Stiffness Ratio	1.0 -	1.13 (1.0)	1.21 (1.07)

Note *: Assume the same width with girder

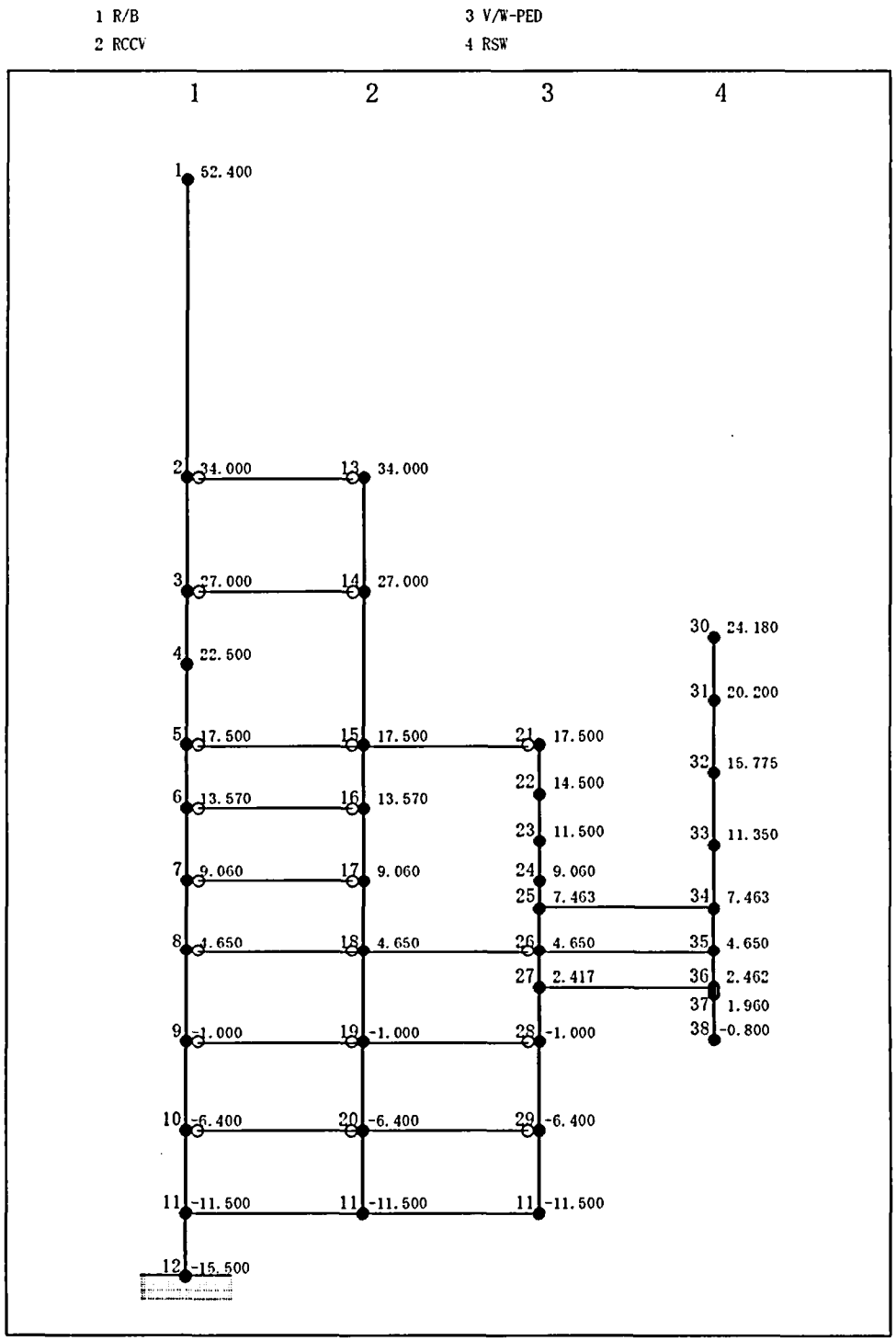

Figure 3.8-41(32) Analysis Model for Vent Wall

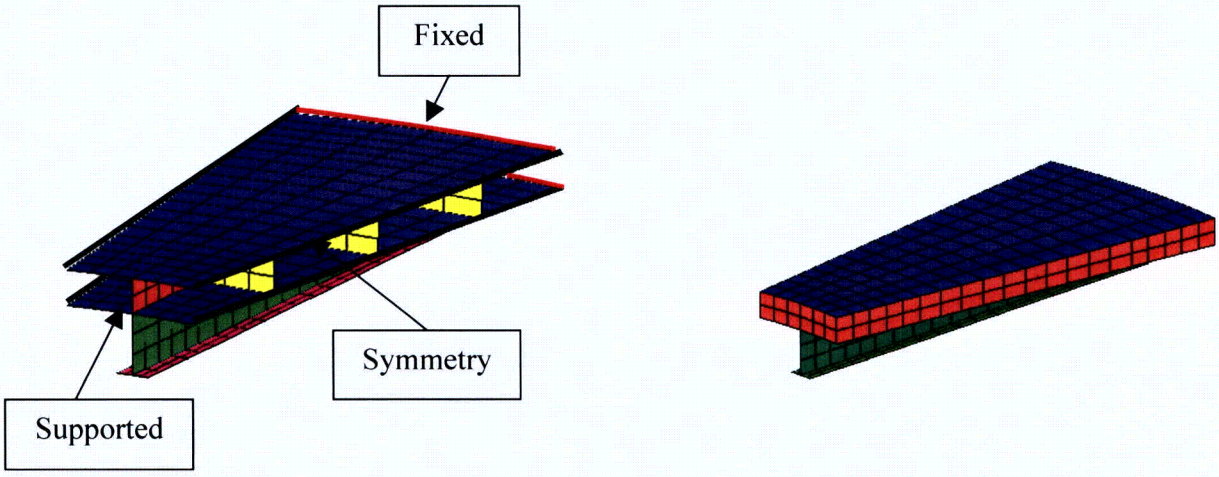

Figure 3.8-41(33) Analysis Model for Diaphragm Floor

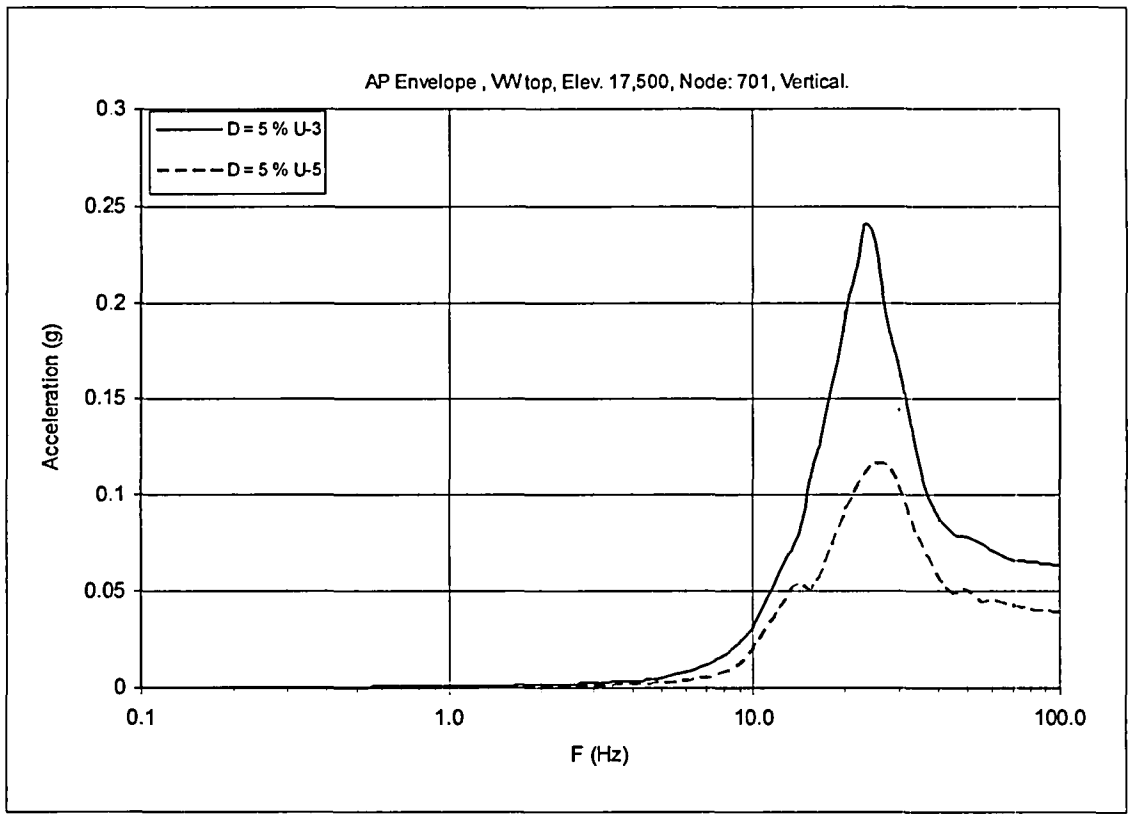

Figure 3.8-41(34) Floor Response Spectrum - AP Envelope, Node: 701, Vertical

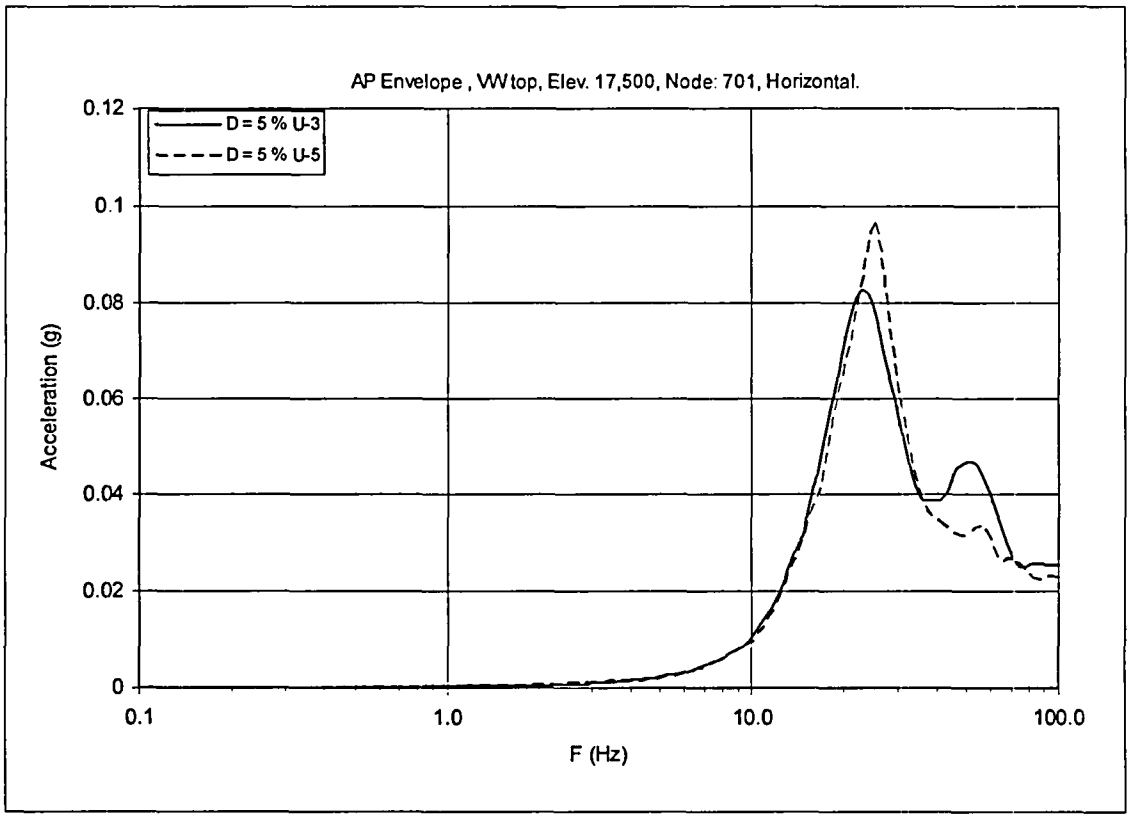

Figure 3.8-41(35) Floor Response Spectrum - AP Envelope, Node: 701, Horizontal

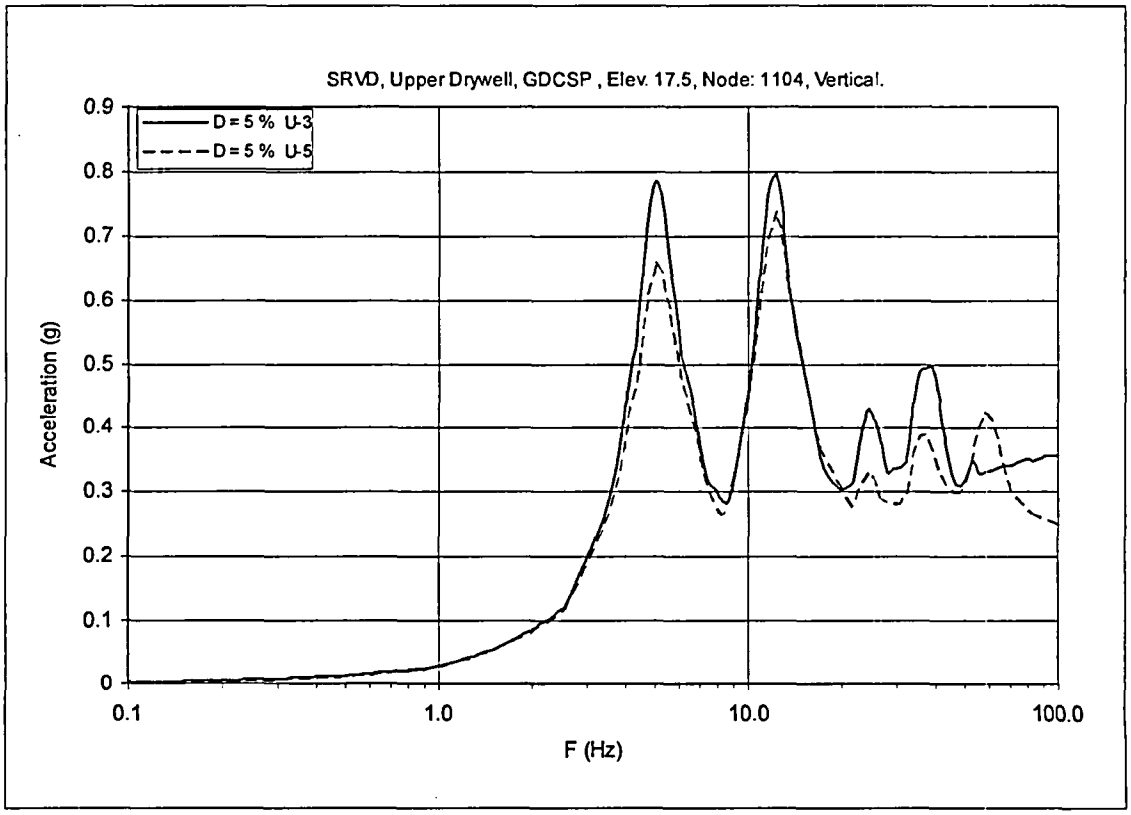

Figure 3.8-41(36) Floor Response Spectrum – SRVD Envelope, Node: 1104, Vertical

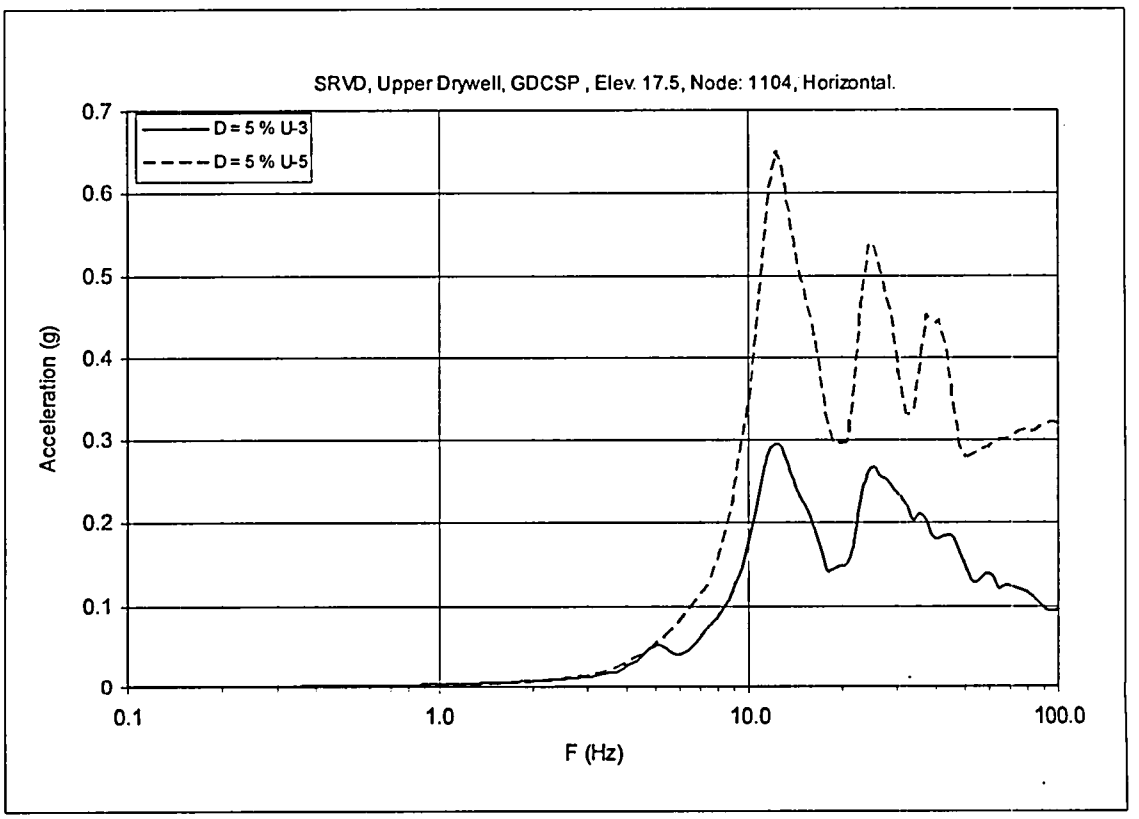

Figure 3.8-41(37) Floor Response Spectrum – SRVD Envelope, Node: 1104, Horizontal

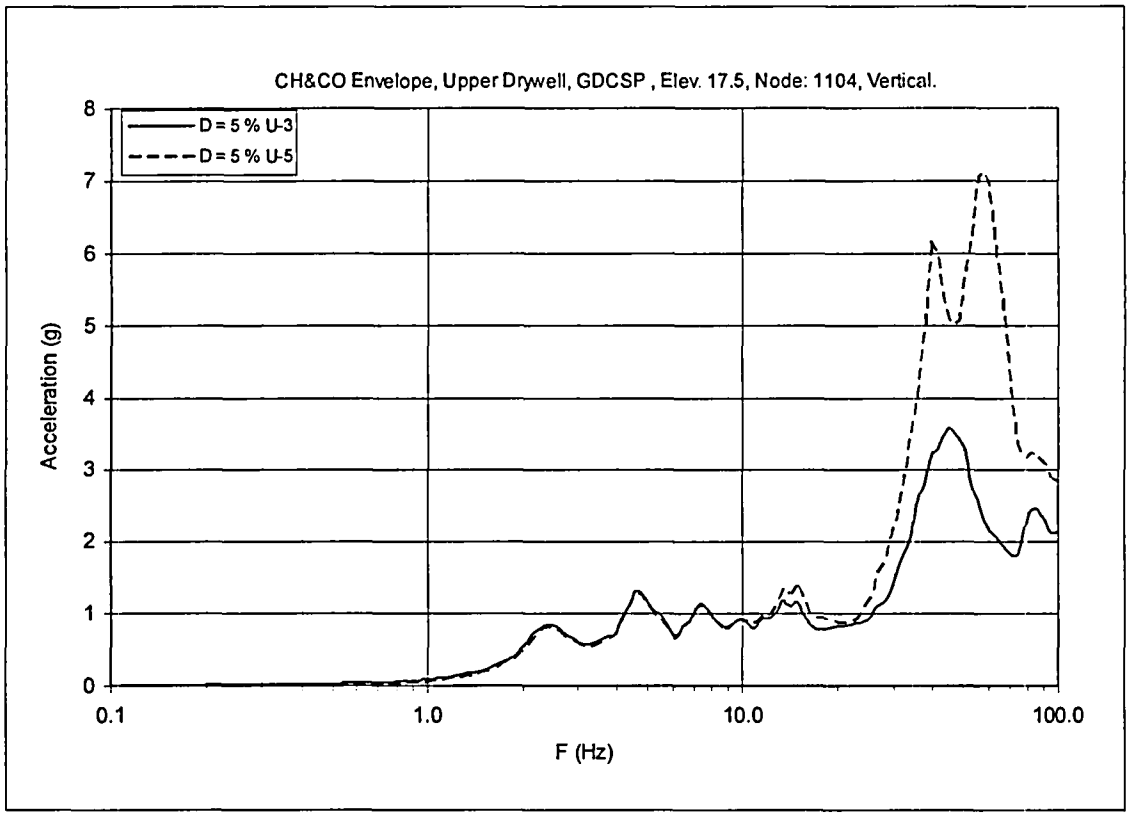

Figure 3.8-41(38) Floor Response Spectrum – CH & CO Envelope. Node: 1104, Vertical

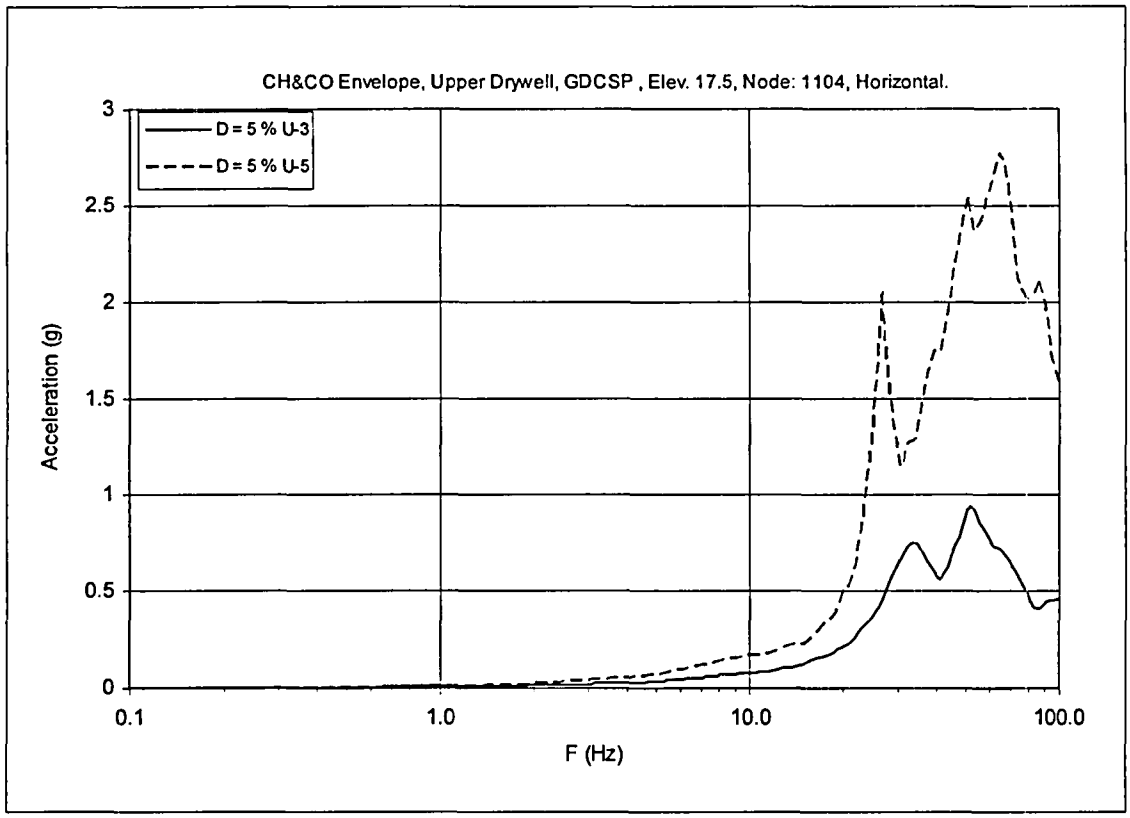

Figure 3.8-41(39) Floor Response Spectrum – CH & CO Envelope. Node: 1104, Horizontal

DCD Impact

No DCD change was made in response to this RAI Supplement.

NRC RAI 3.8-41, Supplement 5

GEH response dated December 12, 2007, provided information requested for four items related to the effects of the infill concrete within the vent wall and diaphragm floor structures located inside containment. The staff has two concerns as described below.

(1) Based on the prior analytical results, consideration of 50% of the (unreinforced) infill concrete stiffness had a pronounced effect on the structural responses from seismic loadings and so GEH has indicated that it would envelop these results with those from the original seismic design case of 0% concrete stiffness. From the information provided in the current response it is still not evident that if 100% of the concrete stiffness was considered then the increase in member forces and response spectra would be negligible. The basis provided in the response for the small effect on frequency caused by increasing the concrete stiffness from 50% to 100% is still questionable, as well as the effect of this frequency shift on the member forces and response spectra. GEH needs to either consider the entire range of concrete stiffness in its analysis and design of the ESBWR or clearly demonstrate that the member forces and response spectra are not affected. Also, the current description in the DCD, including Sections 3A.8.4 and 3A.8.5 do not clearly state what percentage of concrete stiffness is considered for the vent wall and diaphragm floor, and it does not clearly state that member forces and response spectra from this set of analyses are enveloped with the results without the infill concrete in the vent wall and diaphragm floor.

(2) This item covers the effect of the infill concrete stiffness for hydrodynamic loadings such as Annulus Pressurization, Safety Relief Valve Discharge, chugging, and condensation oscillation. Since the figures provided in this response show that the hydrodynamic spectra are greater in some locations, GEH needs to consider the entire range of concrete stiffness in its analysis and design of the ESBWR for hydrodynamic loads as well.

GEH Response

(1) GEH has considered the entire range of concrete stiffness. In order to evaluate the entire range of concrete stiffness of infill concrete within the vent wall (VW) and diaphragm floor (D/F) structures, an additional parametric SSI analysis for generic uniform sites is performed for the 100% stiffness case. The analysis results are compared to the site-envelope seismic design loads in DCD Tier 2 Appendix 3A, Revision 4, in which 0% and 50% stiffness cases were considered.

Tables 3.8-41(4) through 3.8-41(8) show member forces of the 100% stiffness case and their percent differences from the DCD Tier 2 Revision 4 design envelope loads. Table 3.8-41(9) shows the vertical acceleration at the D/F. Figures 3.8-41(40) through 3.8-41(58) show comparisons of floor response spectra (FRS) at selected locations.

The most significant effect of the 100% infill concrete stiffness is observed for the member forces in the VW structure, where the shear, moment and torsion at the base are increased by approximately 38%, 30% and 71%, respectively, per Table 3.8-41(6). The largest incremental shear, moment and torsion forces over the design forces considered in the

existing stress analysis are 11 MN, 118 MN-m and 42 MN-m, respectively. The resulting incremental stresses computed as a beam section are 12 MPa bending and 12 MPa shear. They are about 4% and 7% of the highest calculated design bending and shear stresses, respectively, for the governing abnormal/extreme load combination summarized in DCD Tier 2 Revision 5 Table 3G.1-39. The ratio of the total stress (design plus incremental) to the code allowable is 0.7 for bending and 0.76 for shear. Therefore, the higher seismic loads have no impact on the VW design. DCD Tier 2 Subsection 3G.1.5.2.1.13, Revision 6 will be revised to include the above discussion.

Since the results of this parametric analysis for the 100% infill concrete stiffness case are not fully bounded by the existing seismic design envelope, DCD Tier 2 Appendix 3A has been updated in Revision 5 to include the 100% stiffness results in the updated seismic design envelope for both member forces and response spectra. However, typographical errors have been found in DCD Tier 2 Revision 5 Tables 3A.9-1c and 3A.9-1d and will be corrected in DCD Tier 2 Revision 6.

DCD Tier 2 Subsection 3A.8.4 has been clarified in Revision 5 to indicate that the results of the three infill concrete stiffness cases (0%, 50% and 100%) are included in the seismic design envelope. The analysis model used for the LOCA flooding case (RU-6) described in DCD Tier 2 Subsection 3A.8.5 is the updated model for the reactor shield wall (RSW), VW and D/F properties in which the infill concrete stiffness is 0% (see DCD Tier 2 Table 3A.6-1).

(2) For consistency with the seismic analysis discussed above, the 100% infill concrete case is also added to the response analysis for annulus pressurization (AP), safety relief valve (SRV), condensation oscillation (CO) and chugging (CH) hydrodynamic loads. The results of all three infill concrete stiffness cases (0%, 50% and 100%) are enveloped for design use. DCD Tier 2 Appendix 3F has been updated in Revision 5 accordingly.

In order to better simulate the actual configuration of the Reactor Building (RB) and Fuel Building (FB) the axi-symmetric shell model has been replaced by a 3D shell model in the DCD Tier 2 Appendix 3F Revision 5 analysis for SRV, CO and CH loads. The AP analyses were updated to reflect the revised subcompartment pressures in the annulus between the RSW and the reactor pressure vessel (RPV) due to the postulated break of feedwater line and reactor water cleanup.

The last sentence of the introductory paragraph in DCD Tier 2 Appendix 3G has been revised and a new last sentence has been added in Revision 5 to read "Construction drawings meet the technical licensing commitments made in the DCD but are issued under different contractual/industrial rules than the DCD drawings and reflect detailed design configuration. The final design details, and hence final component stresses may be different from those reported here but they will meet the structural acceptance criteria presented in Section 3.8 in accordance with Tier 1 ITAACs in Tables 2.16.5-2, 2.16.6-2, and 2.16.7-2".

Table 3.8-41(4) Seismic Loads: RB/FB Stick

(a) 100% Infill Concrete Stiffness Results

Elev. (m)	Node No.	Elem No.	Shear		Moment		Torsion (MN-m)
			X-Dir. (MN)	Y-Dir. (MN)	X-Dir. (MN-m)	Y-Dir. (MN-m)	
52.40	110				1611	1793	
		1110	125.7	157.5	3074	4460	1353
34.00	109				4329	5522	
		1109	191.7	151.2	4724	6154	2370
27.00	108				6360	7058	
		1108	421.3	363.3	7210	7968	3333
22.50	107				8060	8578	
		1107	474.7	405.2	9053	10356	5551
17.50	106				9924	10974	
		1106	506.1	468.5	11807	12631	4295
13.57	105				12425	13072	
		1105	536.1	502.9	14710	15073	4650
9.06	104				15220	15416	
		1104	573.0	541.2	17574	17476	5044
4.65	103				17446	17721	
		1103	823.0	736.1	21741	21045	10356
-1.00	102				22428	21408	
		1102	862.3	813.3	26919	25164	10679
-6.40	101				27439	25949	
-11.50	2	1101	931.2	912.5	31882	30195	11572

(b) Percent Difference with DCD Rev. 4 Enveloping Loads *

Elev. (m)	Node No.	Elem No.	Shear		Moment		Torsion
			X-Dir.	Y-Dir.	X-Dir.	Y-Dir.	
52.40	110				-1.9%	-0.9%	
		1110	-17.2%	-0.4%	-28.6%	-0.1%	-1.8%
34.00	109				-22.5%	0.5%	
		1109	0.5%	-1.2%	-27.1%	-2.6%	-1.4%
27.00	108				-17.2%	-0.7%	
		1108	-1.0%	-9.3%	-19.6%	-7.3%	0.1%
22.50	107				-18.6%	-6.7%	
		1107	-1.8%	-12.7%	-21.0%	-8.3%	-8.9%
17.50	106				-19.9%	-8.1%	
		1106	-5.0%	-15.6%	-14.3%	-8.9%	-15.2%
13.57	105				-13.1%	-9.1%	
		1105	-5.8%	-16.2%	-11.3%	-10.0%	-11.3%
9.06	104				-10.3%	-10.3%	
		1104	-6.1%	-17.3%	-9.3%	-11.2%	-15.7%
4.65	103				-8.5%	-12.2%	
		1103	-2.0%	-15.6%	-6.1%	-13.3%	-9.4%
-1.00	102				-5.3%	-14.2%	
		1102	-1.0%	-13.3%	-2.7%	-14.0%	-7.3%
-6.40	101				-2.4%	-13.6%	
-11.50	2	1101	-0.3%	-11.4%	-1.1%	-14.4%	-1.0%

Note *: (100% Infill Concrete Stiffness - DCD Rev. 4 Envelope) / DCD Rev. 4 Envelope

Table 3.8-41(5) Seismic Loads: RCCV Stick

(a) 100% Infill Concrete Stiffness Results

Elev. (m)	Node No.	Elem No.	Shear		Moment		Torsion (MN-m)
			X-Dir. (MN)	Y-Dir. (MN)	X-Dir. (MN-m)	Y-Dir. (MN-m)	
34.00	209				191	581	
		1209	117.1	177.7	883	1409	35
27.00	208				1702	2486	
		1208	162.7	247.6	2866	4047	1681
17.50	206				3315	4368	
		1206	222.3	263.5	3924	5182	1692
13.57	205				4144	5350	
		1205	249.0	283.2	4897	6474	1938
9.06	204				5159	6706	
		1204	300.4	296.2	6316	7934	2205
4.65	203				6518	8180	
		1203	227.3	256.3	7605	9487	2602
-1.00	202				7720	9662	
		1202	272.4	291.9	9003	11082	2711
-6.40	201				9113	11219	
-11.50	2	1201	261.7	268.4	10346	12464	1944

(b) Percent Difference with DCD Rev. 4 Enveloping Loads *

Elev. (m)	Node No.	Elem No.	Shear		Moment		Torsion
			X-Dir.	Y-Dir.	X-Dir.	Y-Dir.	
34.00	209				-1.7%	0.7%	
		1209	-14.5%	-3.0%	-16.5%	-5.8%	-1.4%
27.00	208				-0.3%	-1.8%	
		1208	-1.3%	-0.4%	-3.1%	-7.3%	-7.4%
17.50	206				0.3%	-7.4%	
		1206	-3.4%	-9.2%	-5.4%	-10.1%	-14.6%
13.57	205				-4.2%	-10.1%	
		1205	-5.5%	-13.2%	-9.4%	-10.9%	-11.4%
9.06	204				-8.3%	-10.8%	
		1204	-1.3%	-19.0%	-6.9%	-11.0%	-15.7%
4.65	203				-6.8%	-10.8%	
		1203	0.7%	-11.4%	-4.4%	-10.3%	-9.4%
-1.00	202				-4.4%	-10.0%	
		1202	0.3%	-11.7%	-4.4%	-11.5%	-7.4%
-6.40	201				-4.4%	-11.3%	
-11.50	2	1201	0.1%	-11.6%	-4.5%	-12.2%	-0.9%

Note *: (100% Infill Concrete Stiffness - DCD Rev. 4 Envelope) / DCD Rev. 4 Envelope

Table 3.8-41(6) Seismic Loads: VW/Pedestal Stick

(a) 100% Infill Concrete Stiffness Results

Elev. (m)	Node No.	Elem No.	Shear		Moment		Torsion (MN-m)
			X-Dir. (MN)	Y-Dir. (MN)	X-Dir. (MN-m)	Y-Dir. (MN-m)	
17.50	701				58	56	
		701	35.0	37.0	114	136	116
14.50	702				117	148	
		702	36.4	39.3	226	260	118
11.50	703				229	269	
		703	37.0	41.8	340	390	120
8.50	704				341	396	
		704	37.8	44.7	379	438	122
7.4625	705				359	438	
		705	40.7	40.5	456	525	101
4.65	706,303				581	621	
		1303	23.7	31.8	599	667	128
2.4165	377				732	817	
		1377	36.7	47.3	778	922	156
-1.00	302				839	959	
		1302	63.1	65.0	928	1050	135
-2.75	376				928	1050	
		1376	63.2	65.3	1116	1243	135
-6.40	301				1149	1265	
-11.50	2	1301	103.6	104.8	1655	1734	117

(b) Percent Difference with DCD Rev. 4 Enveloping Loads *

Elev. (m)	Node No.	Elem No.	Shear		Moment		Torsion
			X-Dir.	Y-Dir.	X-Dir.	Y-Dir.	
17.50	701				-25.5%	-33.9%	
		701	25.0%	30.0%	14.6%	11.1%	58.9%
14.50	702				-1.4%	6.7%	
		702	23.2%	28.7%	23.1%	19.9%	57.2%
11.50	703				23.4%	19.5%	
		703	22.8%	25.9%	23.2%	23.6%	55.9%
8.50	704				23.5%	23.6%	
		704	24.5%	26.8%	23.4%	24.5%	55.1%
7.4625	705				24.6%	28.4%	
		705	31.2%	37.9%	27.9%	29.2%	70.8%
4.65	706,303				6.2%	12.5%	
		1303	-27.6%	-29.1%	5.6%	12.3%	-9.4%
2.4165	377				5.5%	11.9%	
		1377	-23.7%	-28.6%	4.1%	6.2%	-9.3%
-1.00	302				3.2%	6.6%	
		1302	-3.9%	-20.1%	2.8%	1.7%	-7.4%
-2.75	376				2.8%	1.7%	
		1376	-4.2%	-20.1%	2.2%	-6.6%	-7.4%
-6.40	301				1.6%	-6.0%	
-11.50	2	1301	-0.8%	-13.5%	1.1%	-11.7%	-0.9%

Note *: (100% Infill Concrete Stiffness - DCD Rev. 4 Envelope) / DCD Rev. 4 Envelope

Table 3.8-41(7) Seismic Loads: RSW Stick

(a) 100% Infill Concrete Stiffness Results

Elev. (m)	Node No.	Elem No.	Shear		Moment		Torsion (MN-m)
			X-Dir. (MN)	Y-Dir. (MN)	X-Dir. (MN-m)	Y-Dir. (MN-m)	
24.18	707				1.7	1.7	
		707	3.0	2.7	13.2	12.4	0.4
20.20	708				18.0	16.8	
		708	11.6	12.3	66.5	68.4	1.3
15.775	709				68.6	71.0	
		709	15.1	14.4	135.4	133.6	1.9
11.35	710				138.0	136.4	
		710	18.8	16.6	210.9	198.7	2.3
7.4625	711				80.6	95.9	
		711	23.2	23.1	130.0	148.0	23.4
4.65	712				125.1	133.0	
		712	10.3	13.8	133.0	150.9	27.4
2.4165	713				3.6	3.2	
		713	1.5	1.3	2.9	2.6	0.2
1.96	714				2.7	2.3	
-0.80	715	714	0.9	0.7	0.5	0.5	0.1

(b) Percent Difference with DCD Rev. 4 Enveloping Loads *

Elev. (m)	Node No.	Elem No.	Shear		Moment		Torsion
			X-Dir.	Y-Dir.	X-Dir.	Y-Dir.	
24.18	707				-16.9%	0.1%	
		707	2.9%	-0.1%	1.3%	1.6%	-2.7%
20.20	708				-2.2%	3.9%	
		708	-20.1%	4.9%	-15.7%	6.3%	-2.3%
15.775	709				-16.2%	6.2%	
		709	-12.6%	5.2%	-14.5%	6.4%	-2.3%
11.35	710				-13.3%	6.3%	
		710	-5.6%	4.7%	-10.7%	5.9%	-1.6%
7.4625	711				-59.1%	-47.8%	
		711	-43.6%	-35.2%	-55.5%	-41.1%	6.3%
4.65	712				6.5%	12.0%	
		712	-27.7%	-29.1%	5.3%	11.0%	-9.4%
2.4165	713				7.5%	-1.2%	
		713	3.9%	2.1%	8.0%	-1.4%	0.1%
1.96	714				7.1%	-1.0%	
-0.80	715	714	5.2%	0.0%	5.9%	0.8%	-1.7%

Note *: (100% Infill Concrete Stiffness - DCD Rev. 4 Envelope) / DCD Rev. 4 Envelope

Table 3.8-41(8) Seismic Loads: RPV Stick

(a) 100% Infill Concrete Stiffness Results

Elev. (m)	Node No.	Elem No.	Shear		Moment	
			X-Dir. (MN)	Y-Dir. (MN)	X-Dir. (MN-m)	Y-Dir. (MN-m)
Shroud	845				13.0	14.3
Bottom	846	844	6.9	7.0	18.2	17.3
RPV	815				143.8	135.5
Support	711	871	17.8	17.0	141.3	132.9

(b) Percent Difference with DCD Rev. 4 Enveloping Loads *

Elev. (m)	Node No.	Elem No.	Shear		Moment	
			X-Dir.	Y-Dir.	X-Dir.	Y-Dir.
Shroud	845				-28.8%	-2.6%
Bottom	846	844	-8.1%	-4.5%	-23.8%	0.1%
RPV	815				-16.5%	0.2%
Support	711	871	-5.0%	-6.8%	-15.4%	3.0%

Note *: (100% Infill Concrete Stiffness - DCD Rev. 4 Envelope) / DCD Rev. 4 Envelope

Table 3.8-41(9) D/F Oscillator Acceleration

(a) 100% Infill Concrete Stiffness

Elev. (m)	DF Oscillator Node No.	Max. Vertical Acceleration (g)
17.50	9064	1.29

(b) Percent Difference with DCD Rev. 4 Enveloping Loads *

Elev. (m)	DF Oscillator Node No.	Max. Vertical Acceleration
17.50	9064	-30.0%

Note *: (100% Infill Concrete Stiffness - DCD Rev. 4 Envelope) / DCD Rev. 4 Envelope

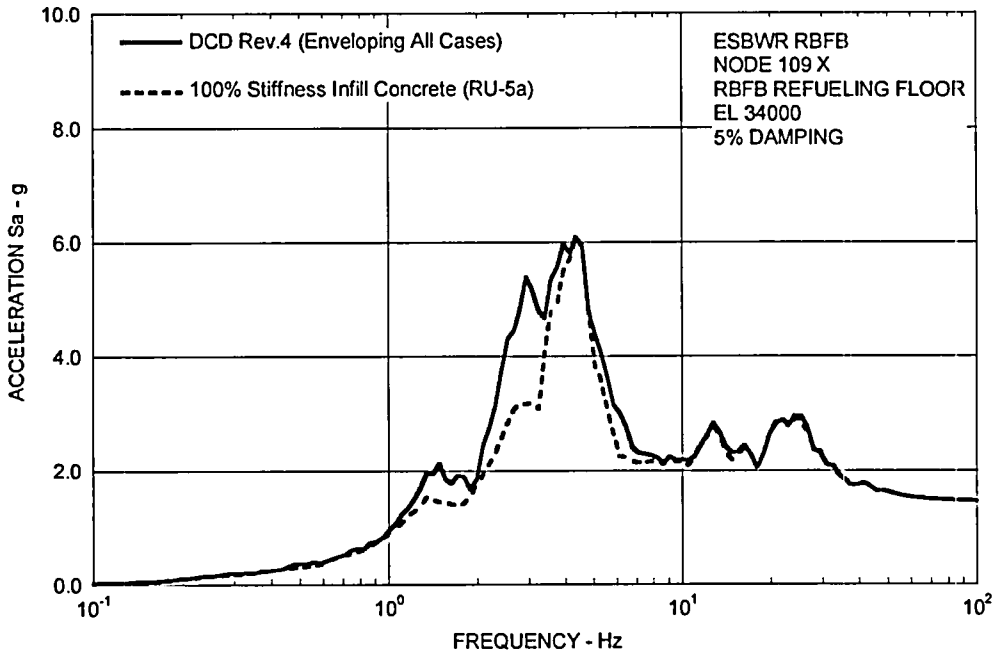

Figure 3.8-41(40) FRS (Comparison of DCD Rev. 4 with 100% Stiffness Infill Concrete) – RB/FB Refueling Floor X

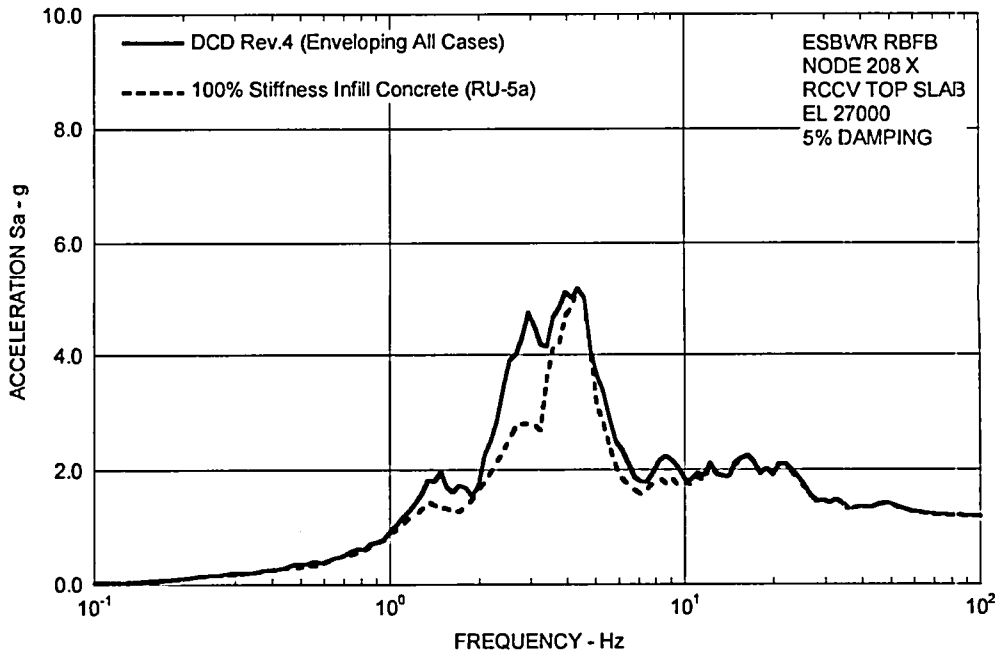

Figure 3.8-41(41) FRS (Comparison of DCD Rev. 4 with 100% Stiffness Infill Concrete) – RCCV Top Slab X

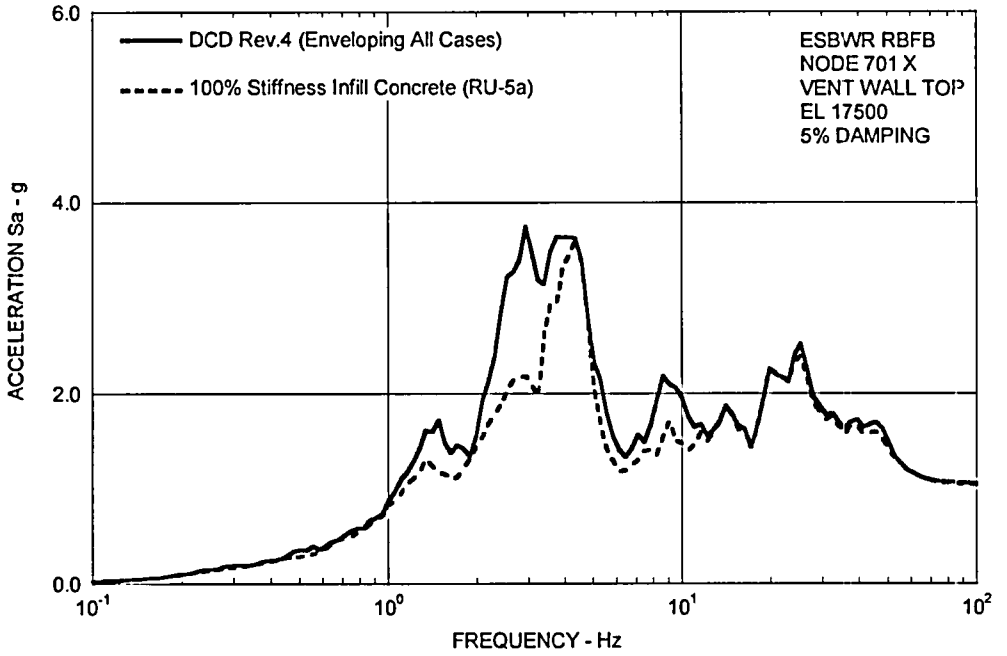

Figure 3.8-41(42) FRS (Comparison of DCD Rev. 4 with 100% Stiffness Infill Concrete) – Vent Wall Top X

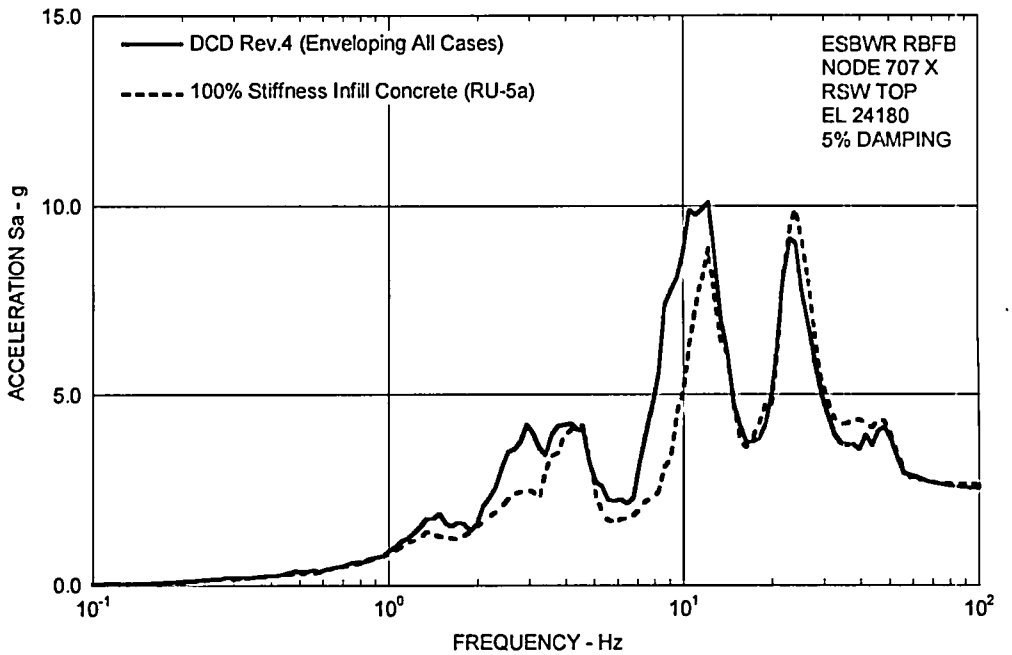

Figure 3.8-41(43) FRS (Comparison of DCD Rev. 4 with 100% Stiffness Infill Concrete) – RSW Top X

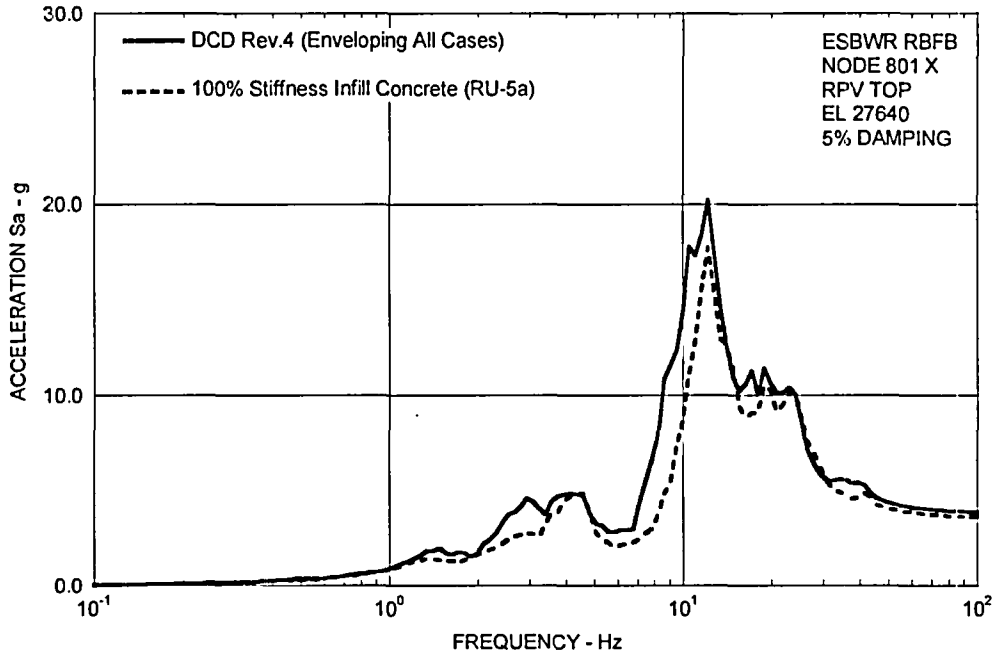

Figure 3.8-41(44) FRS (Comparison of DCD Rev. 4 with 100% Stiffness Infill Concrete) – RPV Top X

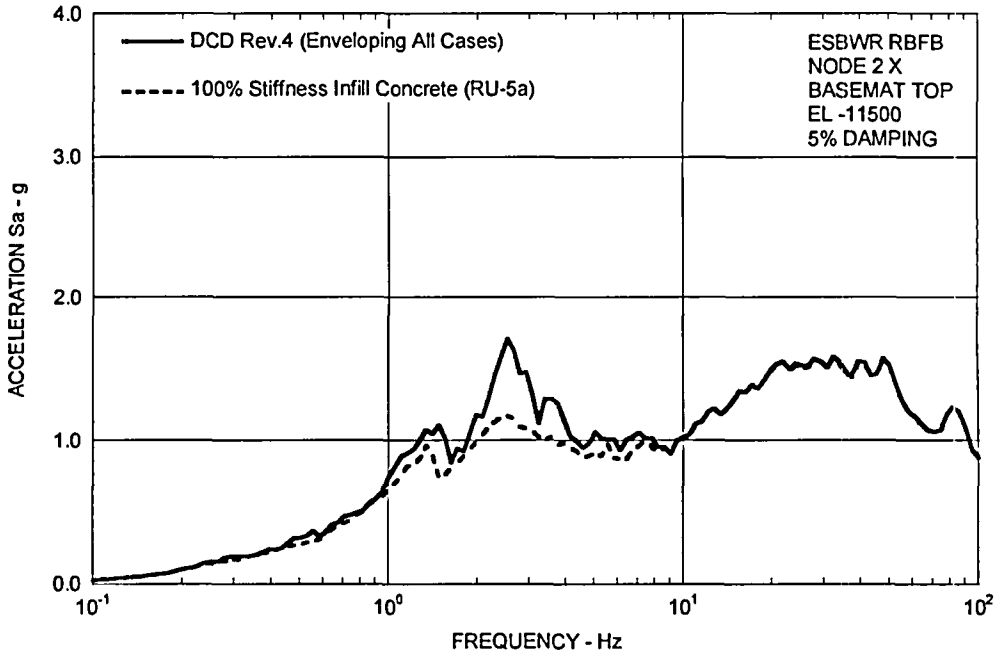

Figure 3.8-41(45) FRS (Comparison of DCD Rev. 4 with 100% Stiffness Infill Concrete) – RB/FB Basemat X

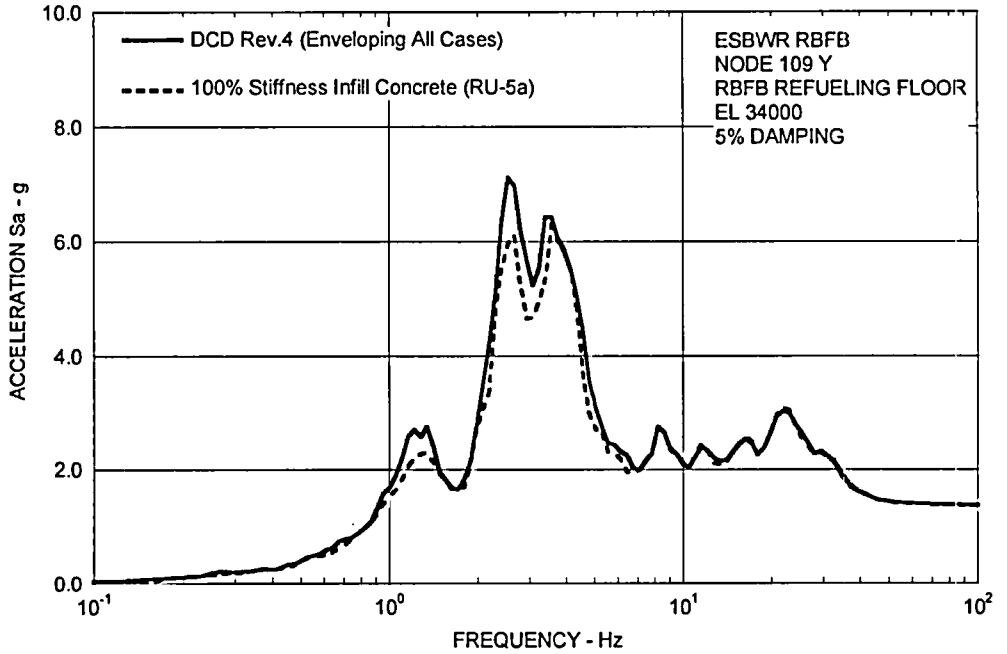

Figure 3.8-41(46) FRS (Comparison of DCD Rev. 4 with 100% Stiffness Infill Concrete) – RB/FB Refueling Floor Y

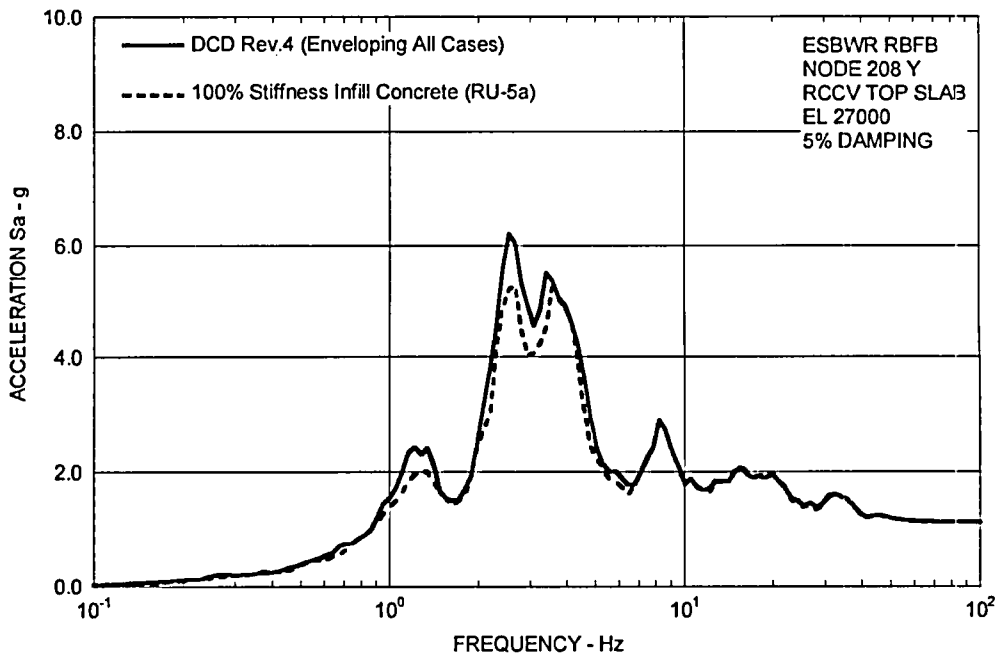

Figure 3.8-41(47) FRS (Comparison of DCD Rev. 4 with 100% Stiffness Infill Concrete) – RCCV Top Slab Y

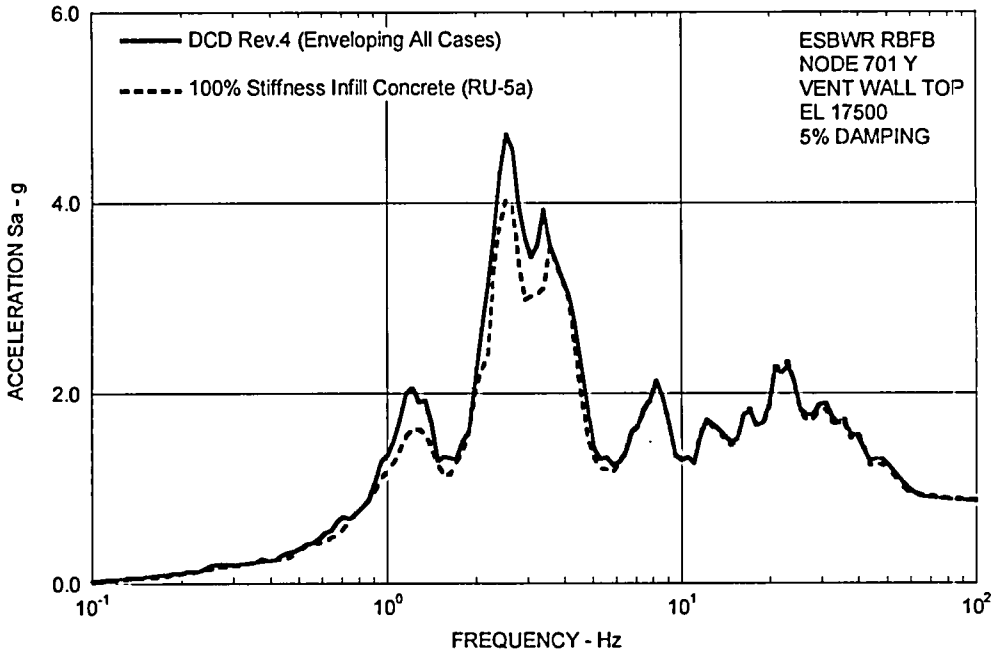

Figure 3.8-41(48) FRS (Comparison of DCD Rev. 4 with 100% Stiffness Infill Concrete) – Vent Wall Top Y

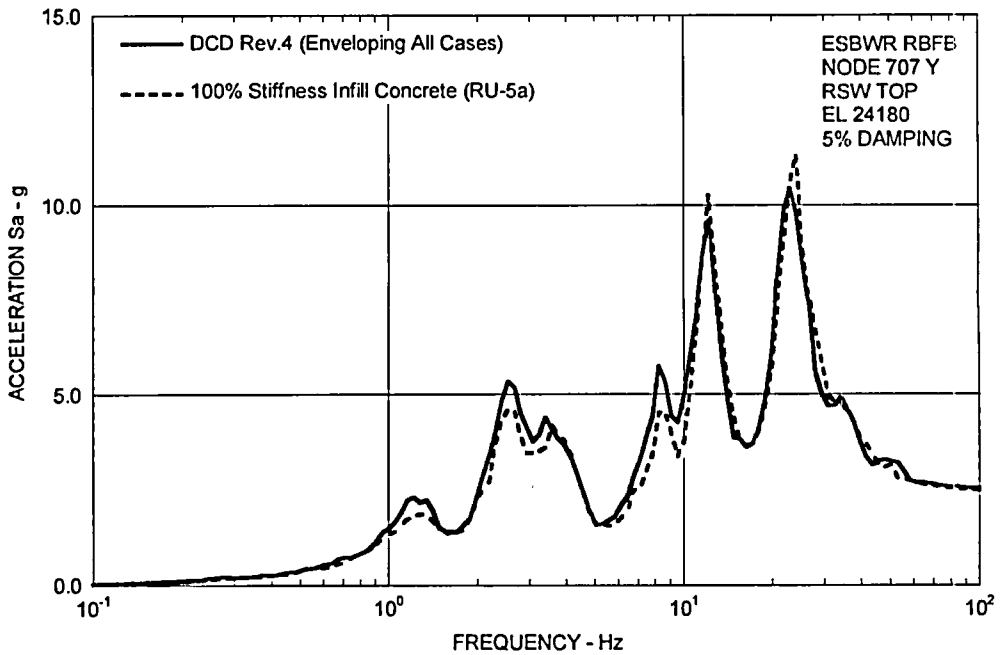

Figure 3.8-41(49) FRS (Comparison of DCD Rev. 4 with 100% Stiffness Infill Concrete) – RSW Top Y

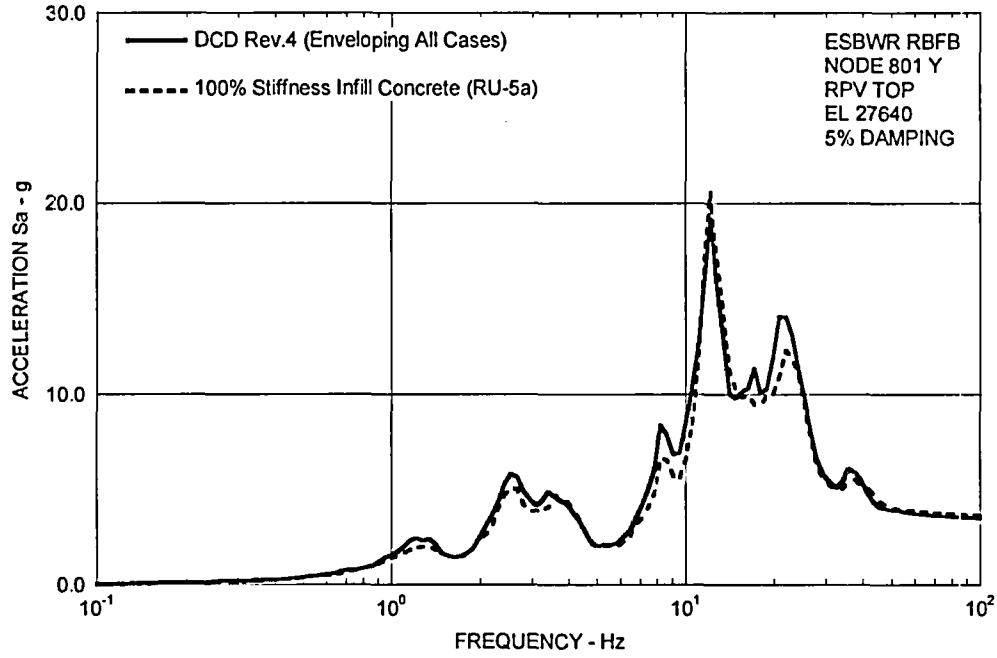

Figure 3.8-41(50) FRS (Comparison of DCD Rev. 4 with 100% Stiffness Infill Concrete) – RPV Top Y

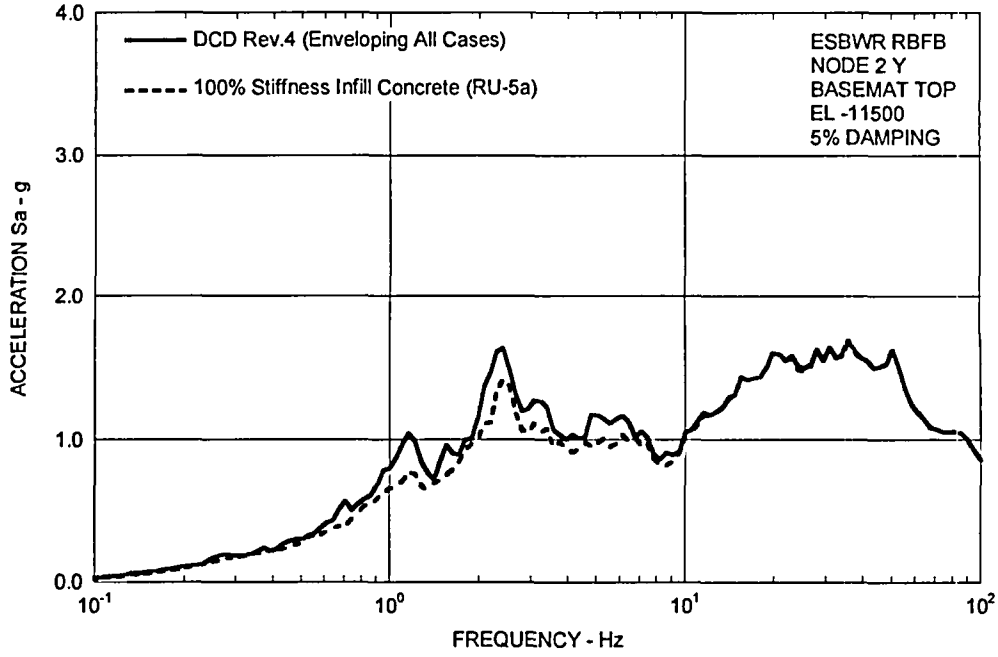

Figure 3.8-41(51) FRS (Comparison of DCD Rev. 4 with 100% Stiffness Infill Concrete) – RB/FB Basemat Y

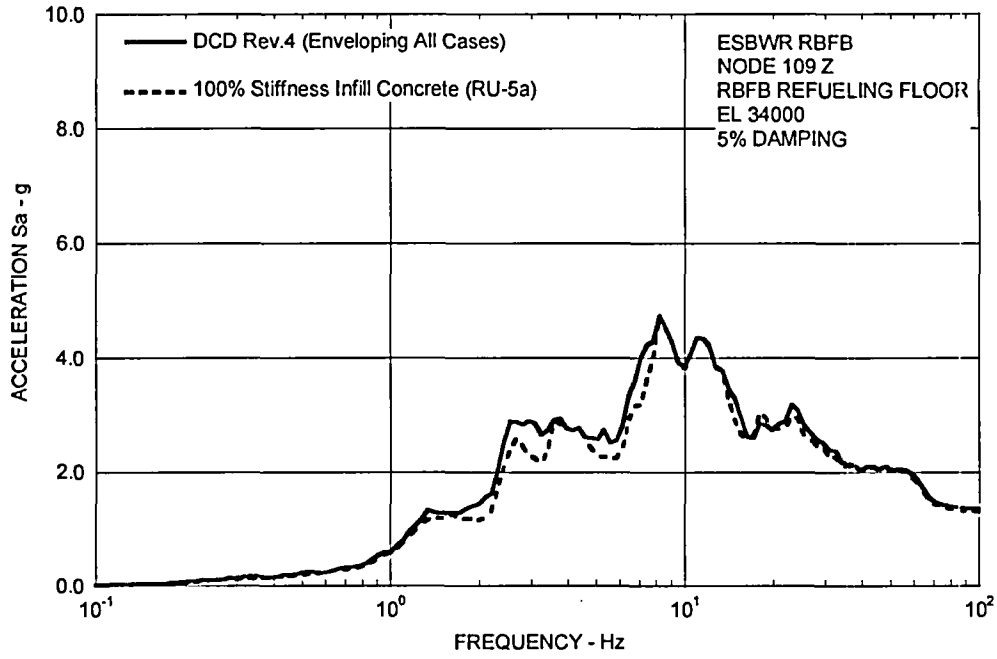

Figure 3.8-41(52) FRS (Comparison of DCD Rev. 4 with 100% Stiffness Infill Concrete) – RB/FB Refueling Floor Z

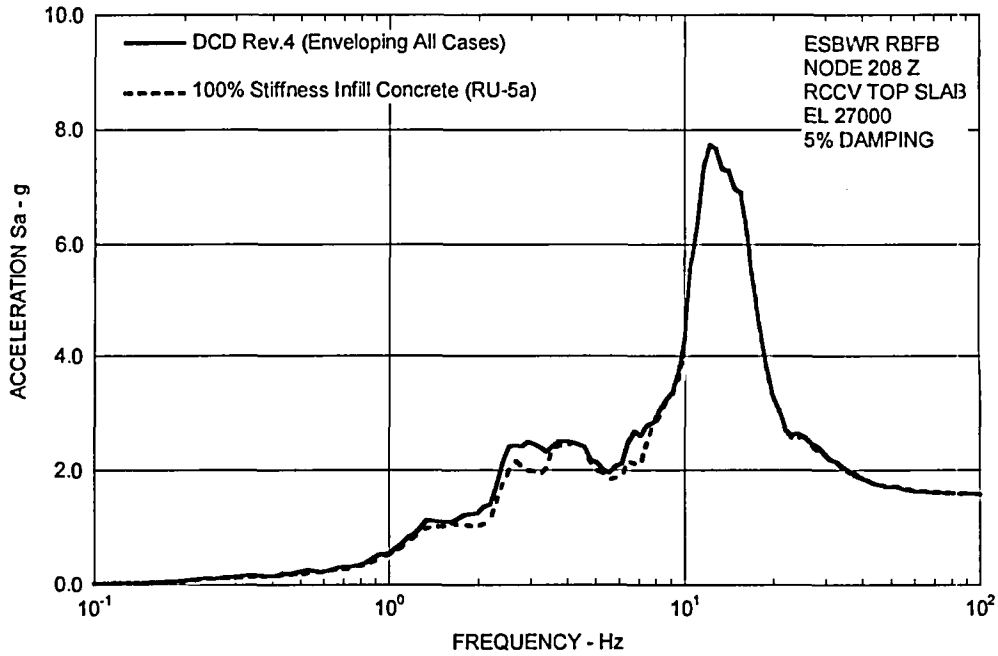

Figure 3.8-41(53) (Comparison of DCD Rev. 4 with 100% Stiffness Infill Concrete) – RCCV Top Slab Z

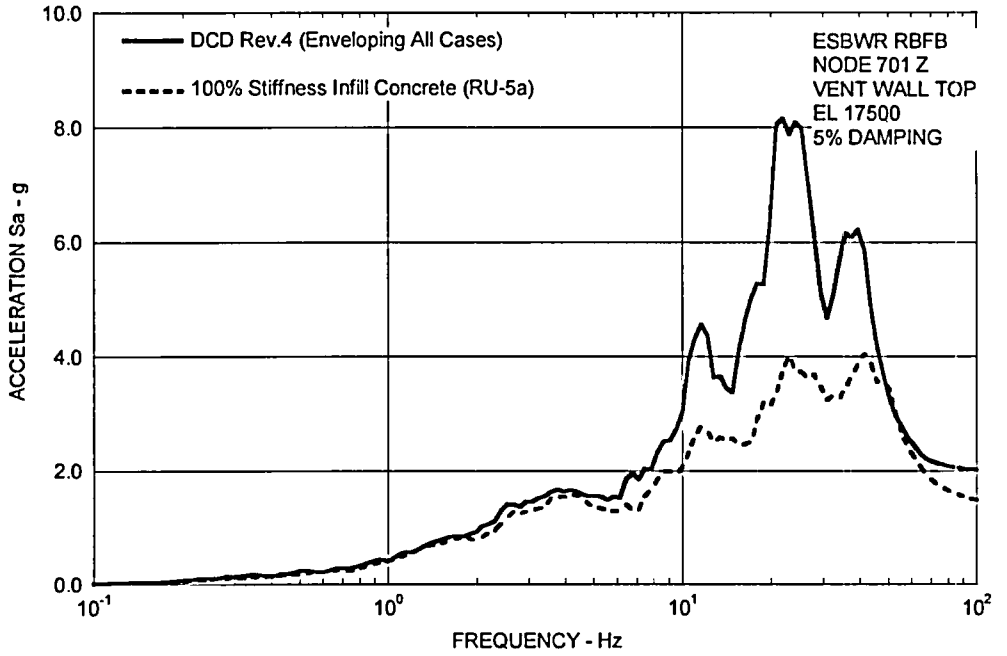

Figure 3.8-41(54) FRS (Comparison of DCD Rev. 4 with 100% Stiffness Infill Concrete) – Vent Wall Top Z

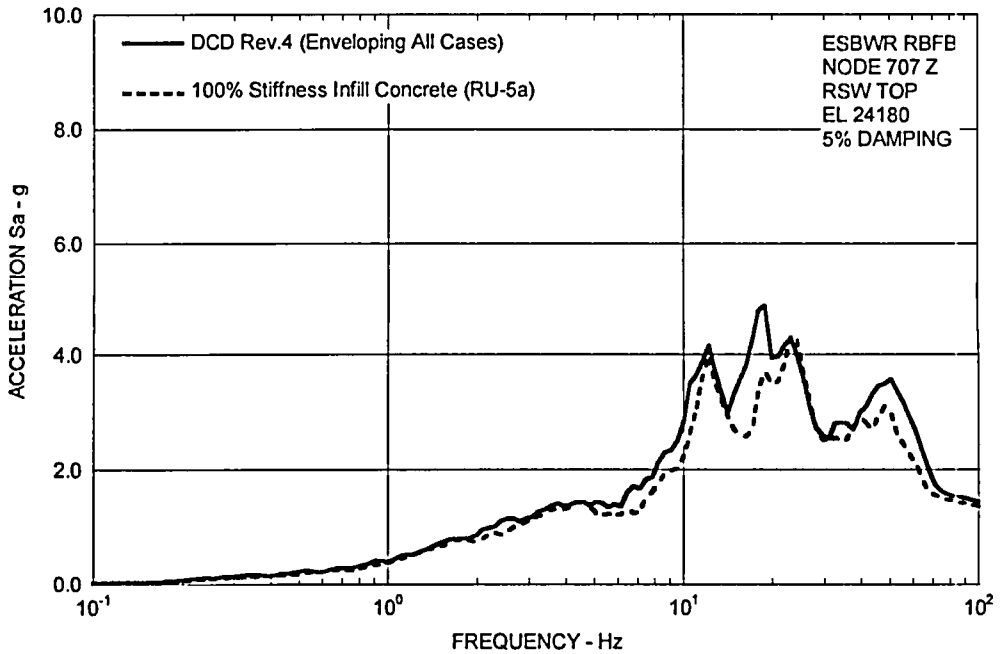

Figure 3.8-41(55) FRS (Comparison of DCD Rev. 4 with 100% Stiffness Infill Concrete) – RSW Top Z

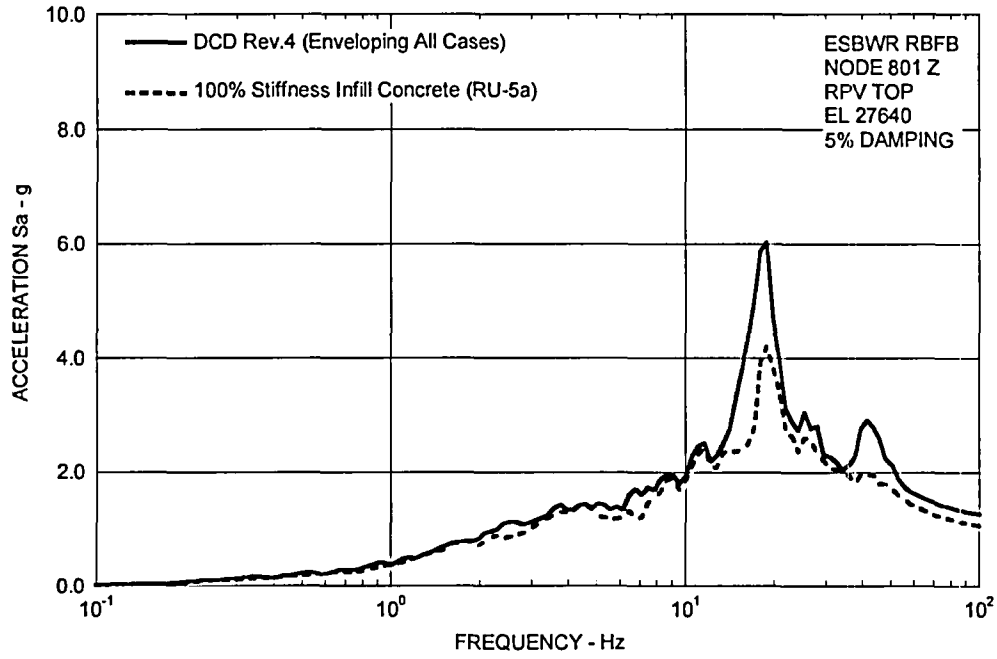

Figure 3.8-41(56) FRS (Comparison of DCD Rev. 4 with 100% Stiffness Infill Concrete) – RPV Top Z

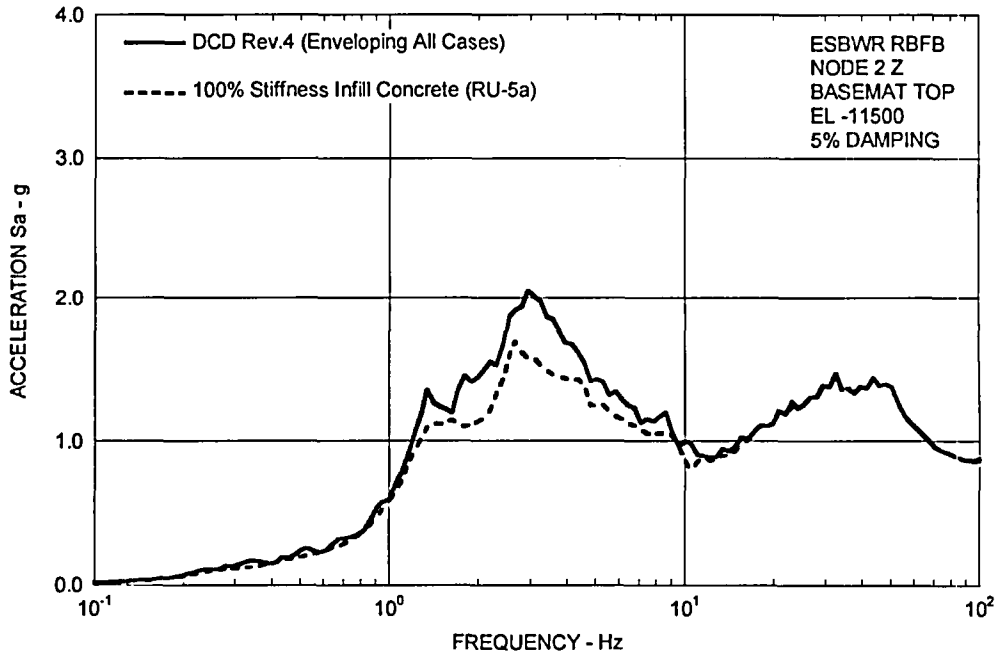

Figure 3.8-41(57) FRS (Comparison of DCD Rev. 4 with 100% Stiffness Infill Concrete) – RB/FB Basemat Z

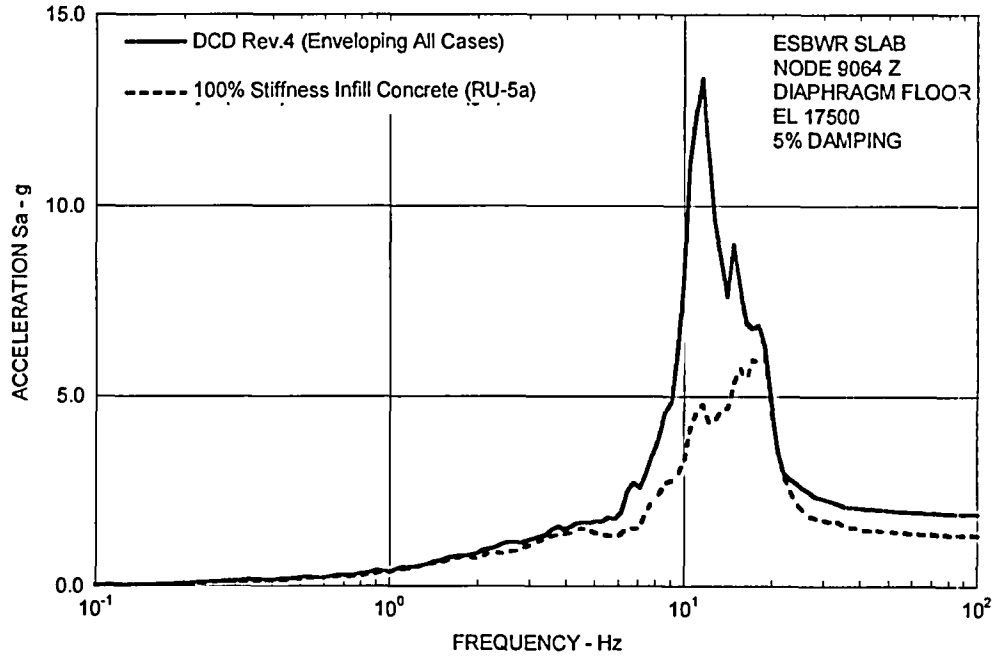

Figure 3.8-41(58) FRS (Comparison of DCD Rev. 4 with 100% Stiffness Infill Concrete) – D/F Oscillator Z

DCD Impact

DCD Tier 2 Subsection 3G.1.5.2.1.13 and Tables 3A.9-1c and 3A.9-1d will be revised in Revision 6 as noted in the attached markups.

NRC RAI 3.8-41, Supplement 6

This RAI relates to the structural analysis and design of the ESBWR using 100 percent of the infill concrete stiffness in the vent wall and diaphragm floor. GEH letter MFN 08-529, dated June 26, 2008, indicated that the response to RAI 3.8-41 Supplement no. 5 was incorporated into DCD Rev. 5 and that no further information is required to complete the RAI response. As discussed during the NRC audit at GEH office the week of June 23, 2008, the following items still need to be addressed:

(a) GEH indicated during the audit that the changes that will be considered in the final design calculation are: (1) consideration of the 100 percent infill concrete, (2) consideration of the revised containment thermal DBA time history (identified in RAI 6.2-180 S01), and (3) widening of the buffer pool gate. GEH also indicated that revisions to DCD Appendix 3G resulting from these changes will not be submitted for review as part of the design certification, but will be performed as part of the detailed design phase. The Design Summary Report and supporting calculations will be prepared to reflect these changes. The staff notes that the introductory paragraph in Appendix 3G of DCD Rev. 5 states that "The final design details, and hence final component stresses may be different from those reported here but they will meet the structural acceptance criteria presented in Section 3.8 in accordance with Tier 1 ITAACs in Tables 2.16.5-2, 2.16.6-2, and 2.16.7-2." Since the three changes listed above may affect the design results, and GEH does not plan to incorporate the changes in the DCD, GEH is requested to (1) identify in the DCD the reported results that did not consider the three changes listed above, (2) perform a quantitative evaluation to demonstrate that structural design will not be affected due to these changes, and (3) include a note in the DCD to state that a quantitative evaluation was performed to conclude that final design will not be affected by the changes.

(b) GEH is requested to clarify whether the introductory paragraph in Appendix 3G of DCD Rev. 5 (quoted in part (a) above) is intended to mean that the final design details, and hence final component stresses, may be different from those reported here but they will meet the structural acceptance criteria presented in Section 3.8 and in Tier 1 ITAACs in Tables 2.16.5-2, 2.16.6-2, and 2.16.7-2? If so, then this clarification should be reflected in the DCD.

GEH Response

(a) To address the request for identifying the DCD reported results that do not consider the three changes, performing a quantitative evaluation to demonstrate that the structural design is not affected by the changes, and including a note in the DCD to summarize this evaluation and its conclusion, GEH has incorporated the changes in the structural analyses as required to confirm their effect on the structural design and the results of the analyses are incorporated in the DCD as detailed below.

(1) Reported results that consider the 100 percent infill concrete case, the revised containment thermal DBA time history and the widening of the buffer pool gate are being included in all appropriate portions of the DCD in Revisions 5 and 6. The DCD

portions related to the 100 percent infill concrete case are included in GEH's response to NRC RAI 3.8-41, Supplement 5, transmitted to the NRC on November 6, 2008 via MFN 06-191 Supplement 9. The DCD portions related to the revised containment thermal DBA time history will be included in GEH's response to NRC RAI 6.2-180, Supplement 1. The DCD portions related to the widening of the buffer pool gate are included in GEH's response to NRC RAI 3.8-41, Supplement 6, Item (a) (2) below.

(2) The quantitative structural evaluation for the 100 percent infill concrete case is included in GEH's response to NRC RAI 3.8-41, Supplement 5, transmitted to the NRC on November 6, 2008 via MFN 06-191 Supplement 9. The quantitative evaluation for the revised containment thermal DBA time history will be included in GEH's response to NRC RAI 6.2-180, Supplement 1.

To evaluate the potential impact of the widening of the buffer pool gate on the design, the following analysis is performed using the updated global finite element (FE) model shown in Figure 3.8-41(59) in which elements associated with the buffer pool gate and adjacent elements in the RCCV top slab have been modified and compared to the DCD Revision 5 FE model. The accident pressure and accident temperature are the most critical loads in these regions and the following loads are analyzed to compare the element force distributions on the RCCV top slab, pool girder and walls:

- Pressure Load: Dry Well Unit Load (1 MPa)
- Thermal Load: LOCA after 72 hours; Winter

Figures 3.8-41(60) through 3.8-41(75) show the element force distributions of the RCCV top slab, pool girder and walls for the pressure load case, and Figures 3.8-41(76) through 3.8-41(91) show those for the thermal load case. The coordinate system for element forces and moments is shown in Figure 3.8-41(92).

As for the thermal load, the element force distributions of all components are almost the same for both models. As for the pressure load, however, the element forces of the 'My' bending moment component around the drywell head opening increase about 20 percent from the DCD Revision 5 element forces as shown in Figure 3.8-41(64). The existing stress margins, which are the ratio of the calculated stress to the allowable stress, in accordance with DCD Tier 2 Tables 3G.1-10 and 3G.1-11 are not sufficient to accommodate the increased accident pressure stress. Therefore, additional bars (1-#14@600) will be added locally and DCD Tier 2 Figure 3G.1-44 will be revised accordingly.

In addition to the RCCV top slab, the equipment storage pool gate and buffer pool gate wall thicknesses need to be increased from 1.3m to 1.6m, and their rebar arrangements need to be changed as shown as Table 3.8-41(10). DCD Tier 1 Table 2.16.5-1 and DCD Tier 2 Figures 3G.1-4 through 3G.1-6, and 3G.1-46 will be revised accordingly.

(3) Please see GEH's response to NRC RAI 3.8-41, Supplement 6, Items (a) (1) and (a) (2) above. Reported results that consider the 100 percent infill concrete case, the revised containment thermal DBA time history and the widening of the buffer pool gate are

being included in all appropriate portions of the DCD in Revisions 5 and 6 which demonstrate that the final design will not be affected by the changes.

(b) The last sentence of the introductory paragraph in DCD Tier 2 Appendix 3G will be revised in Revision 6 to read "The final design details will meet the structural acceptance criteria presented in Section 3.8 and in Tier 1 ITAACs in Tables 2.16.5-2, 2.16.6-2, and 2.16.7-2".

Table 3.8-41(10) Rebar Arrangements of Pool Gate Wall

	Buffer Pool Side			Equipment Storage Pool Side		
	Thickness (m)	Horizontal (EF)	Vertical (EF)	Thickness (m)	Horizontal (EF)	Vertical (EF)
DCD Rev.5	1.3	1-#11@200 +1-#11@400	1-#11@200 +1-#11@400	1.3	1-#11@200 +1-#11@400	1-#11@200 +1-#11@400
Modified	1.6	3-#11@200	3-#11@200	1.6	2-#11@200	2-#11@200

*EF: Each Face

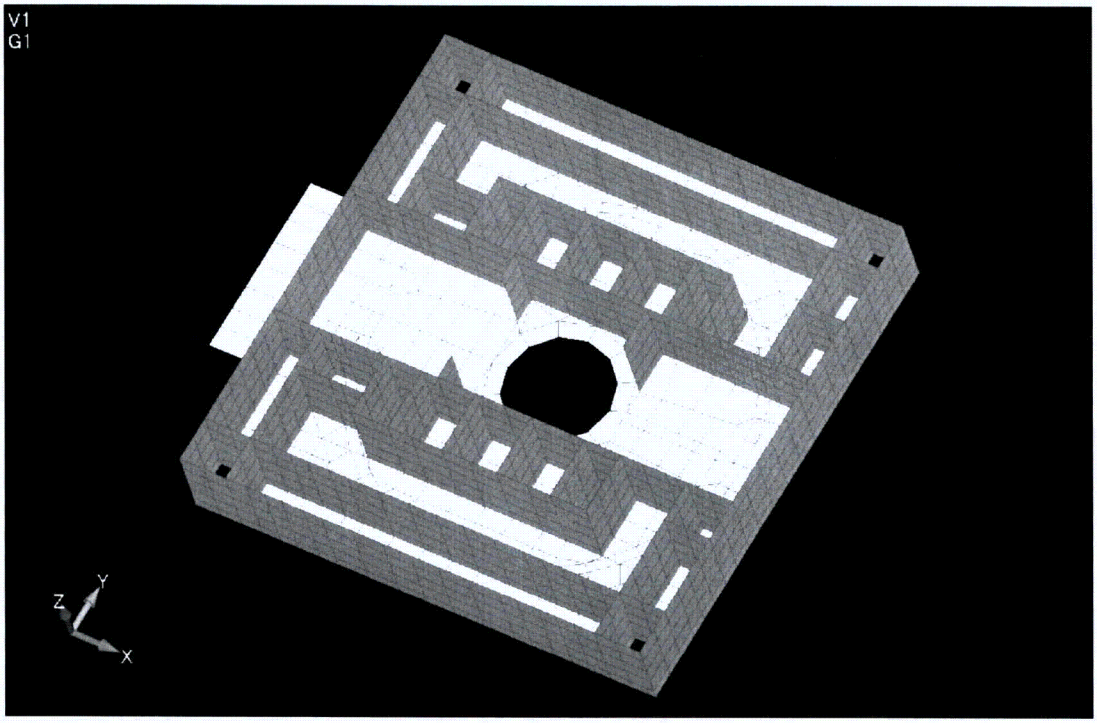

Updated FE Model

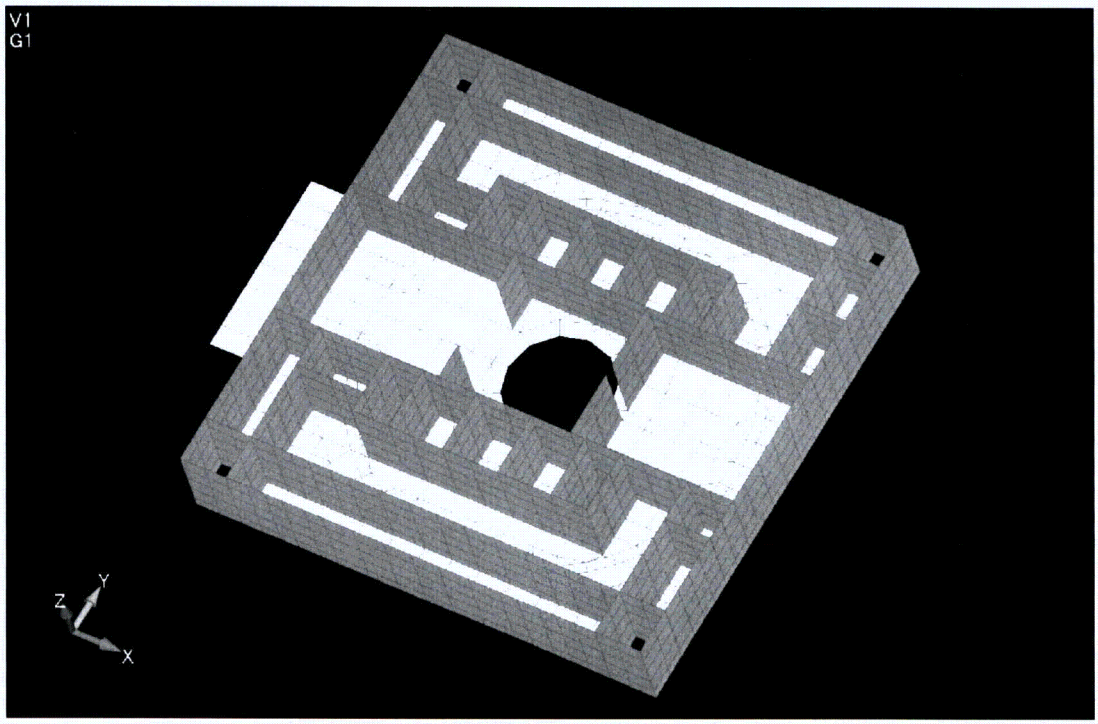

DCD Revision 5 FE Model

Figure 3.8-41(59) Comparison of the FE Model

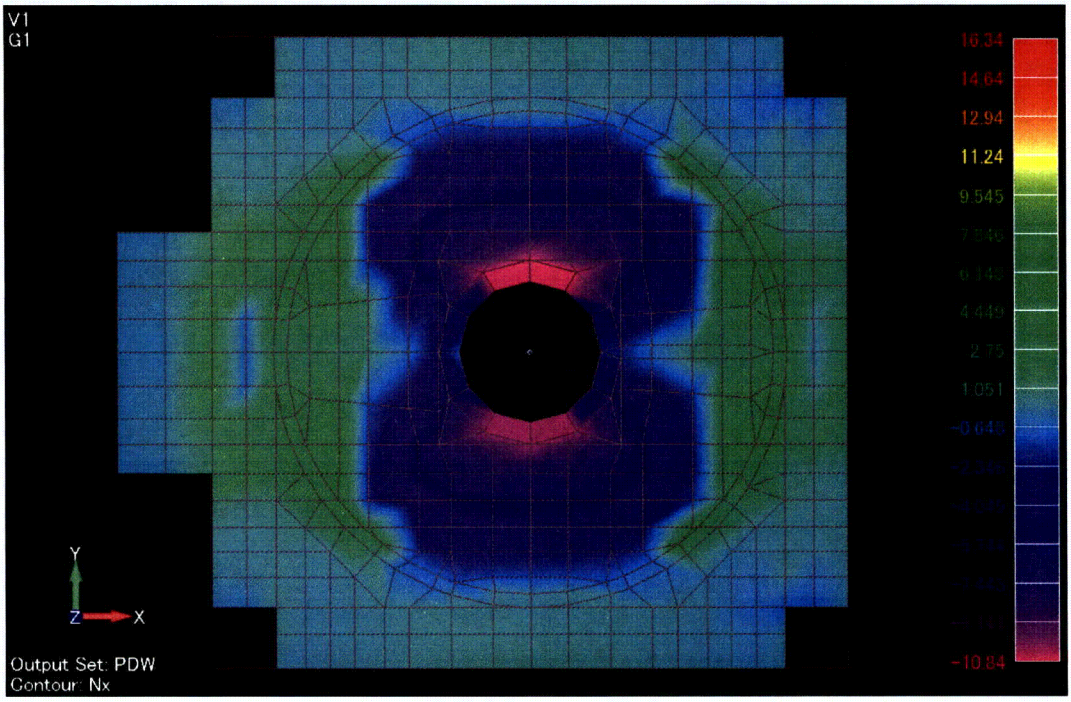

Updated FE Model

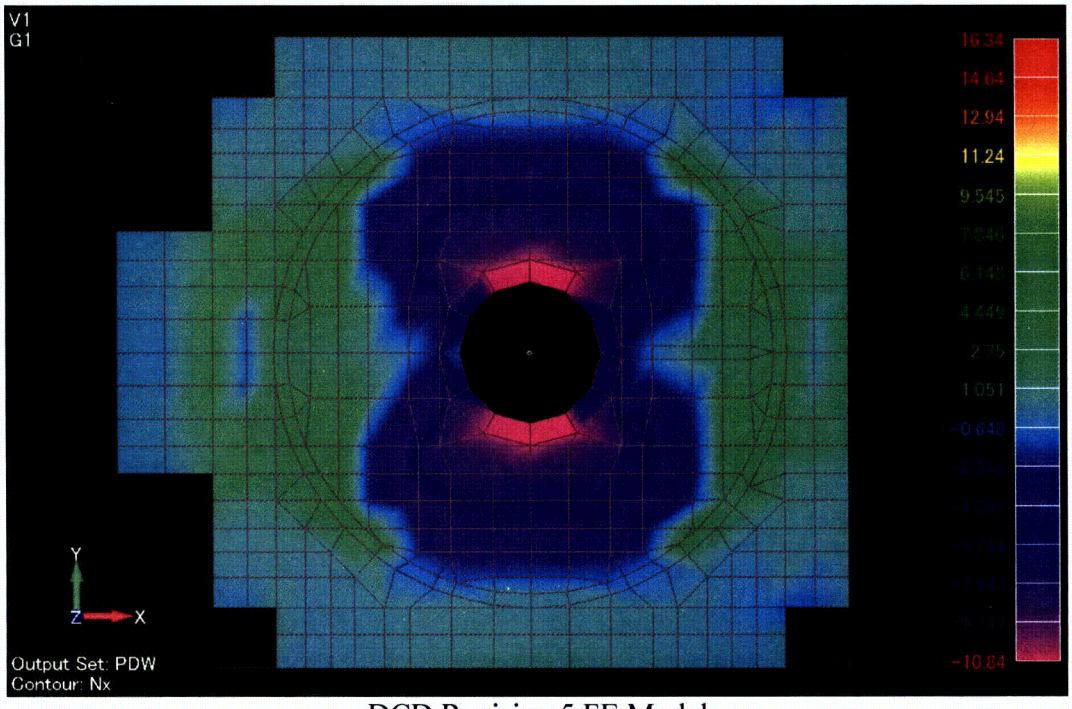

DCD Revision 5 FE Model

[Membrane Force: Nx]

Figure 3.8-41(60) Comparison of Element Force Distribution on RCCV Top Slab (Pressure)

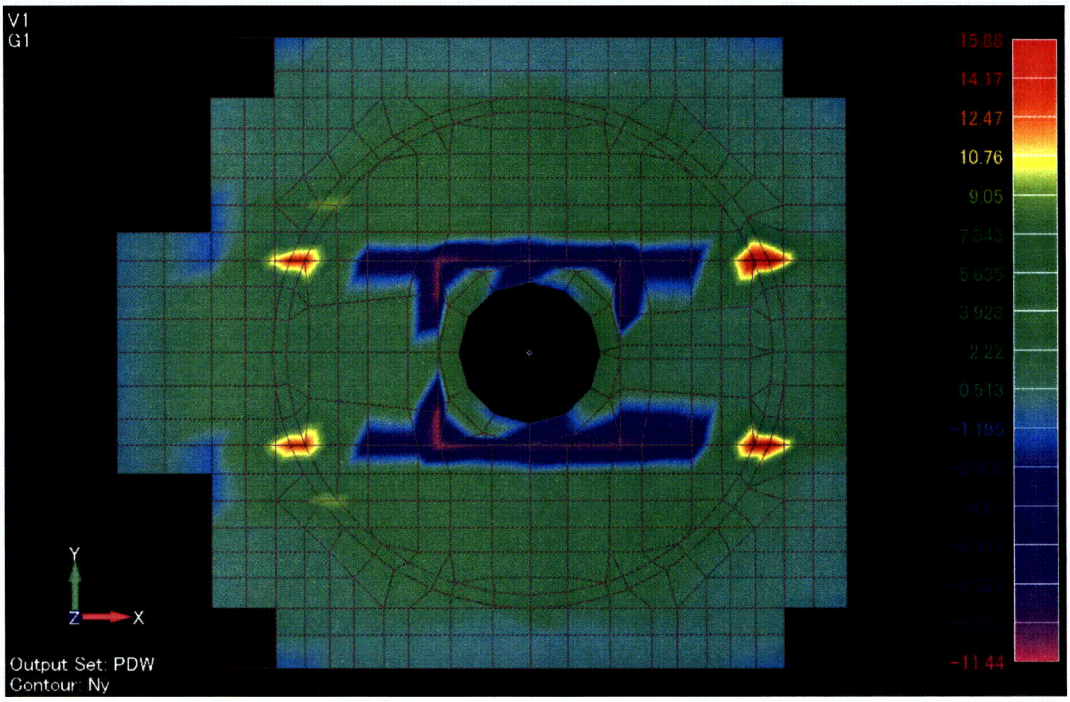

Updated FE Model

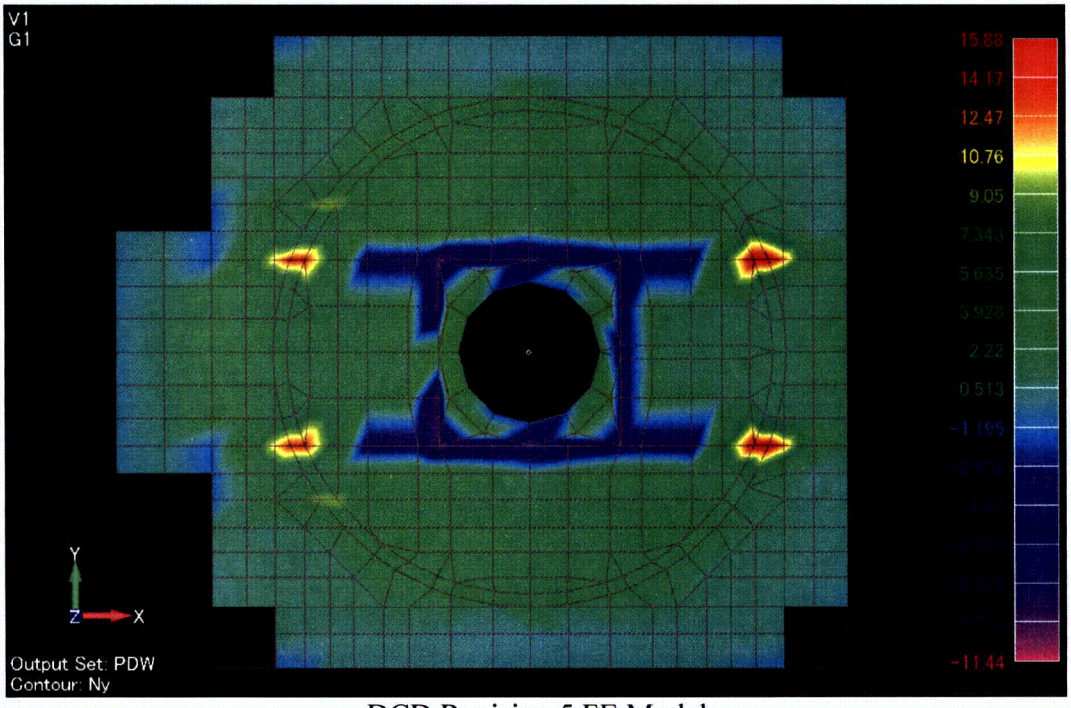

DCD Revision 5 FE Model

[Membrane Force: Ny]

Figure 3.8-41(61) Comparison of Element Force Distribution on RCCV Top Slab (Pressure)

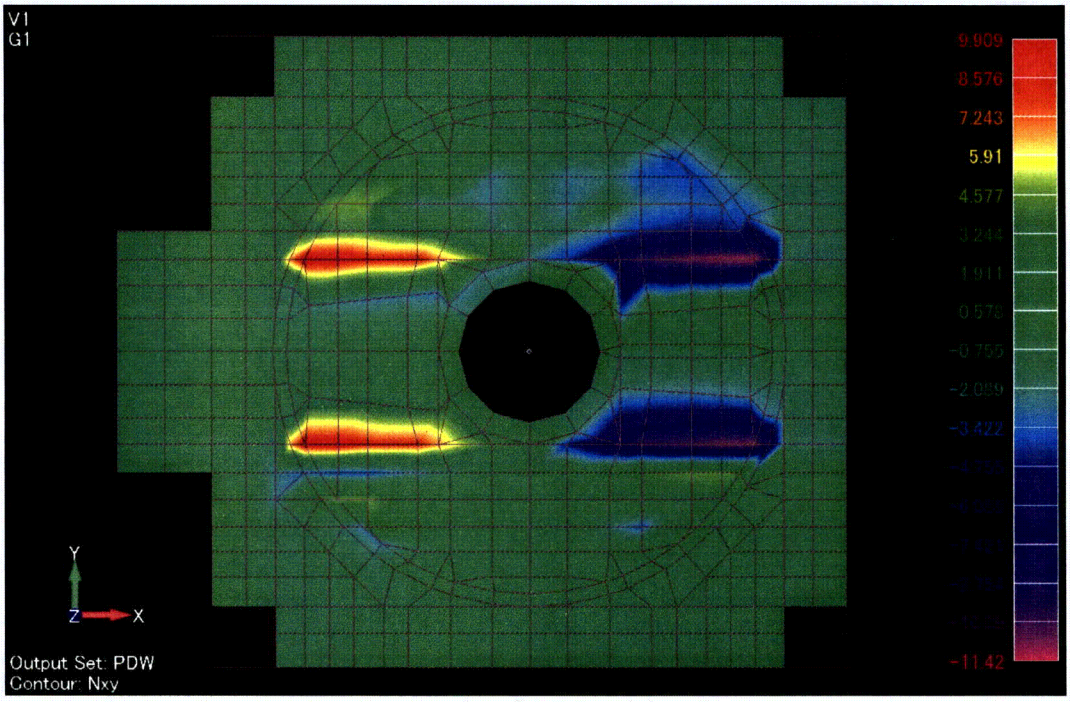

Updated FE Model

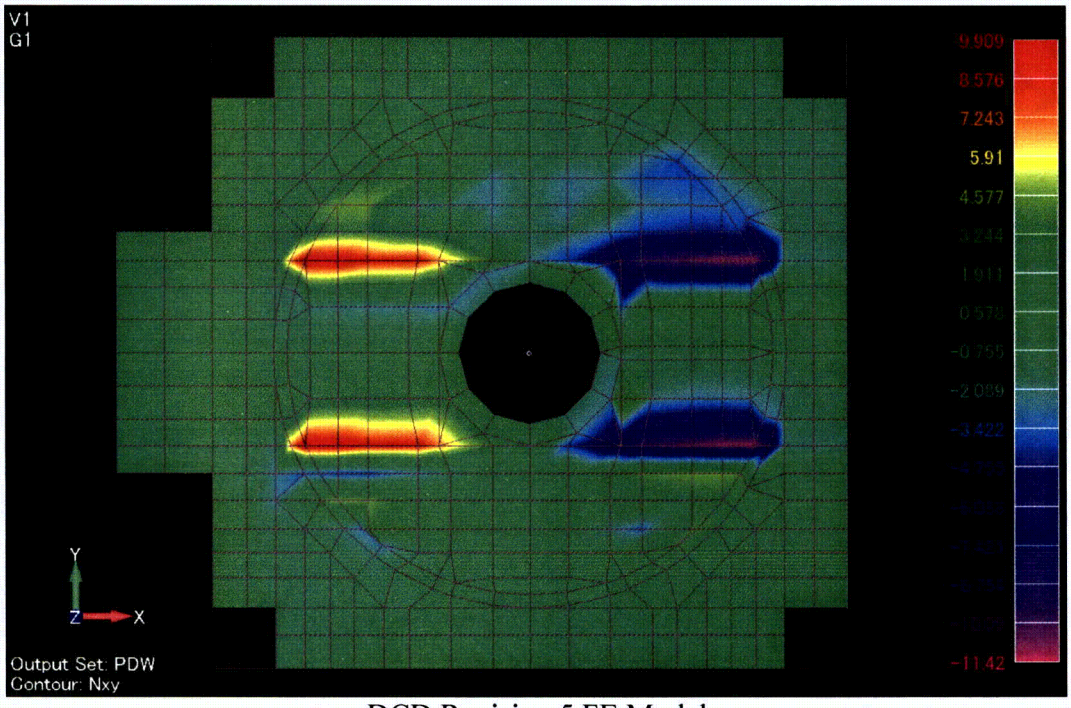

DCD Revision 5 FE Model

[Membrane Force: Nxy]

Figure 3.8-41(62) Comparison of Element Force Distribution on RCCV Top Slab (Pressure)

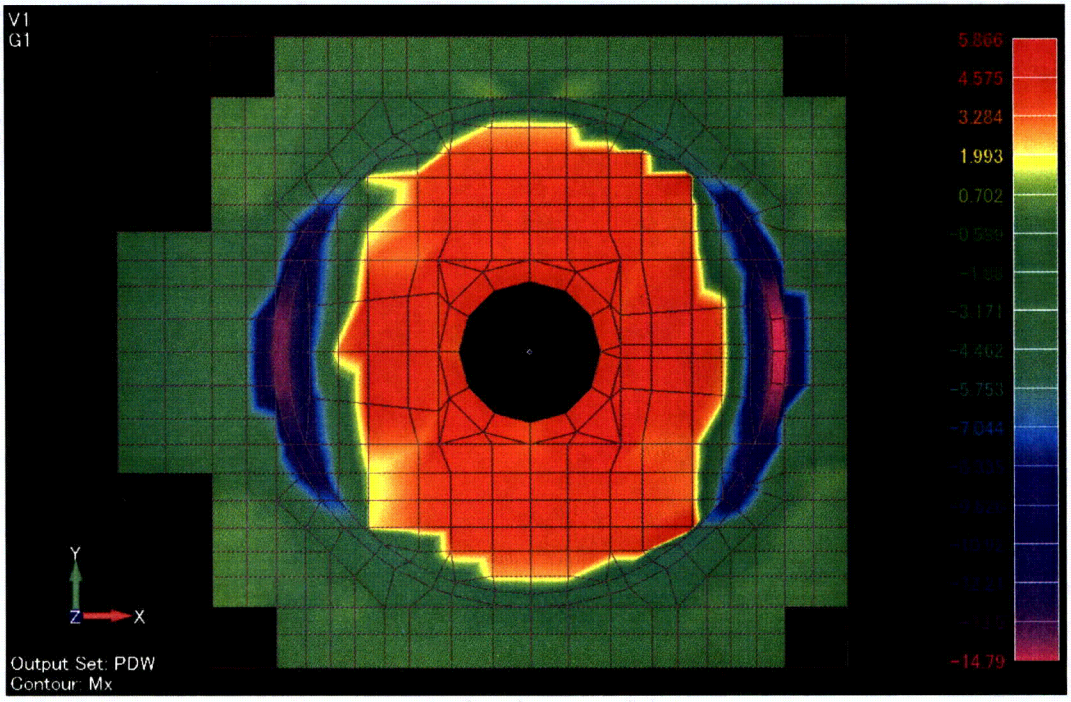

Updated FE Model

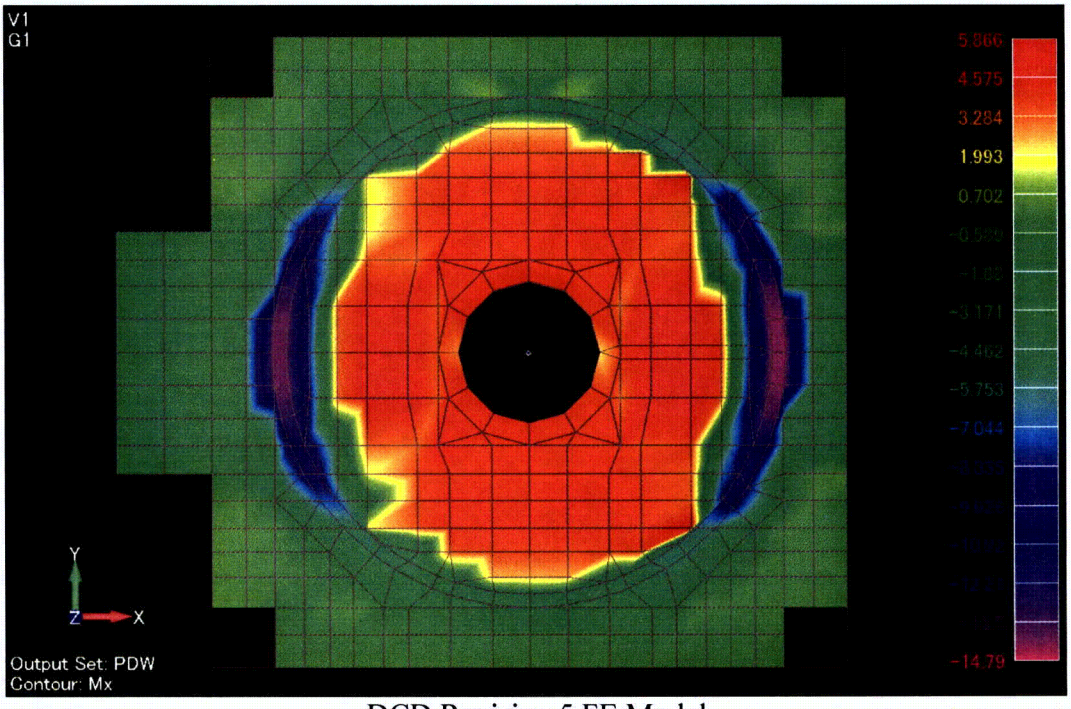

DCD Revision 5 FE Model

[Bending Moment: Mx]

Figure 3.8-41(63) Comparison of Element Force Distribution on RCCV Top Slab (Pressure)

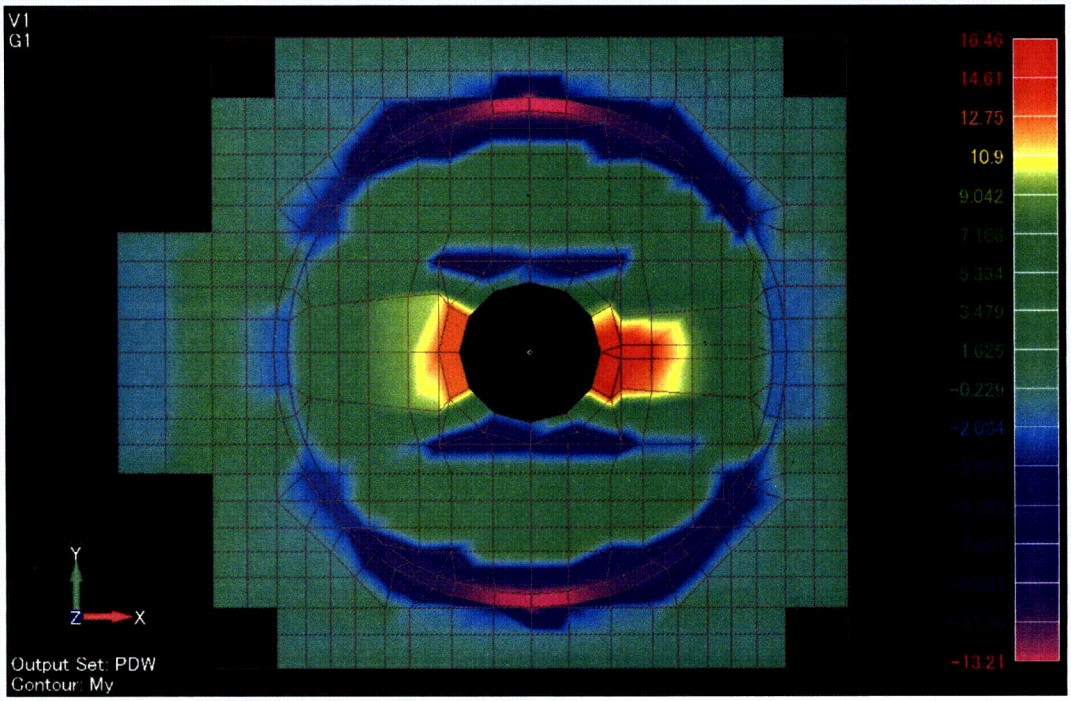

Updated FE Model

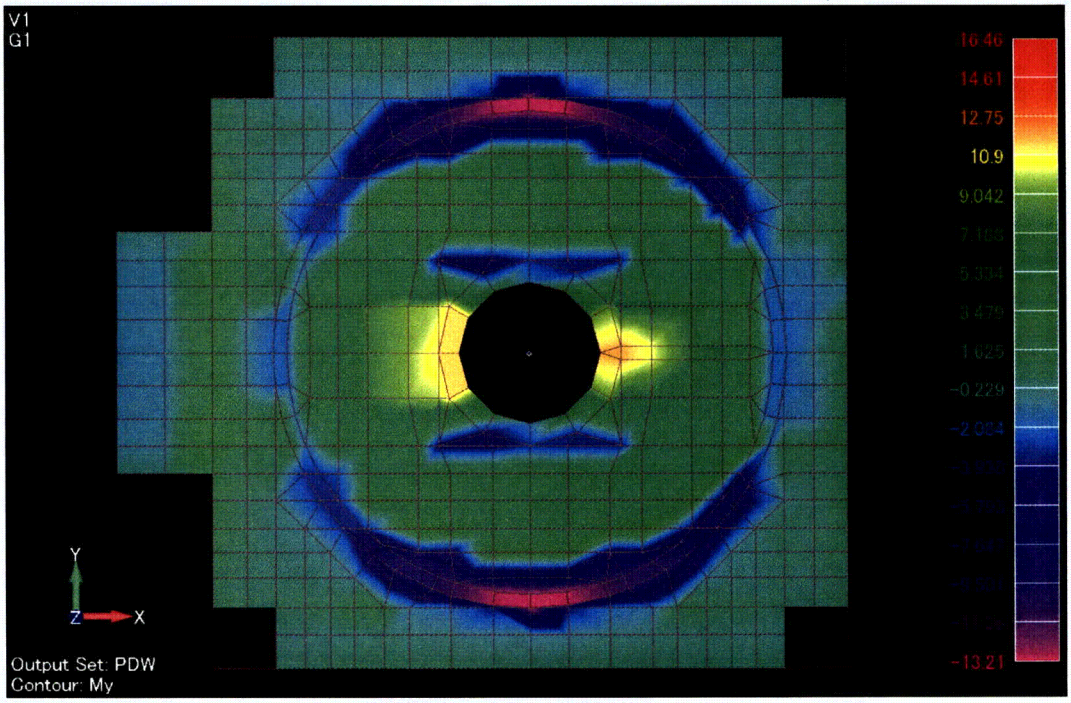

DCD Revision 5 FE Model

[Bending Moment: My]

Figure 3.8-41(64) Comparison of Element Force Distribution on RCCV Top Slab (Pressure)

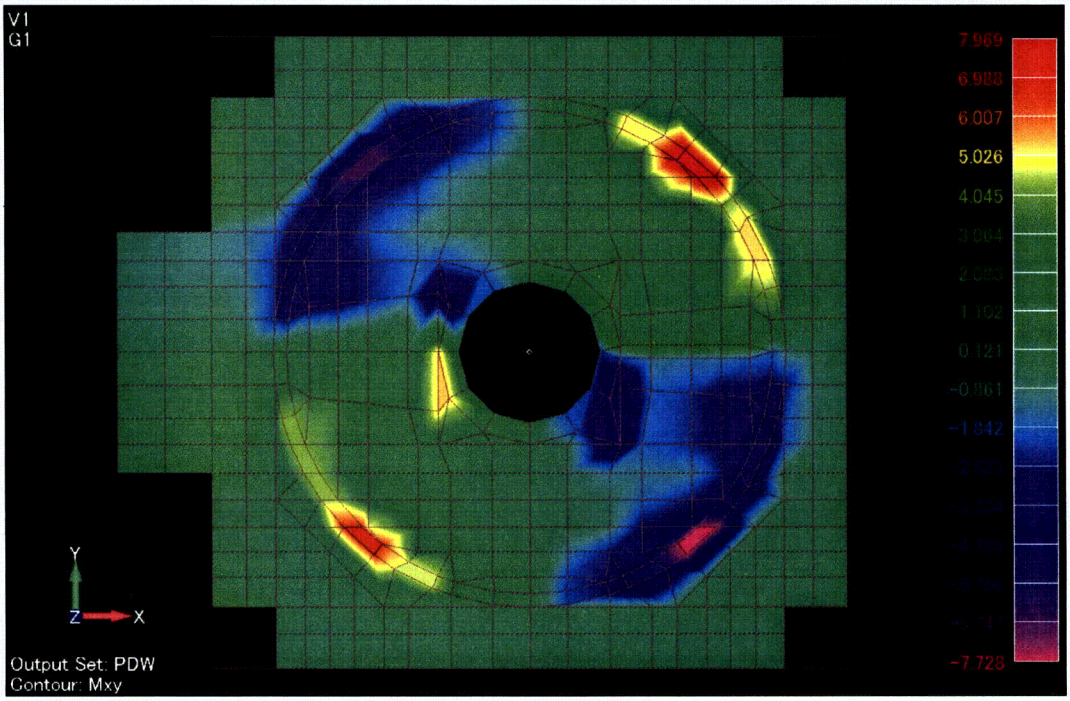

Updated FE Model

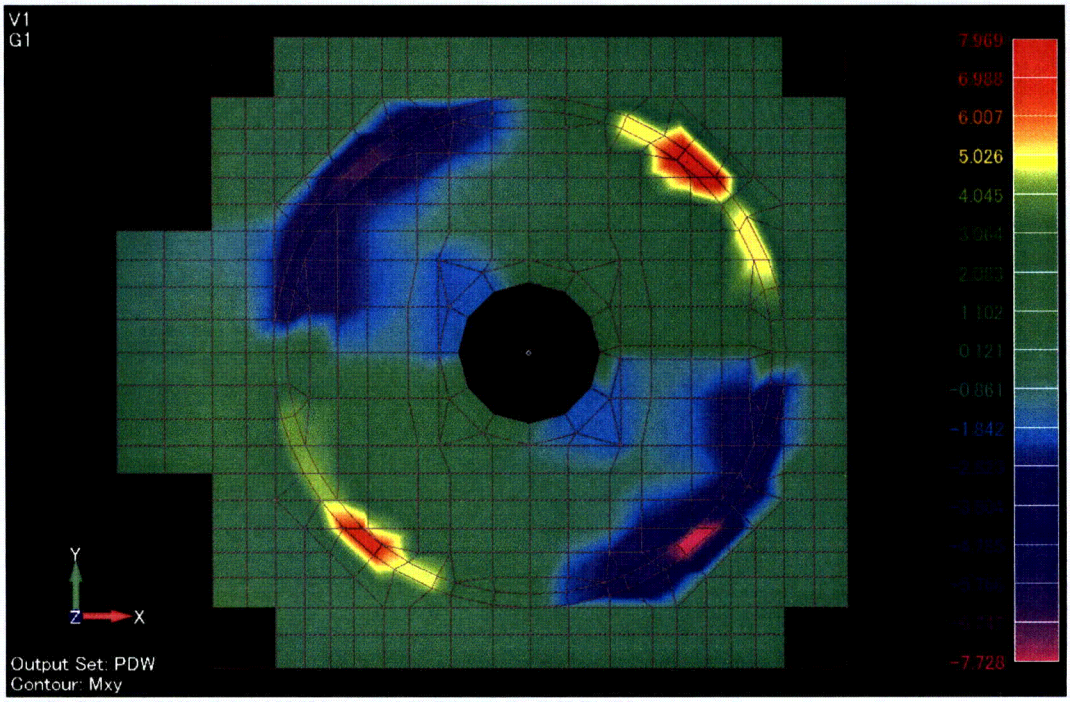

DCD Revision 5 FE Model

[Bending Moment: Mxy]

Figure 3.8-41(65) Comparison of Element Force Distribution on RCCV Top Slab (Pressure)

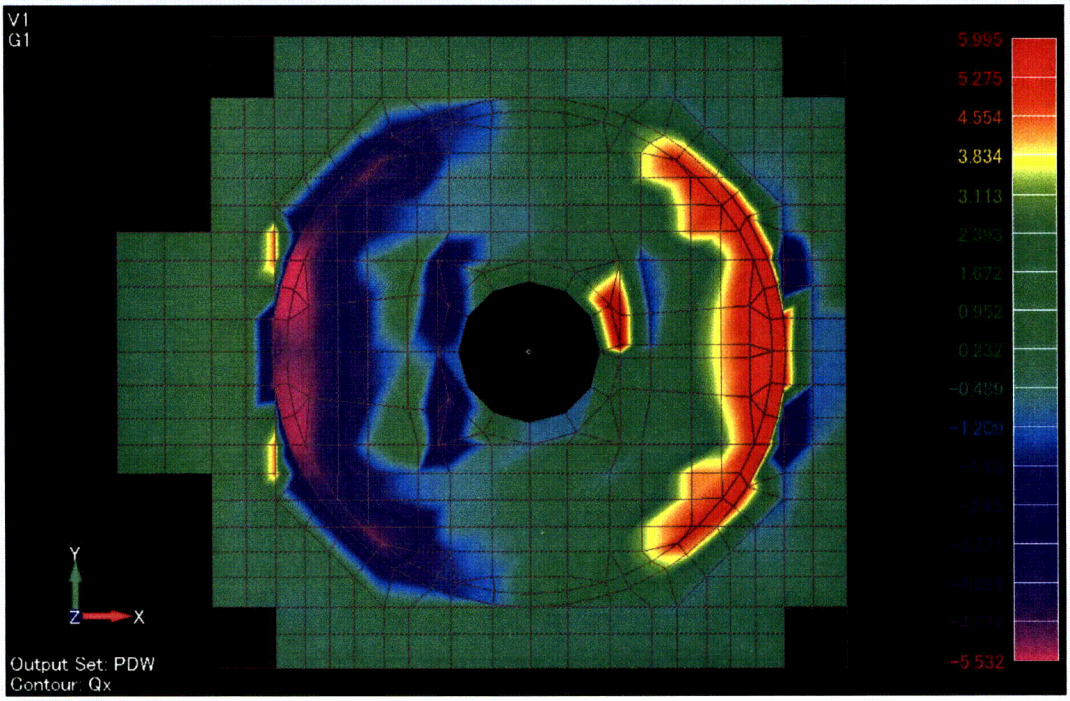

Updated FE Model

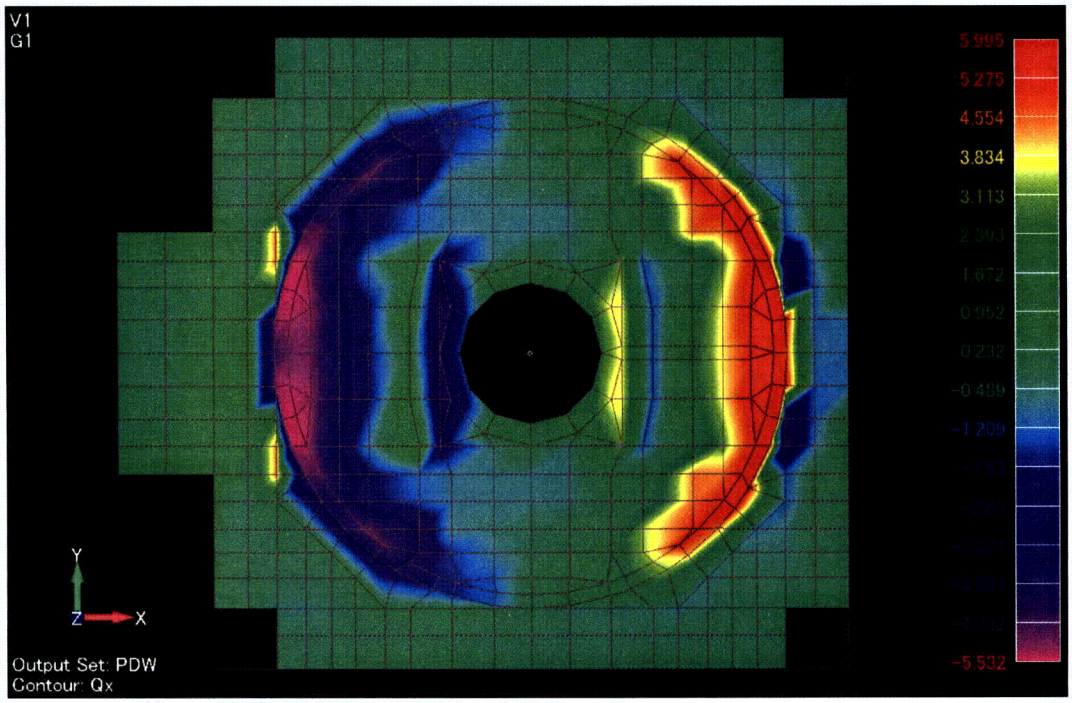

DCD Revision 5 FE Model

[Transverse Shear: Qx]

Figure 3.8-41(66) Comparison of Element Force Distribution on RCCV Top Slab (Pressure)

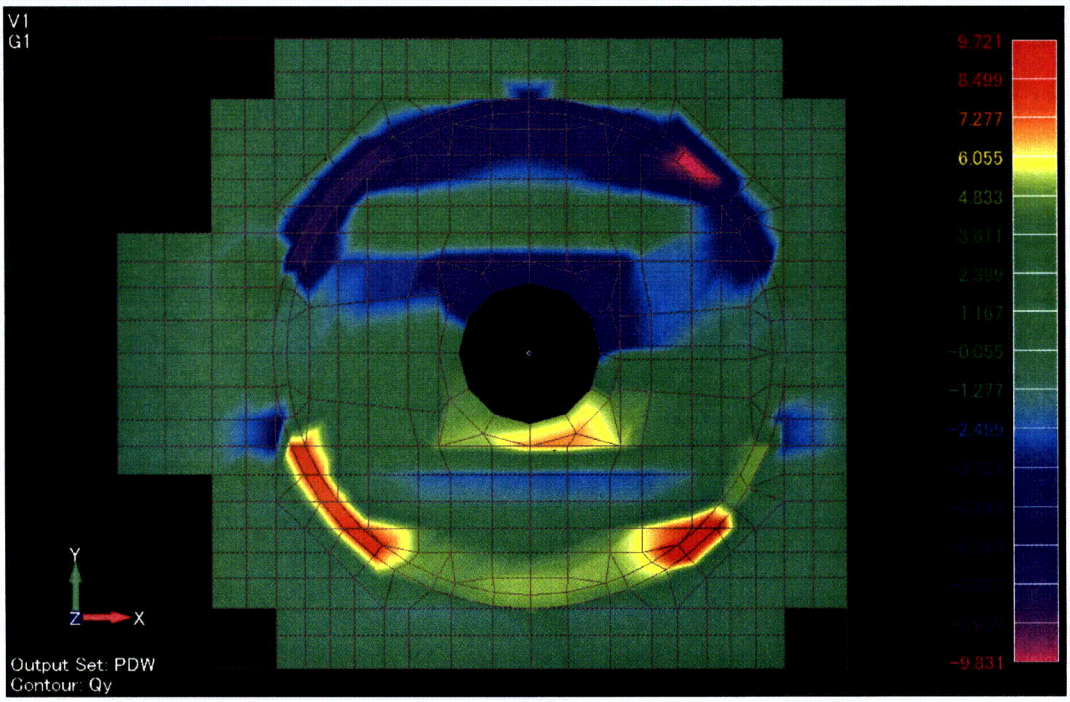

Updated FE Model

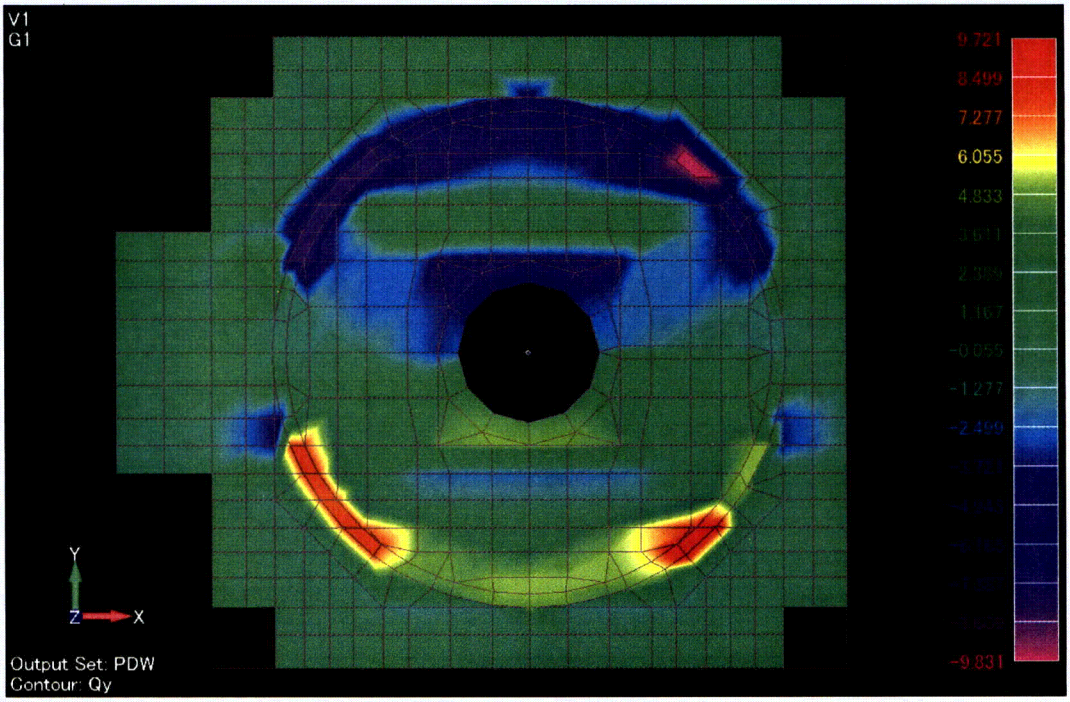

DCD Revision 5 FE Model

[Transverse Shear: Qy]

Figure 3.8-41(67) Comparison of Element Force Distribution on RCCV Top Slab (Pressure)

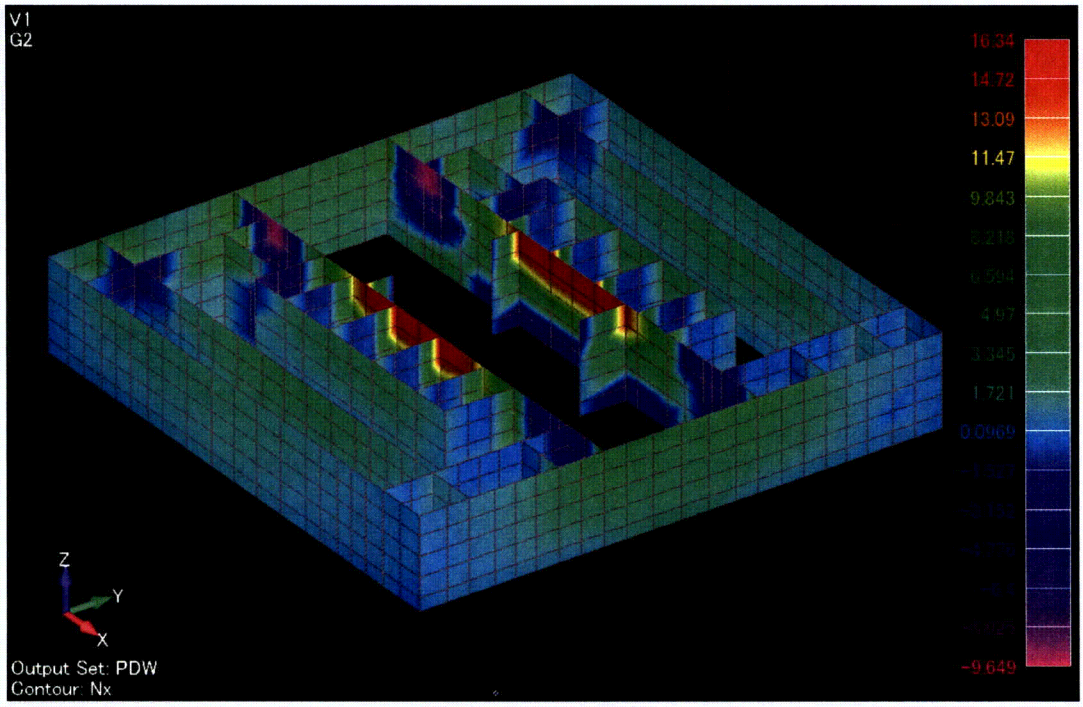

Updated FE Model

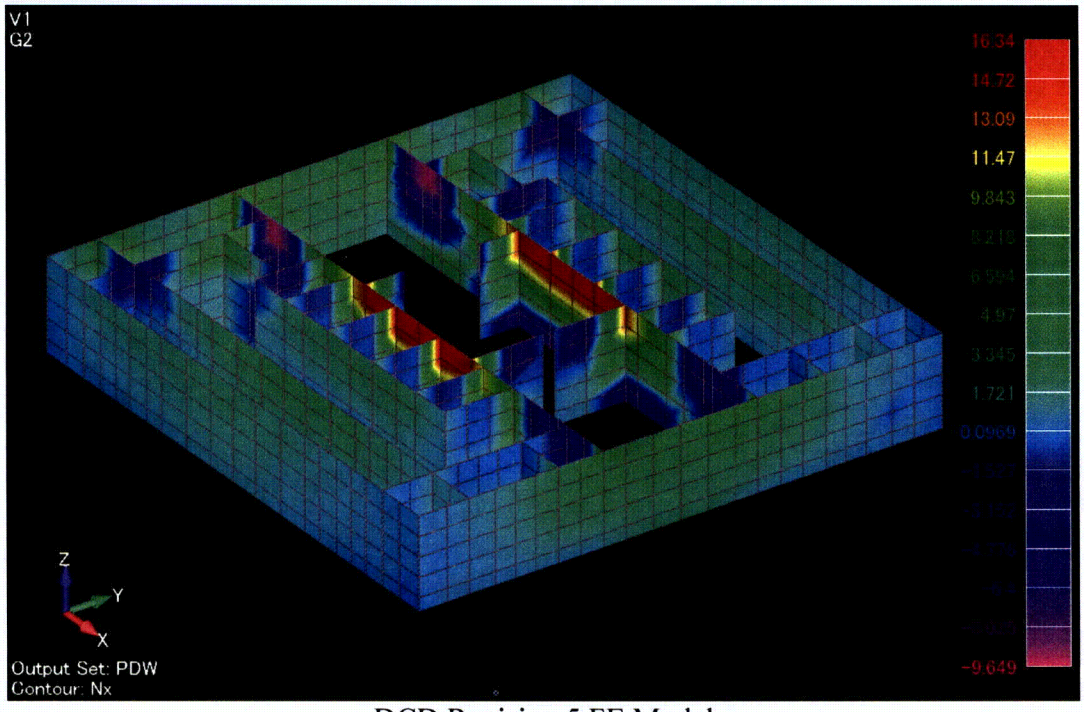

DCD Revision 5 FE Model

[Membrane Force: Nx]

Figure 3.8-41(68) Comparison of Element Force Distribution on Pool Girder and Wall (Pressure)

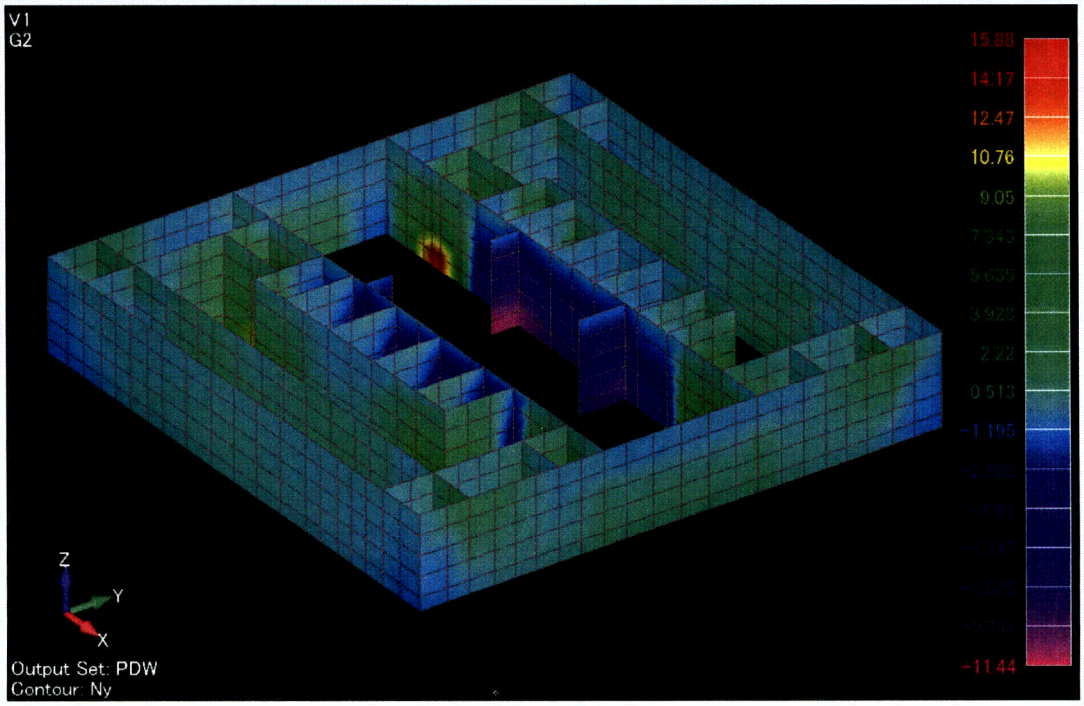

Updated FE Model

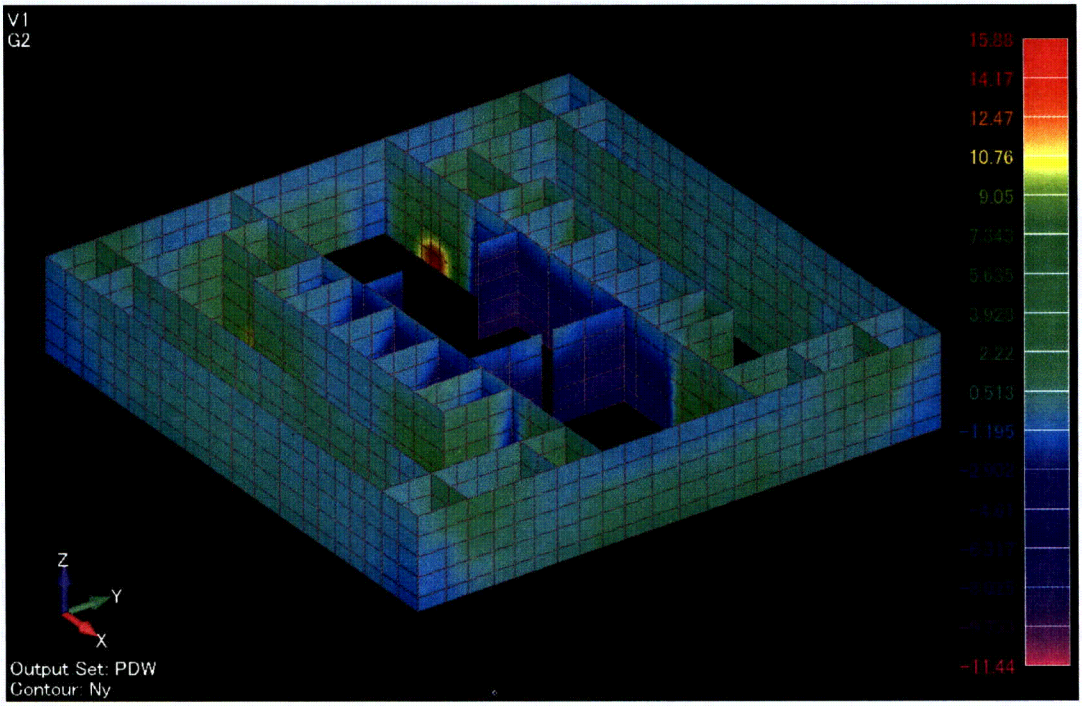

DCD Revision 5 FE Model

[Membrane Force: Ny]

Figure 3.8-41(69) Comparison of Element Force Distribution on Pool Girder and Wall (Pressure)

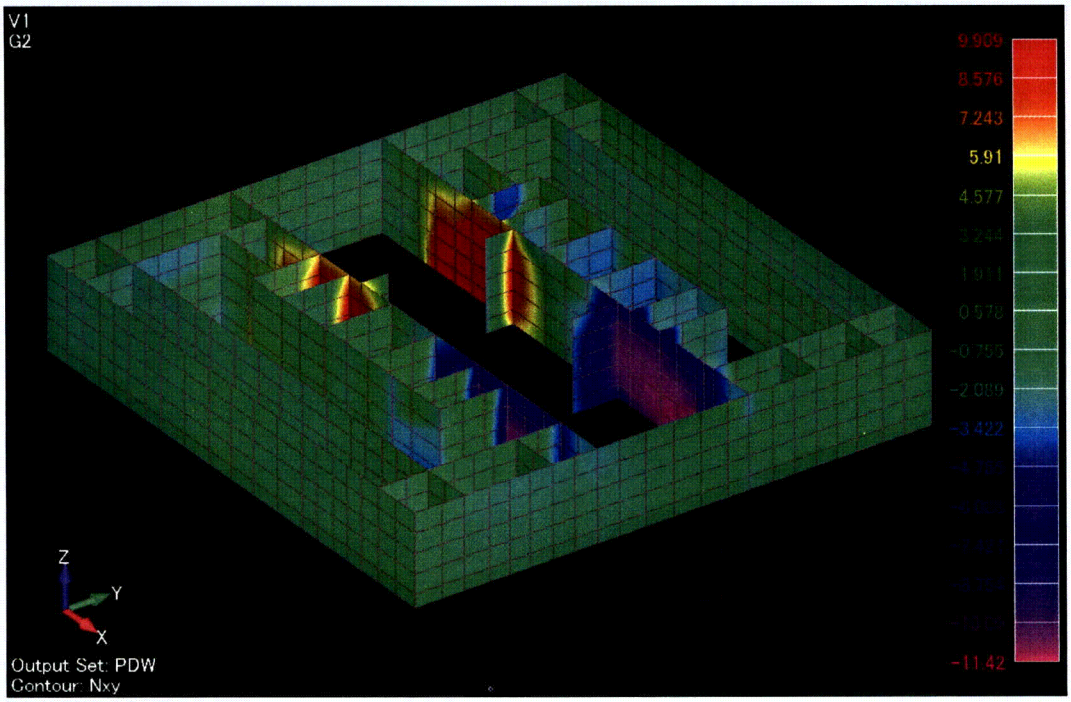

Updated FE Model

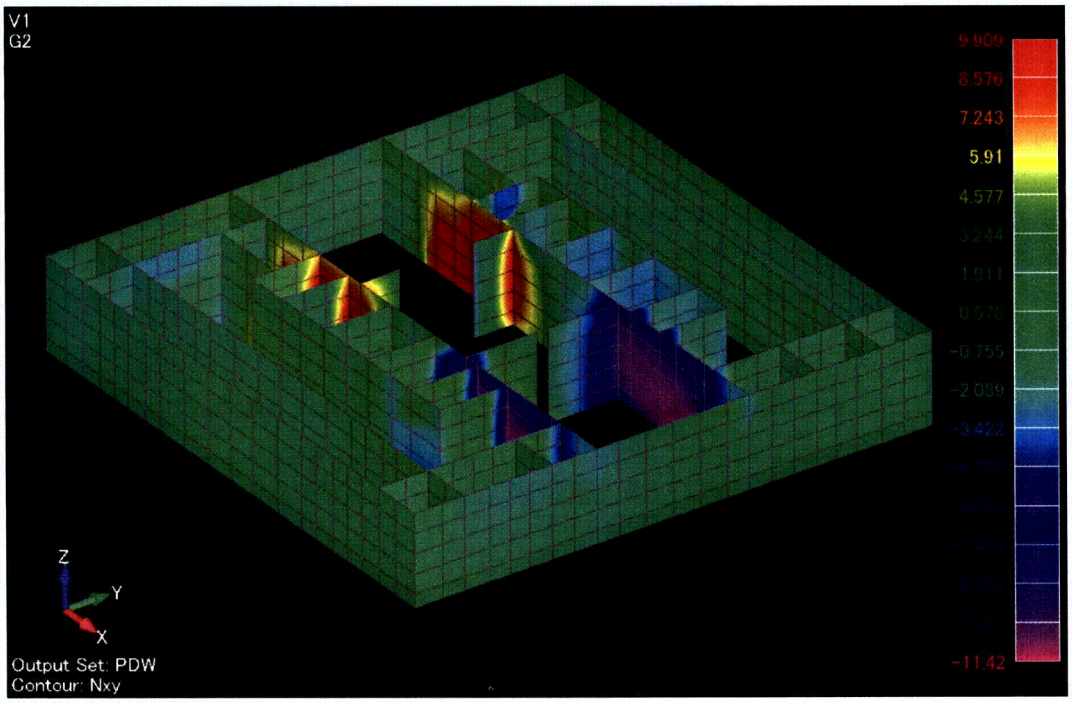

DCD Revision 5 FE Model

[Membrane Force: Nxy]

Figure 3.8-41(70) Comparison of Element Force Distribution on Pool Girder and Wall (Pressure)

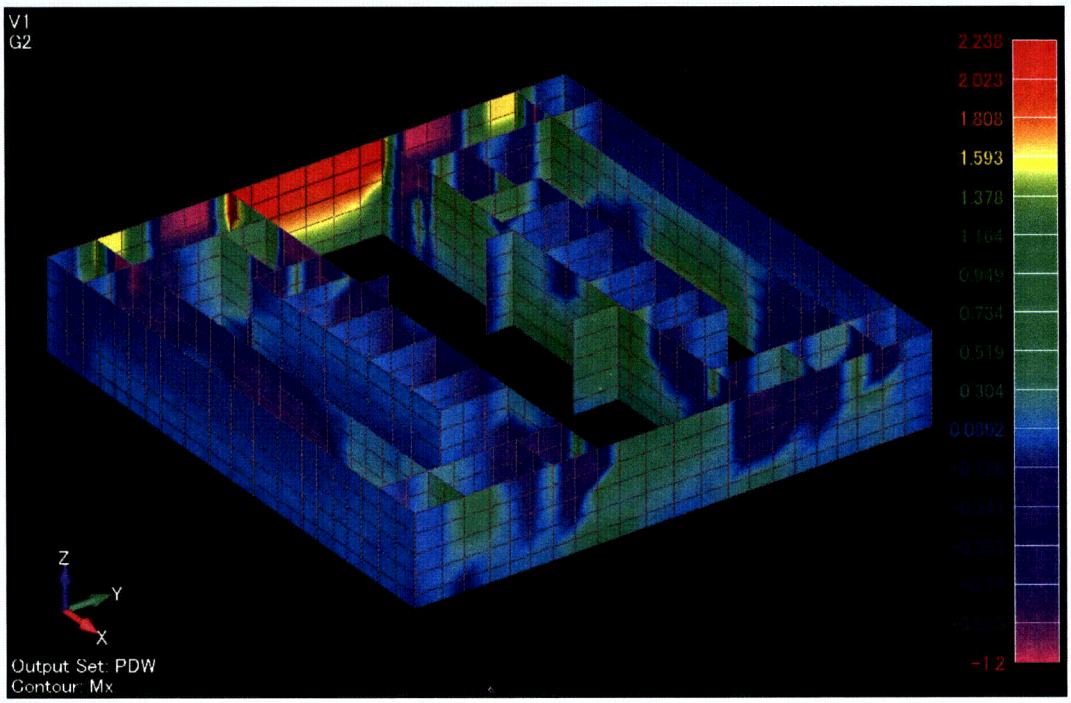

Updated FE Model

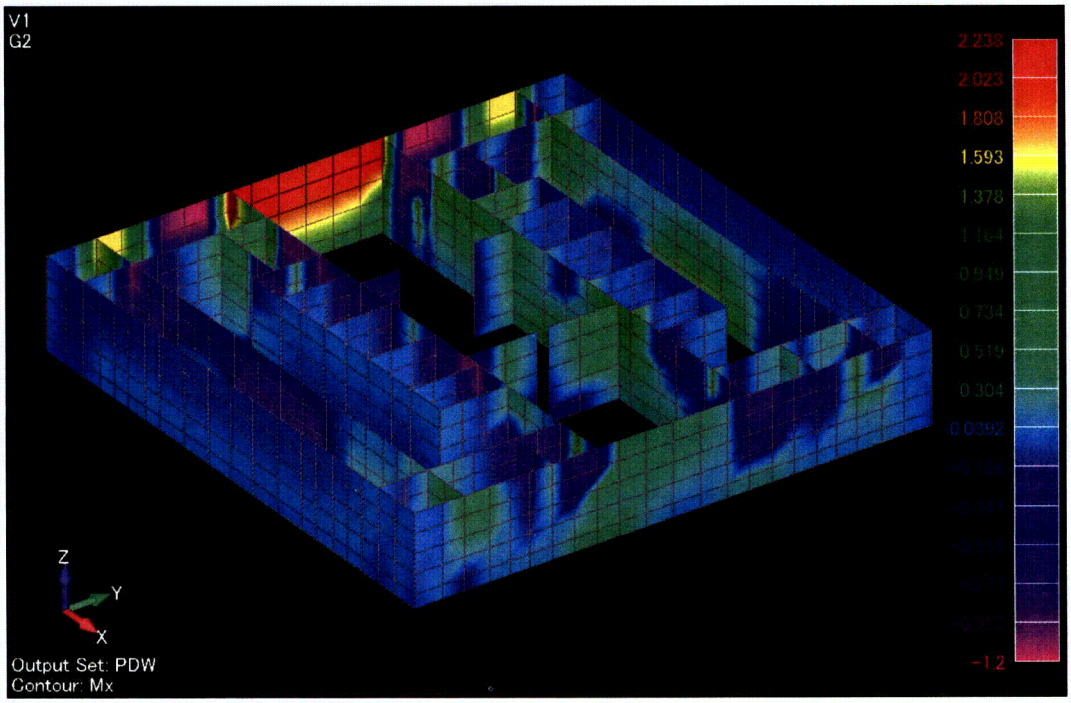

DCD Revision 5 FE Model

[Bending Moment: Mx]

Figure 3.8-41(71) Comparison of Element Force Distribution on Pool Girder and Wall (Pressure)

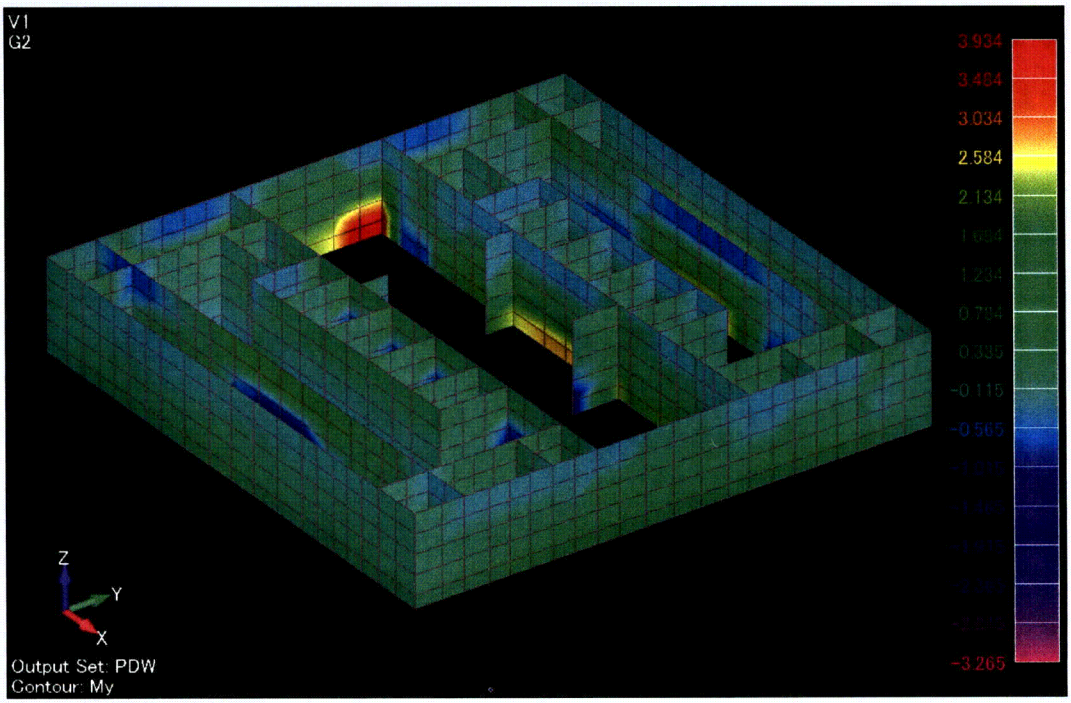

Updated FE Model

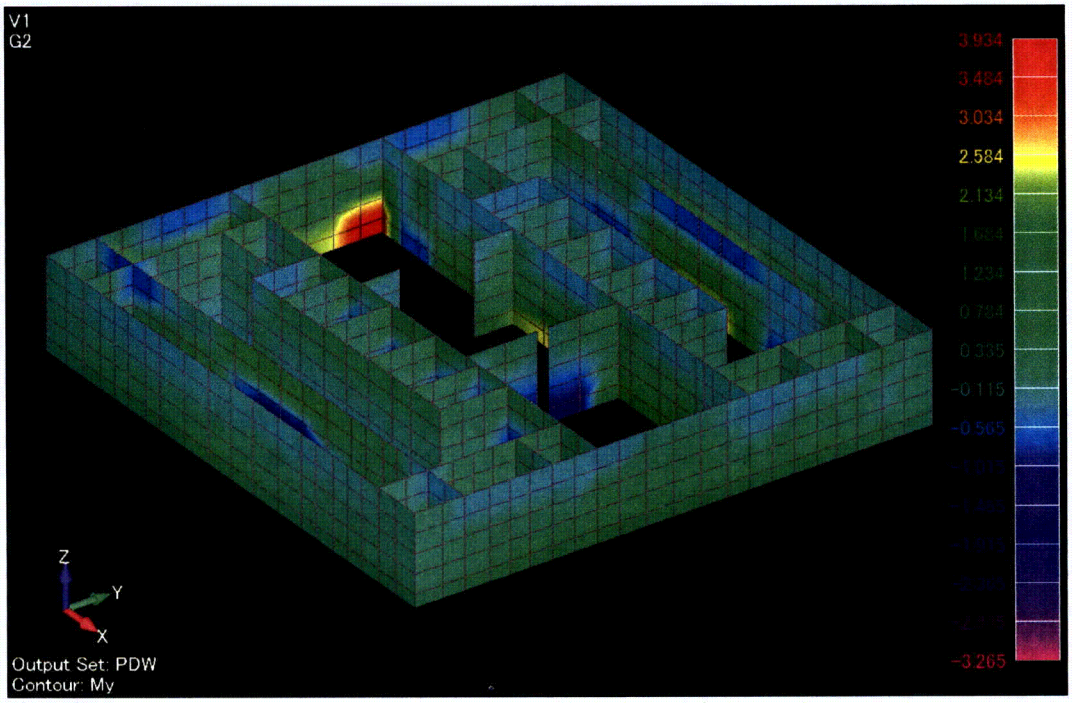

DCD Revision 5 FE Model

[Bending Moment: My]

Figure 3.8-41(72) Comparison of Element Force Distribution on Pool Girder and Wall (Pressure)

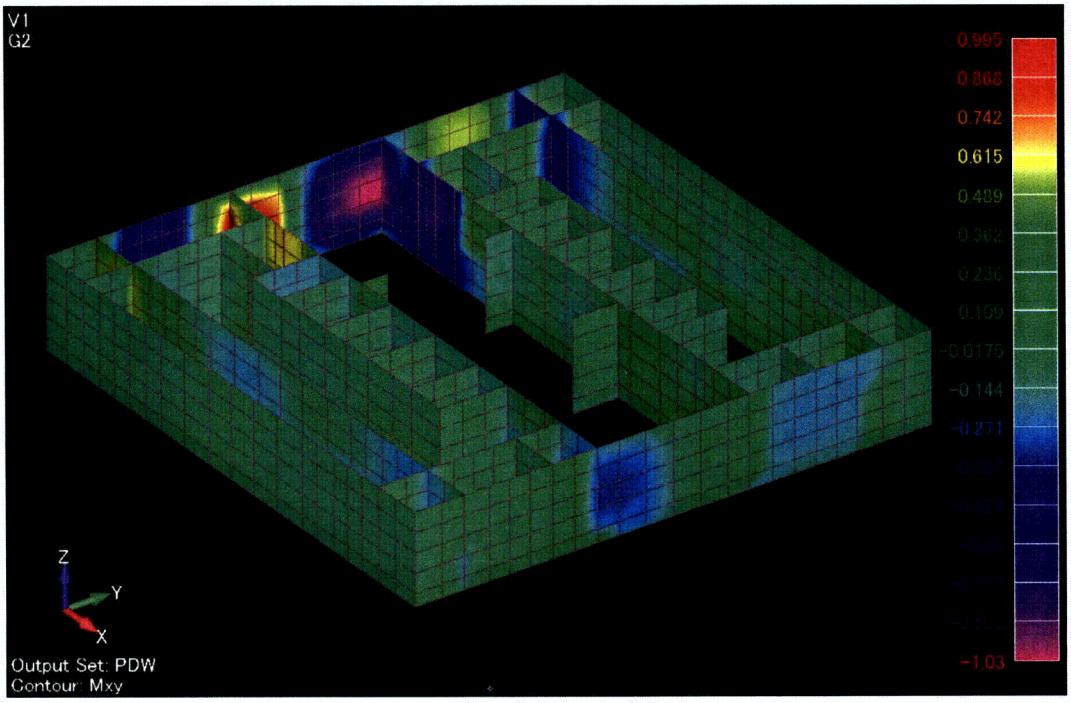

Updated FE Model

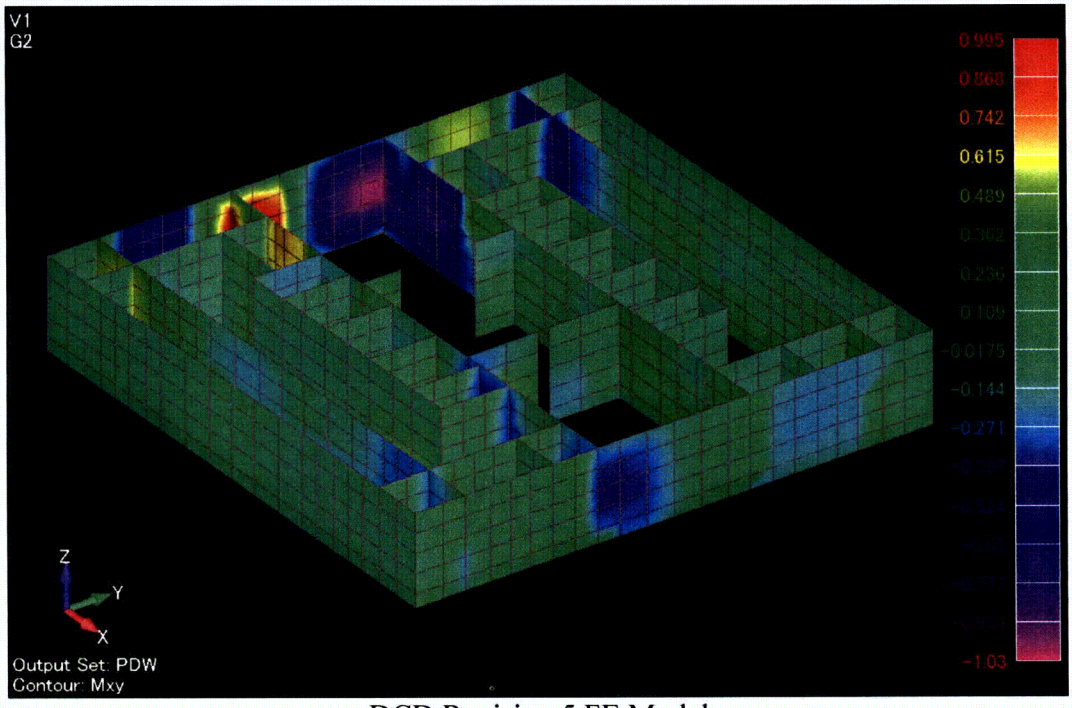

DCD Revision 5 FE Model

[Bending Moment: Mxy]

Figure 3.8-41(73) Comparison of Element Force Distribution on Pool Girder and Wall (Pressure)

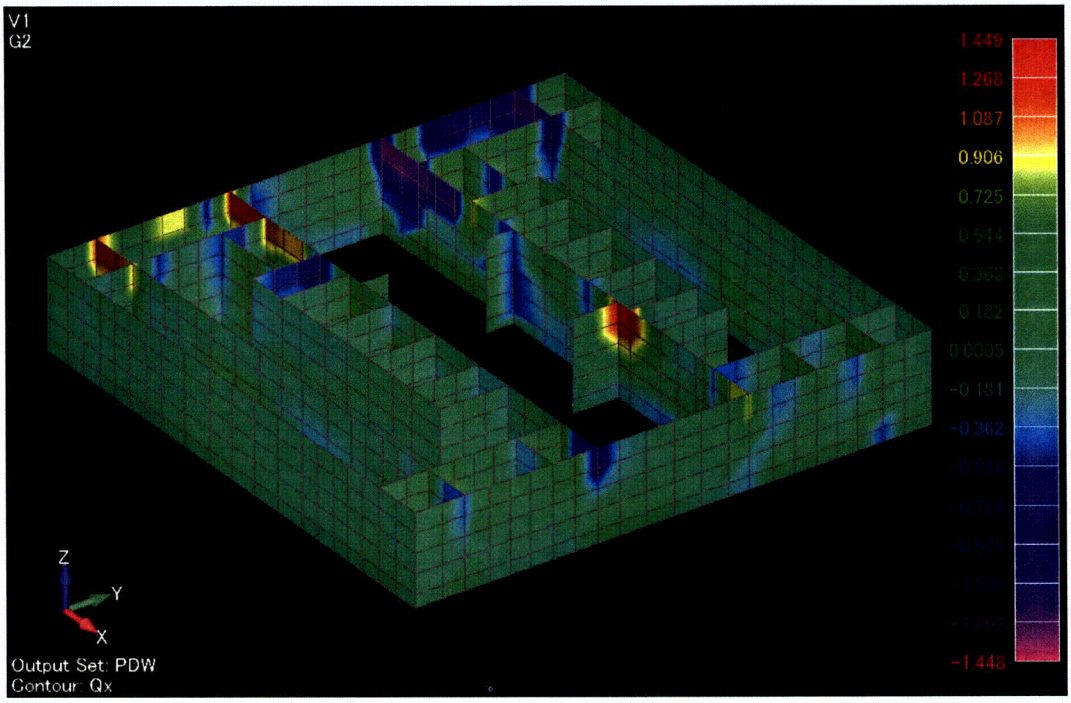

Updated FE Model

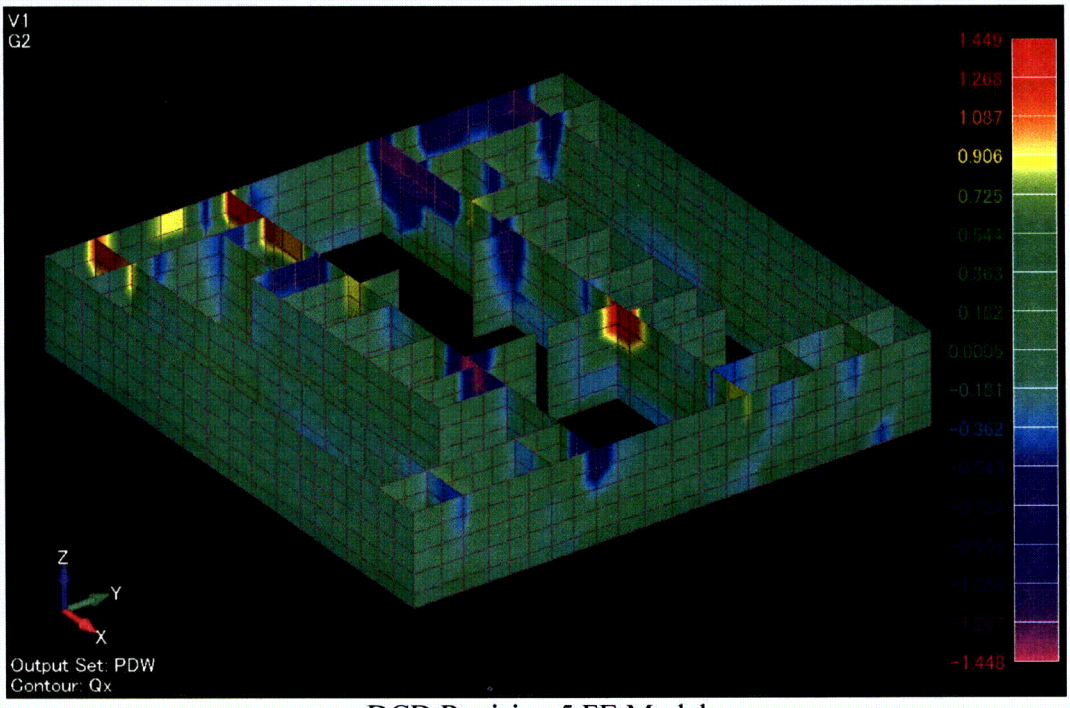

DCD Revision 5 FE Model

[Transverse Shear: Qx]

Figure 3.8-41(74) Comparison of Element Force Distribution on Pool Girder and Wall (Pressure)

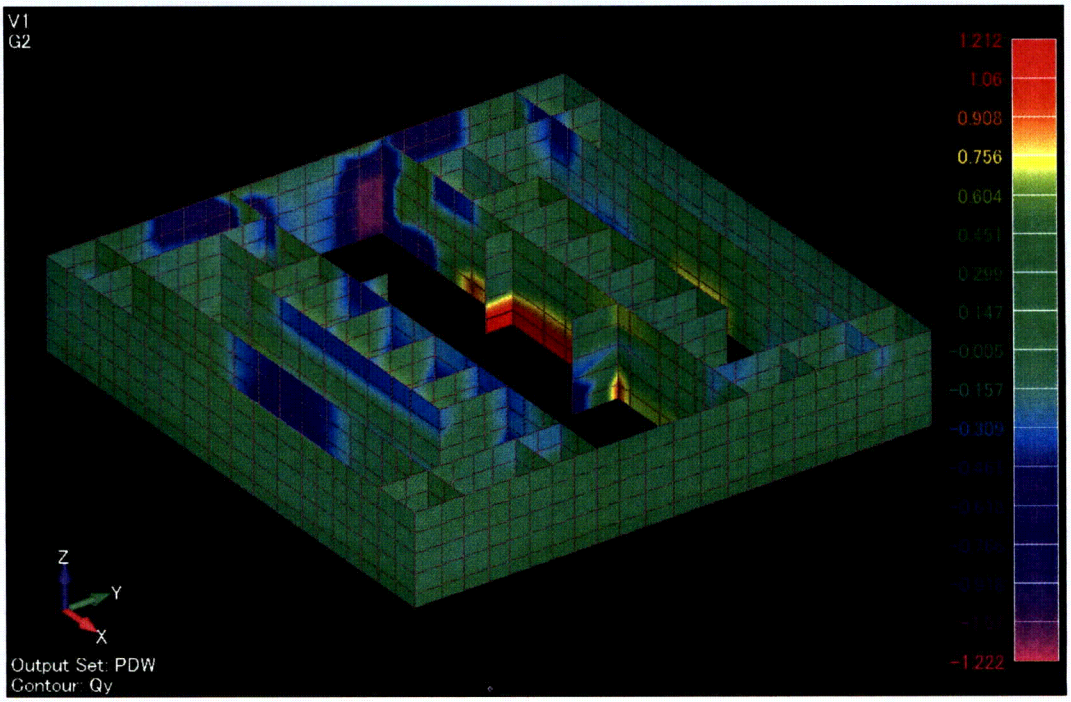

Updated FE Model

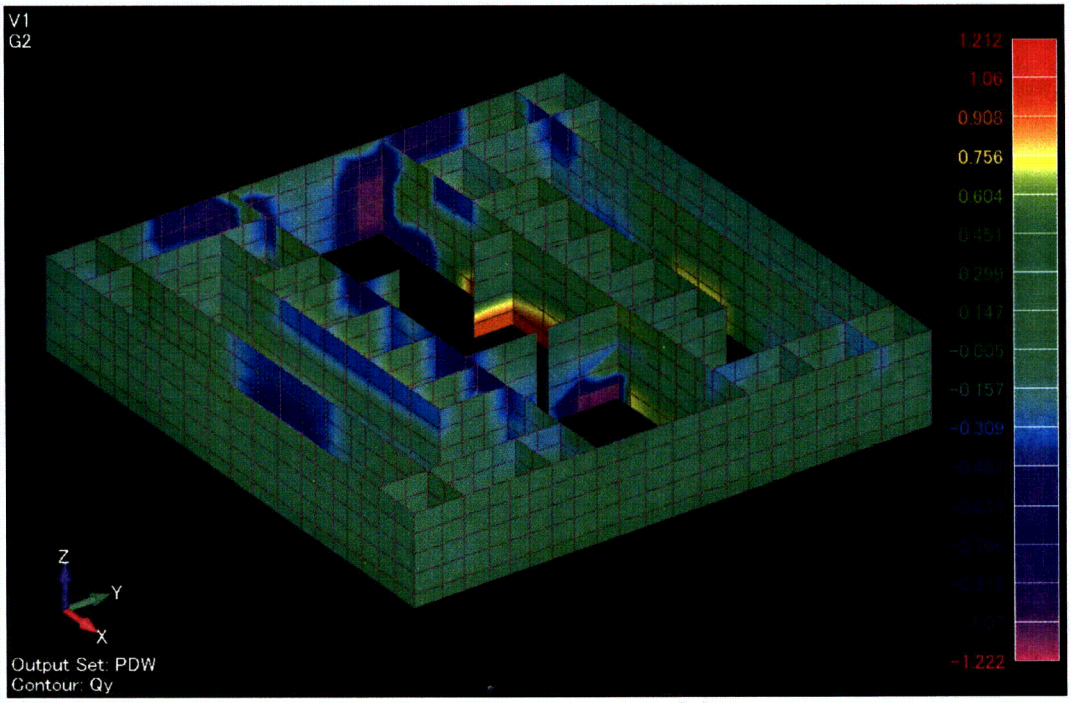

DCD Revision 5 FE Model

[Transverse Shear: Qy]

Figure 3.8-41(75) Comparison of Element Force Distribution on Pool Girder and Wall (Pressure)

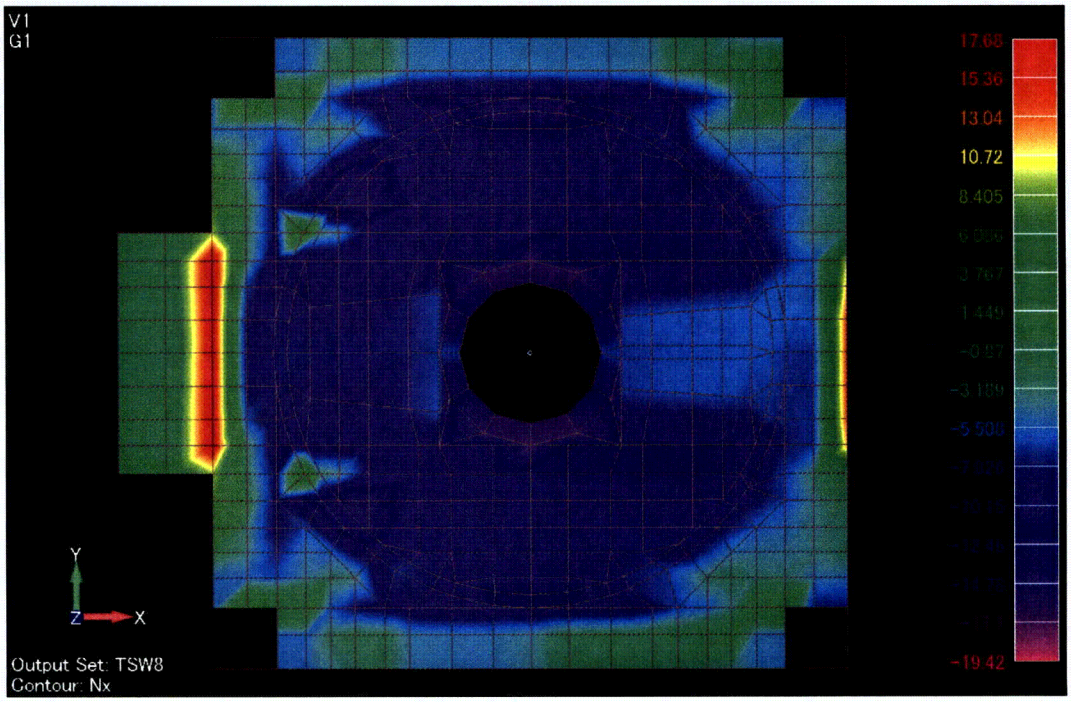

Updated FE Model

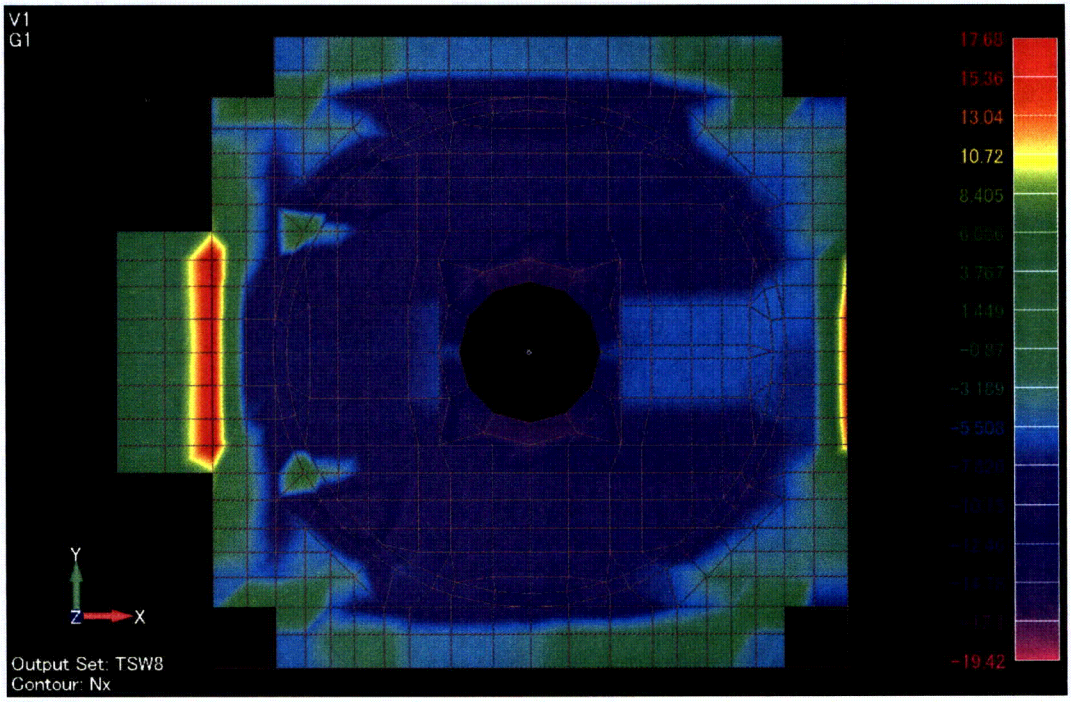

DCD Revision 5 FE Model

[Membrane Force: Nx]

Figure 3.8-41(76) Comparison of Element Force Distribution on RCCV Top Slab (Thermal)

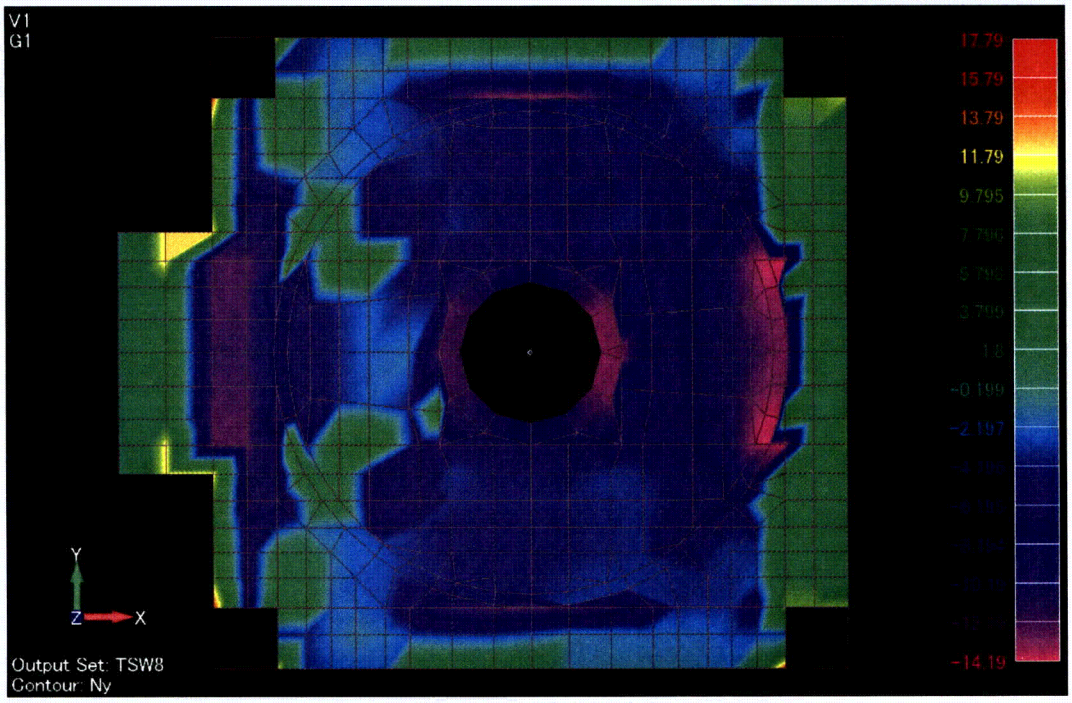

Updated FE Model

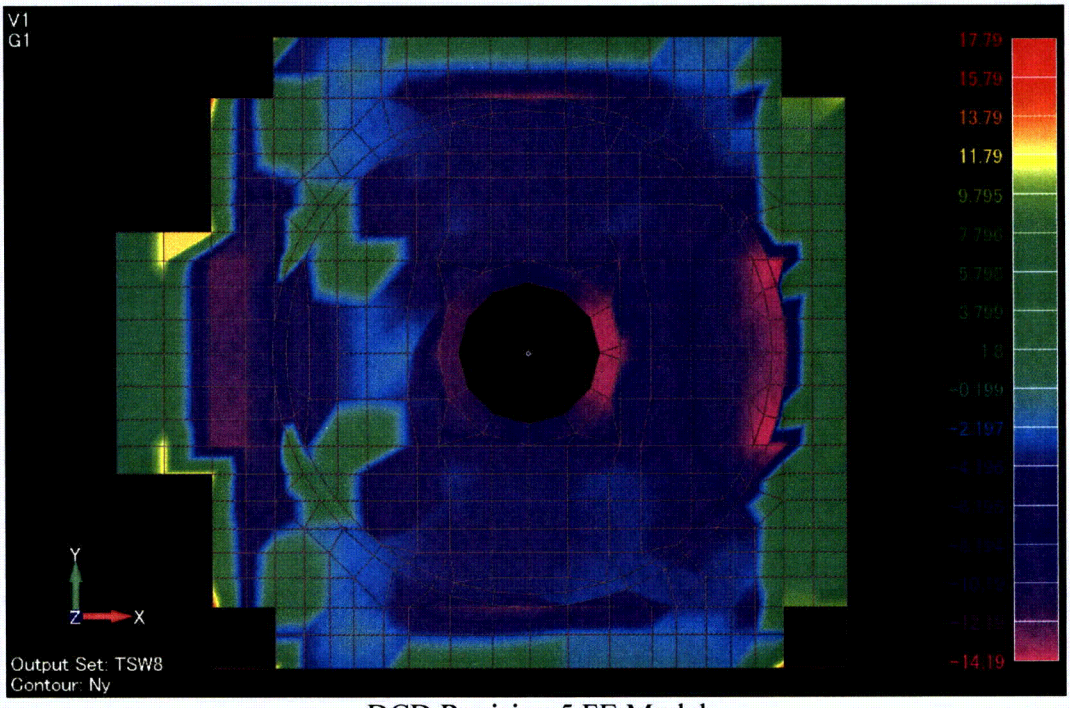

DCD Revision 5 FE Model

[Membrane Force: Ny]

Figure 3.8-41(77) Comparison of Element Force Distribution on RCCV Top Slab (Thermal)

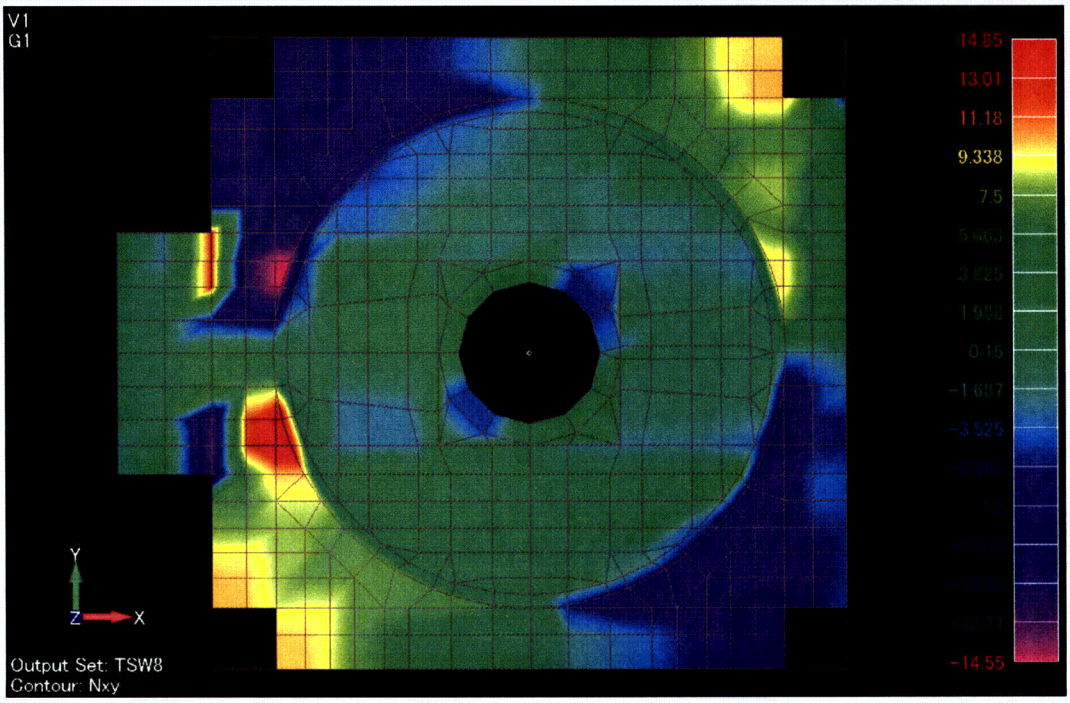

Updated FE Model

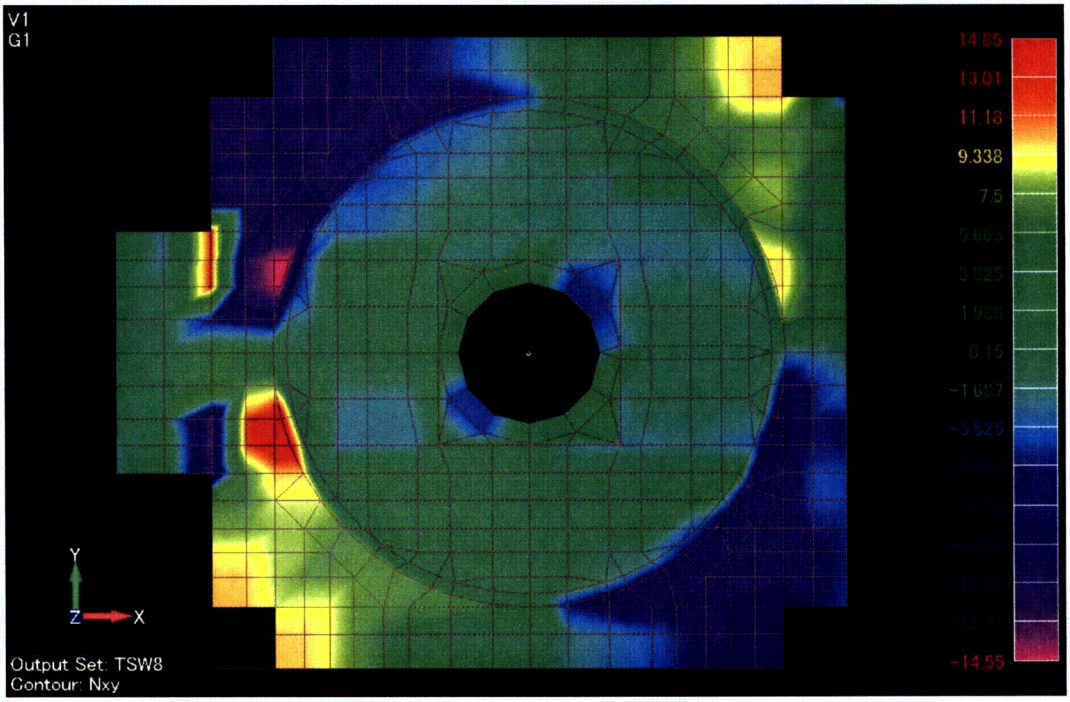

DCD Revision 5 FE Model

[Membrane Force: Nxy]

Figure 3.8-41(78) Comparison of Element Force Distribution on RCCV Top Slab (Thermal)

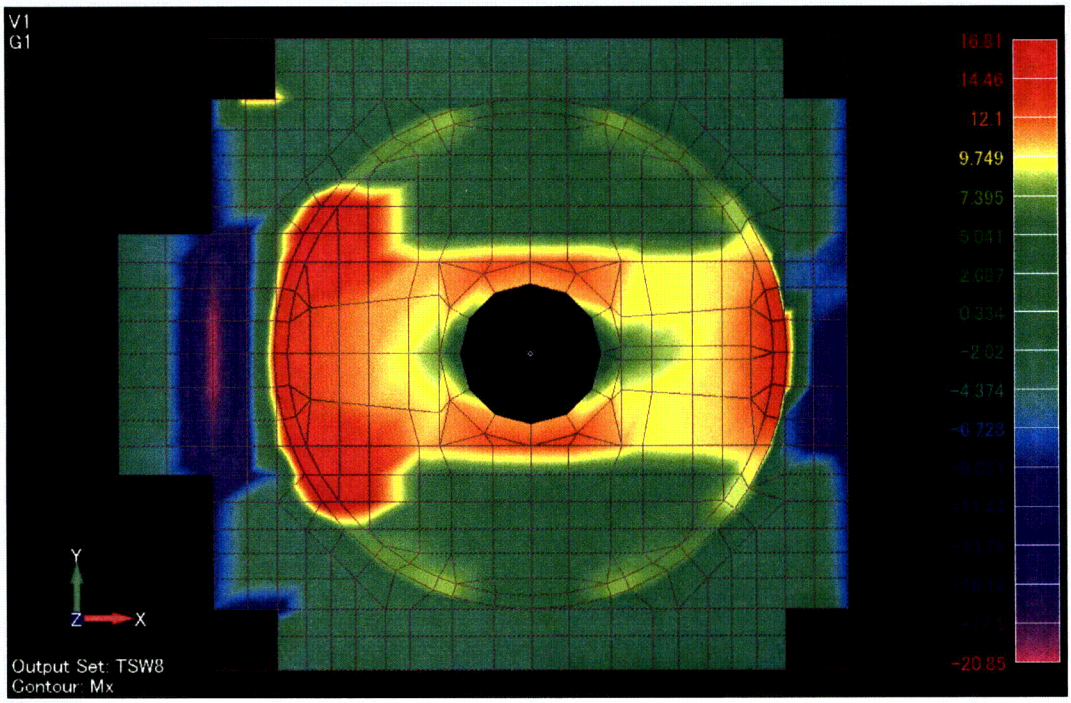

Updated FE Model

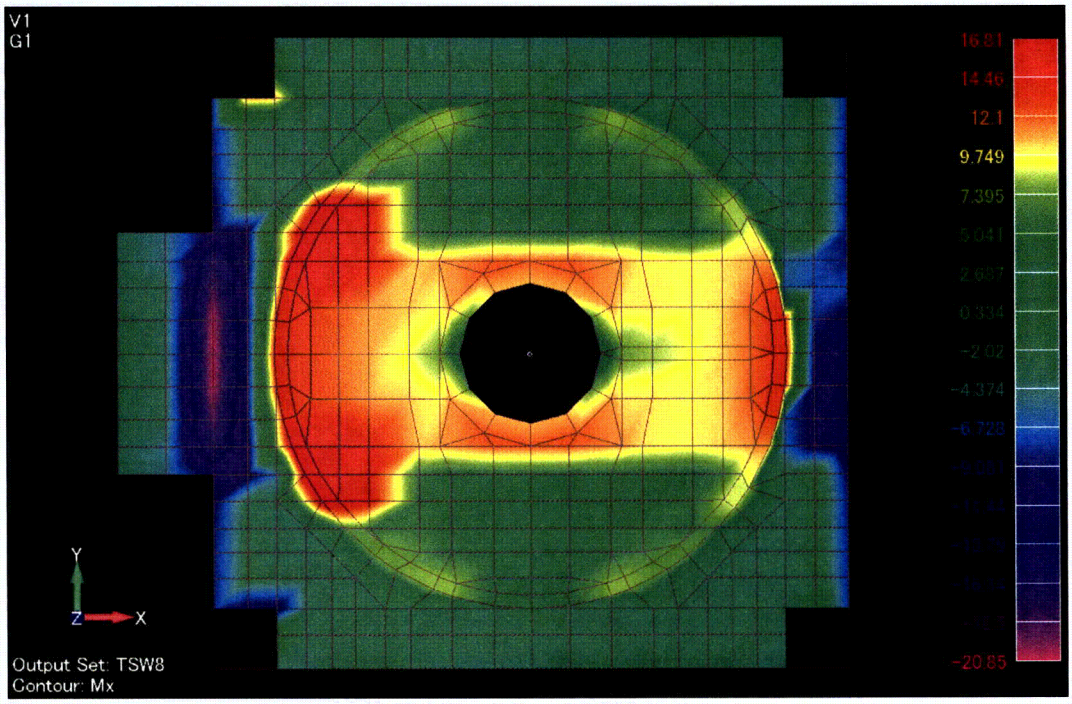

DCD Revision 5 FE Model

[Bending Moment: Mx]

Figure 3.8-41(79) Comparison of Element Force Distribution on RCCV Top Slab (Thermal)

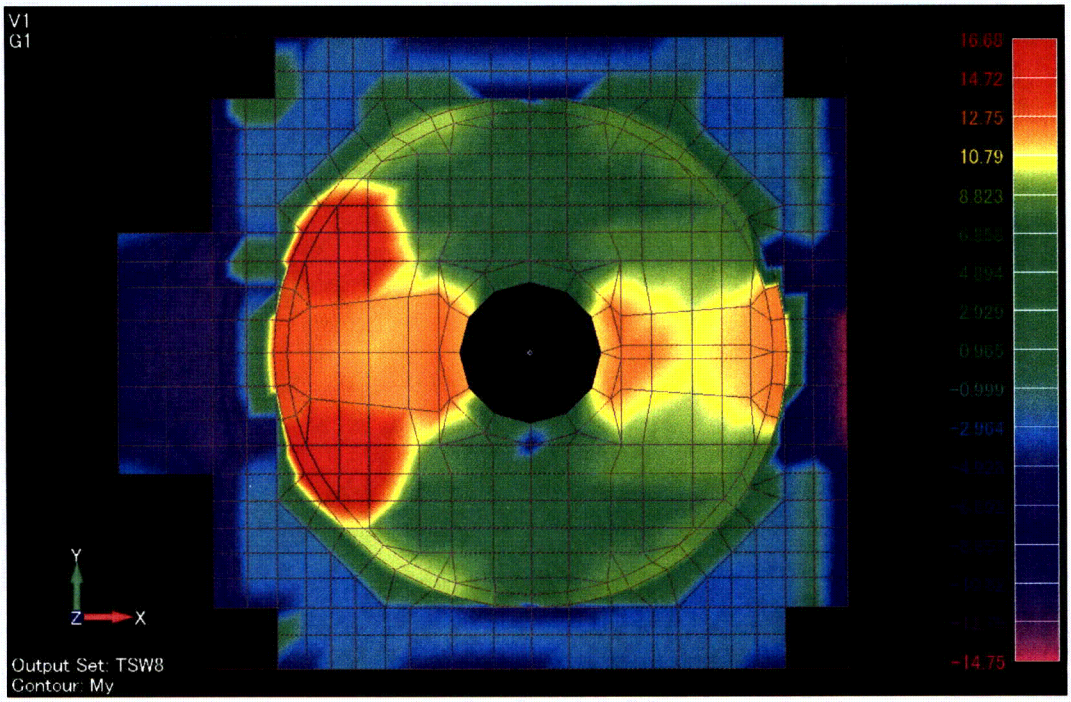

Updated FE Model

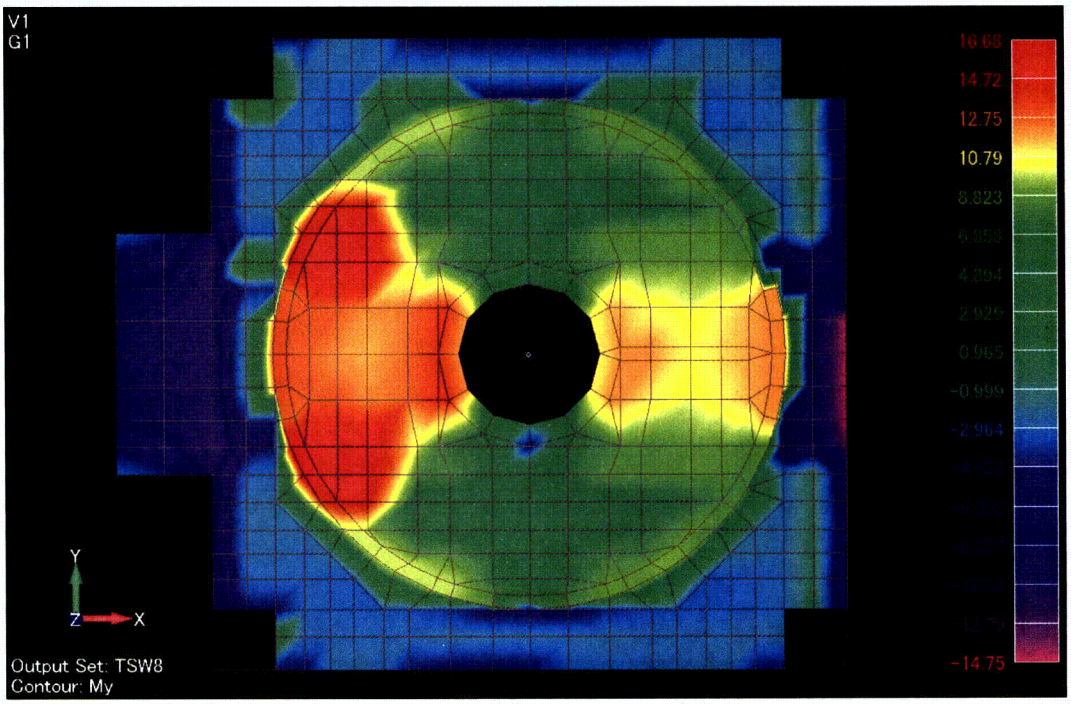

DCD Revision 5 FE Model

[Bending Moment: My]

Figure 3.8-41(80) Comparison of Element Force Distribution on RCCV Top Slab (Thermal)

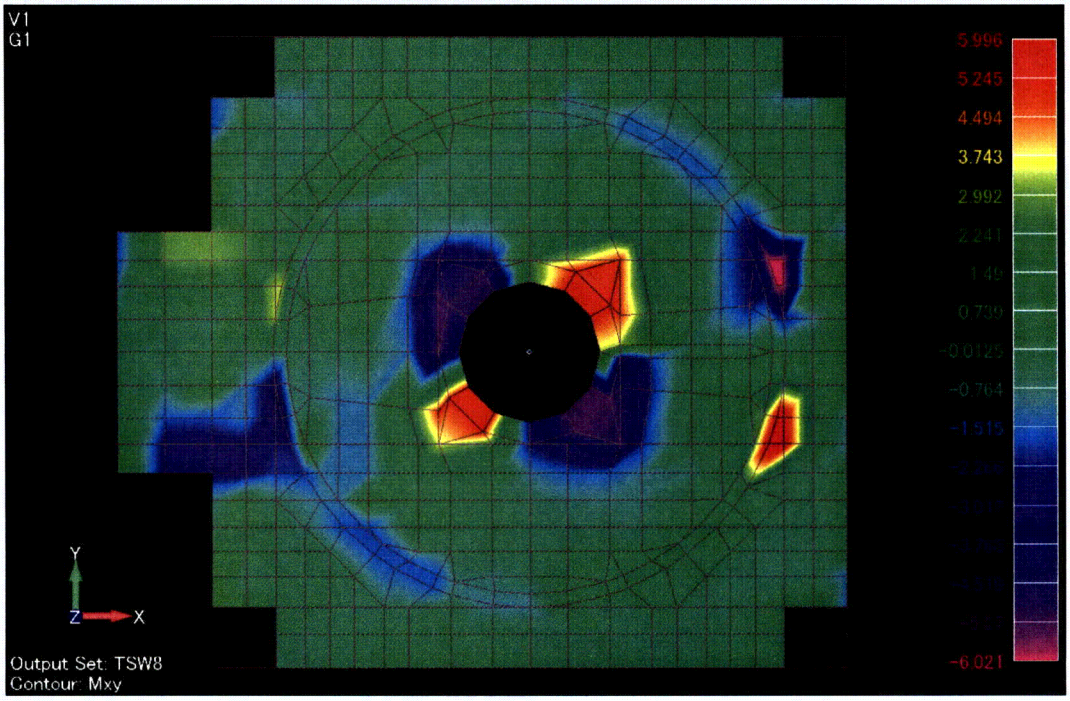

Updated FE Model

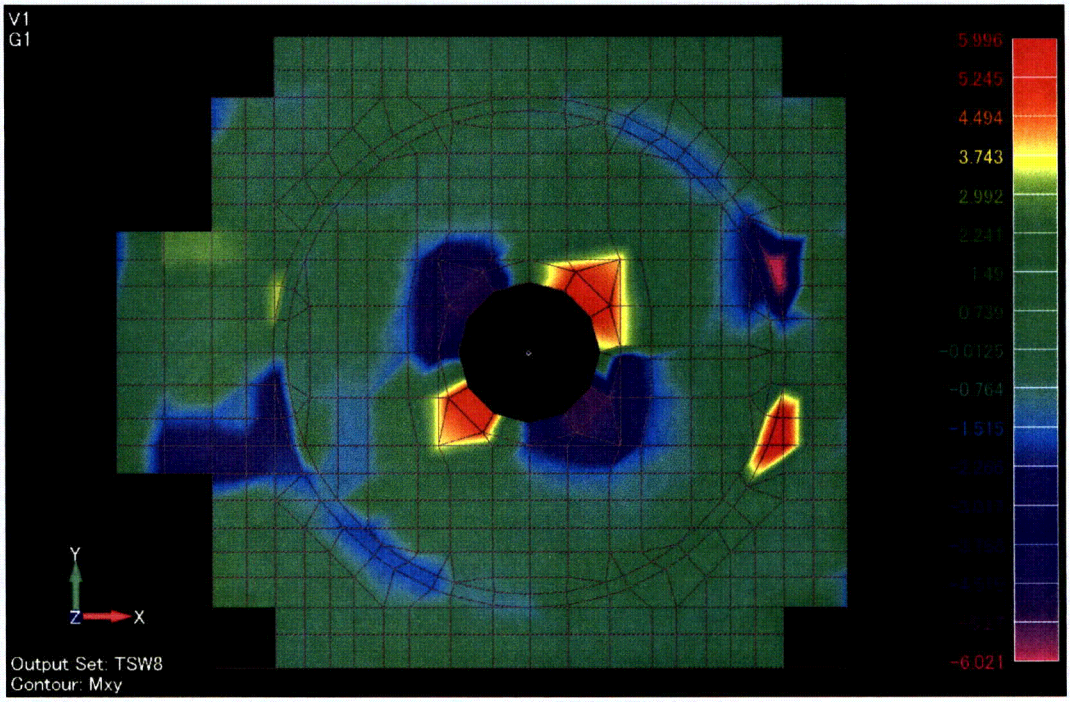

DCD Revision 5 FE Model

[Bending Moment: Mxy]

Figure 3.8-41(81) Comparison of Element Force Distribution on RCCV Top Slab (Thermal)

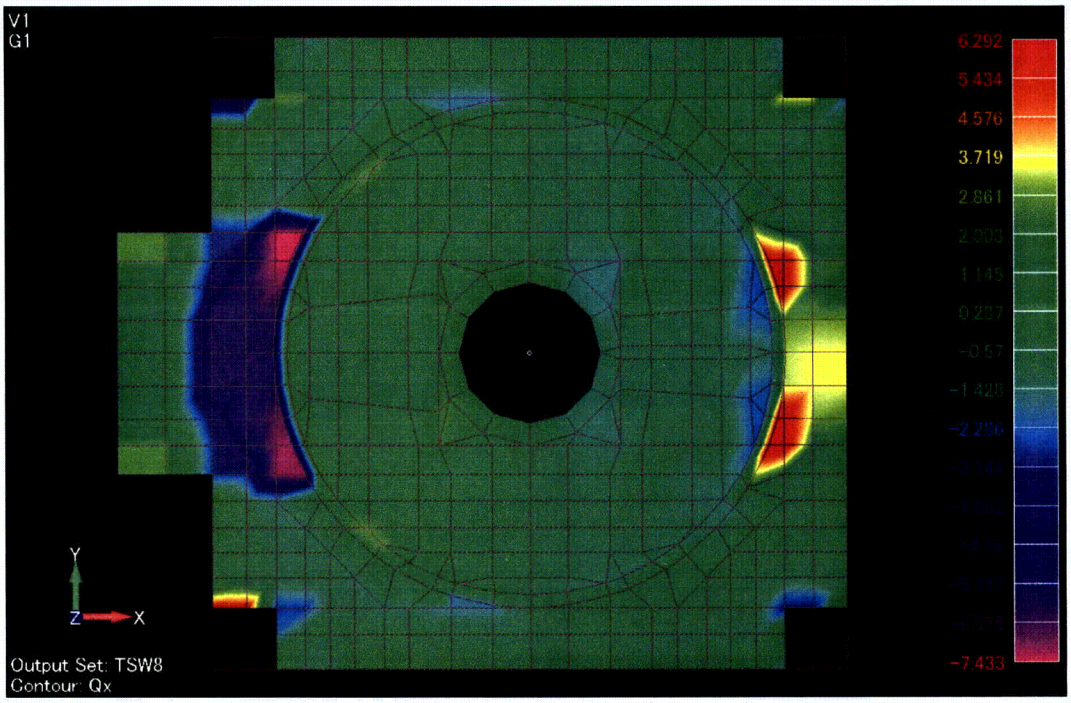

Updated FE Model

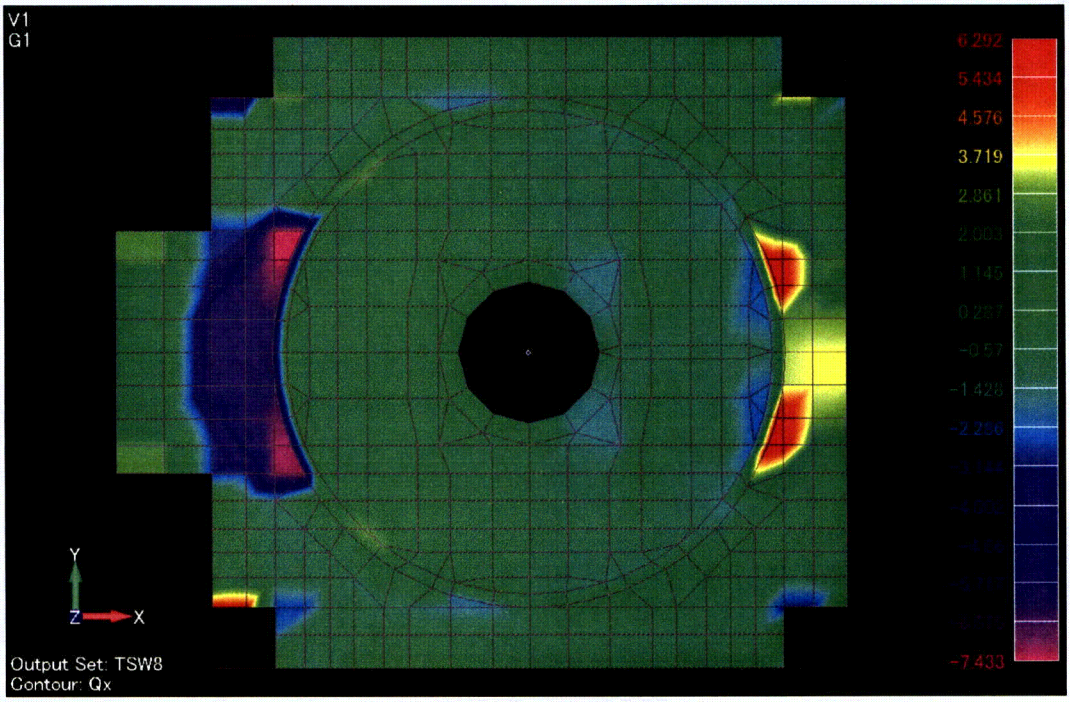

DCD Revision 5 FE Model

[Transverse Shear: Qx]

Figure 3.8-41(82) Comparison of Element Force Distribution on RCCV Top Slab (Thermal)

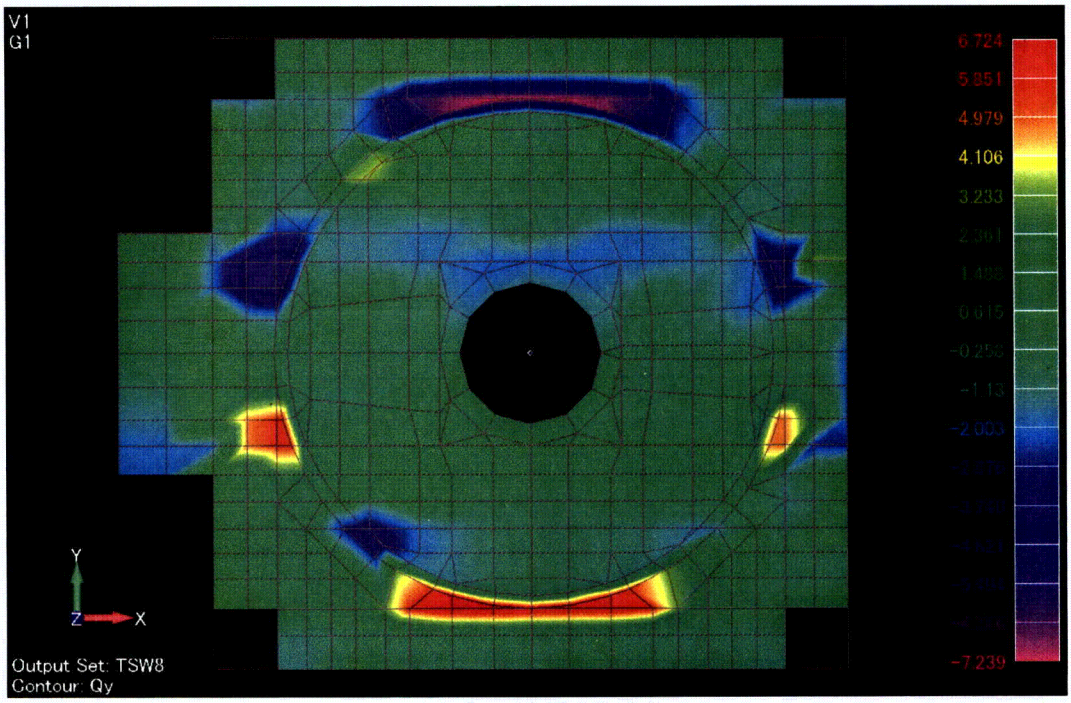

Updated FE Model

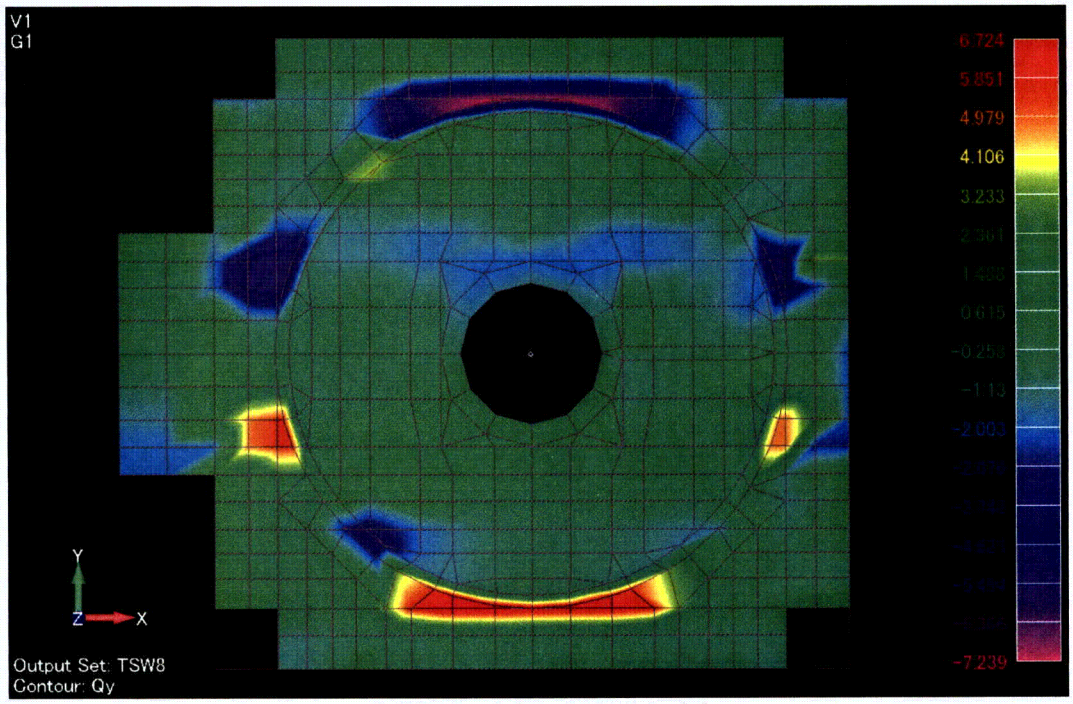

DCD Revision 5 FE Model

[Transverse Shear: Qy]

Figure 3.8-41(83) Comparison of Element Force Distribution on RCCV Top Slab (Thermal)

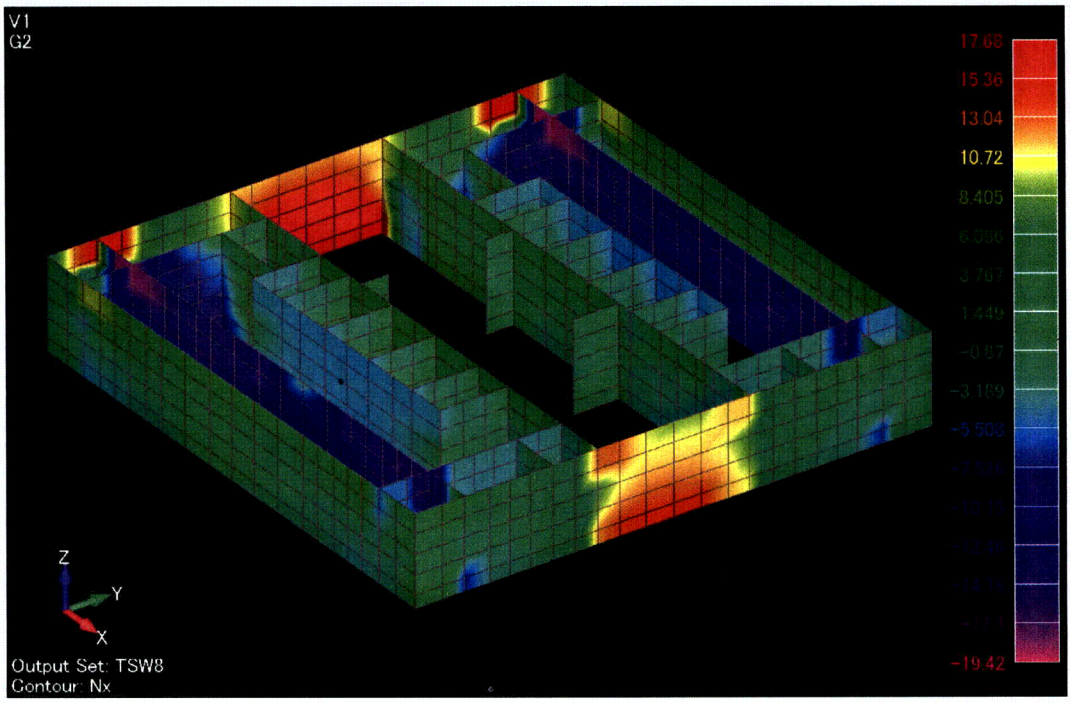

Updated FE Model

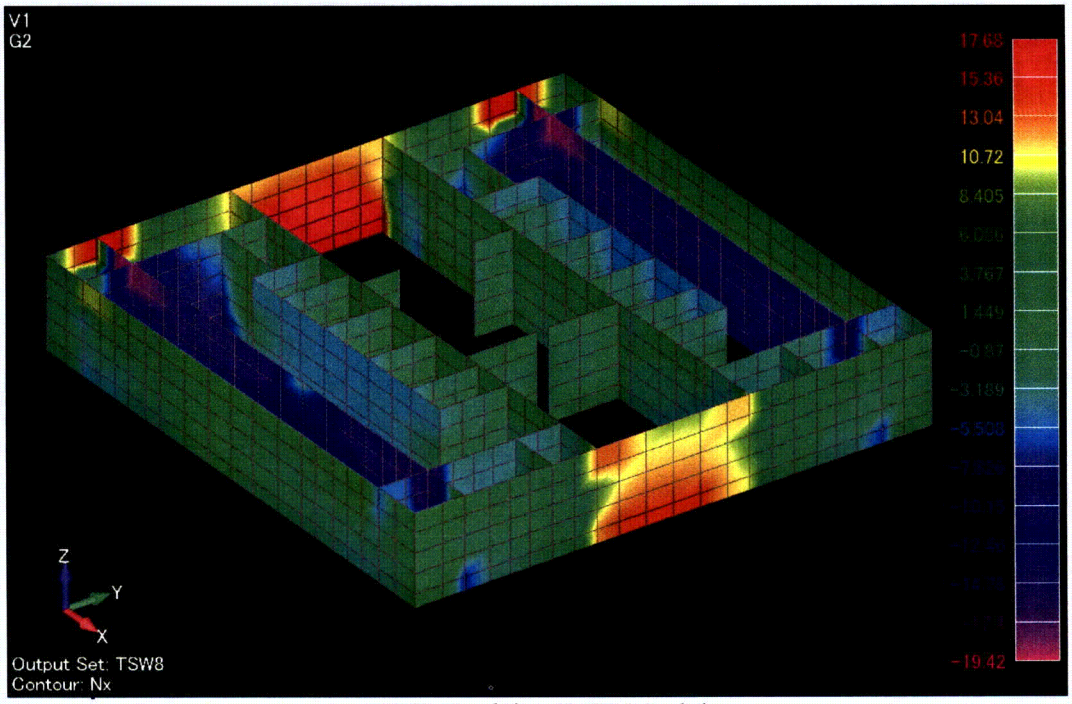

DCD Revision 5 FE Model

[Membrane Force: Nx]

Figure 3.8-41(84) Comparison of Element Force Distribution on Pool Girder and Wall (Thermal)

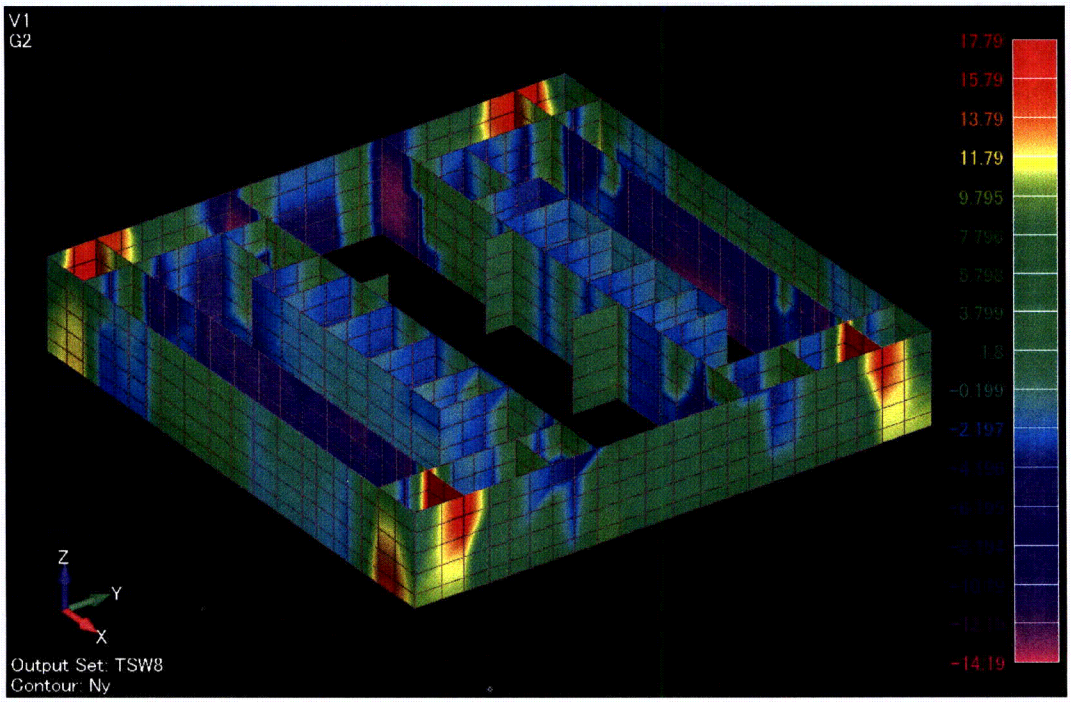

Updated FE Model

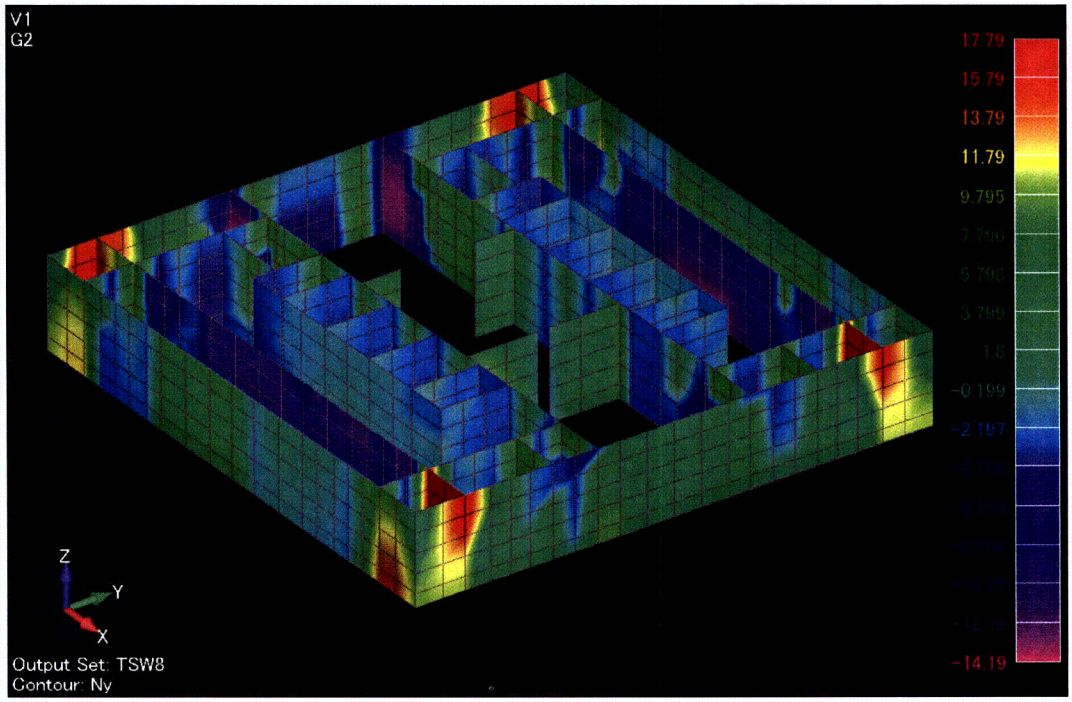

DCD Revision 5 FE Model

[Membrane Force: Ny]

Figure 3.8-41(85) Comparison of Element Force Distribution on Pool Girder and Wall (Thermal)

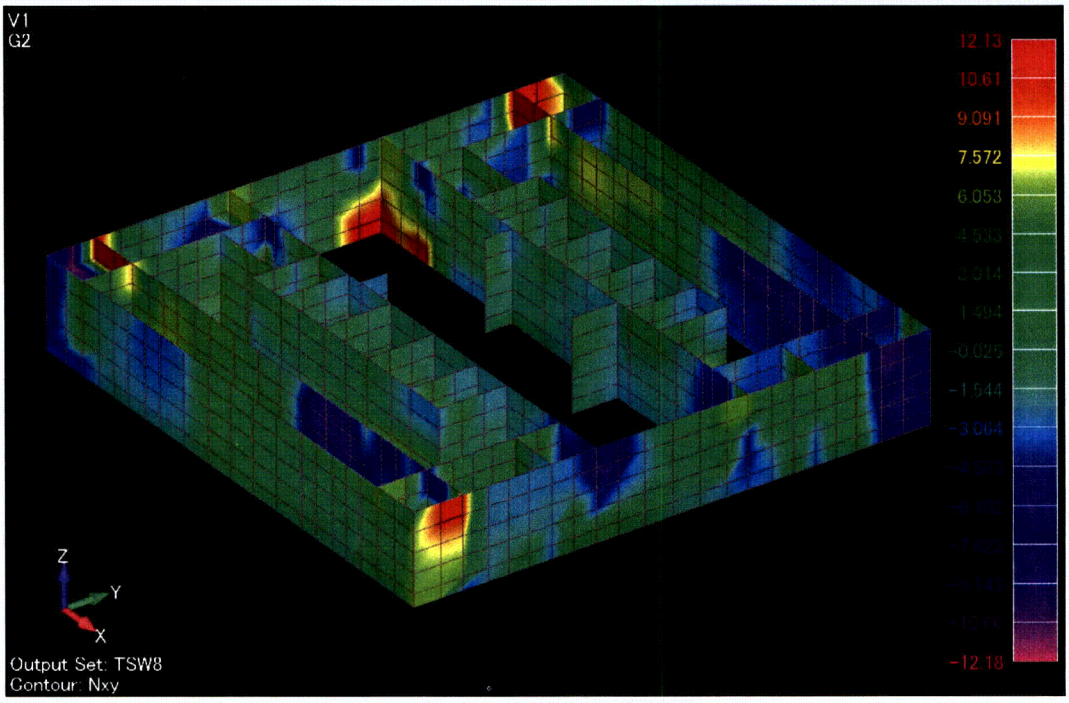

Updated FE Model

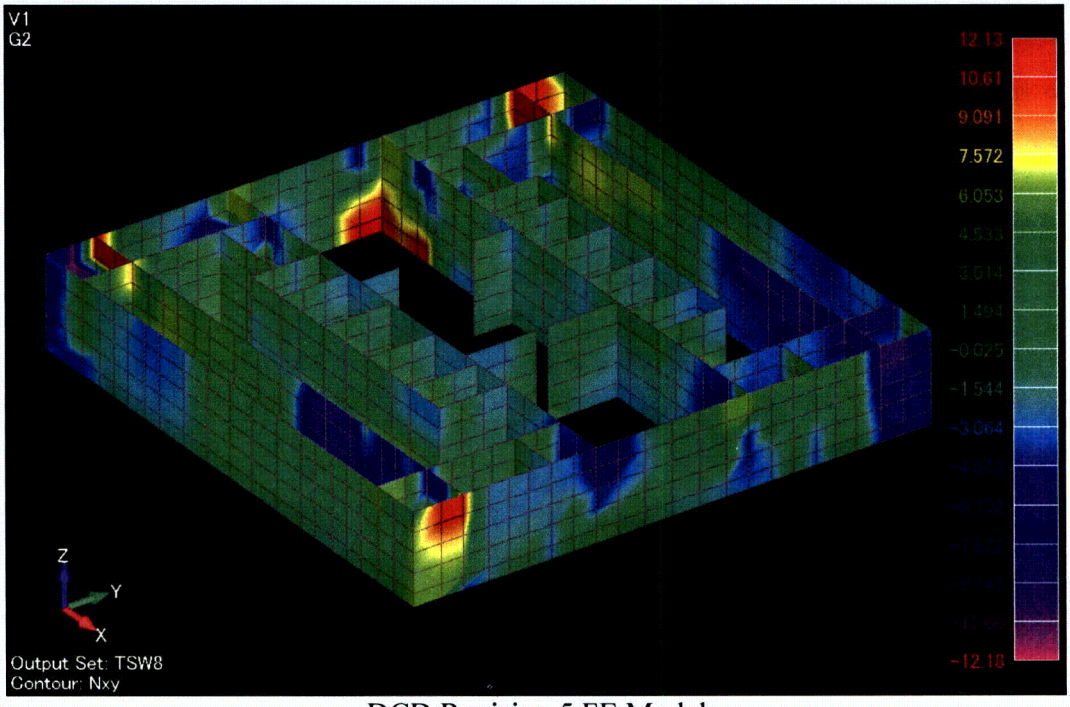

DCD Revision 5 FE Model

[Membrane Force: Nxy]

Figure 3.8-41(86) Comparison of Element Force Distribution on Pool Girder and Wall (Thermal)

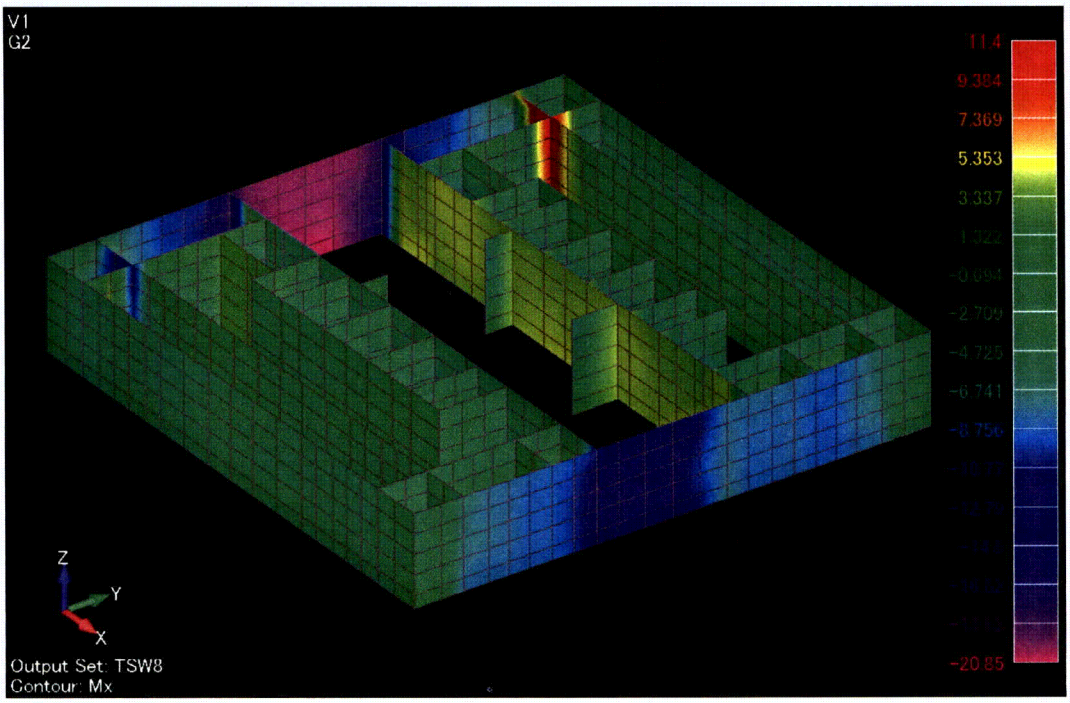

Updated FE Model

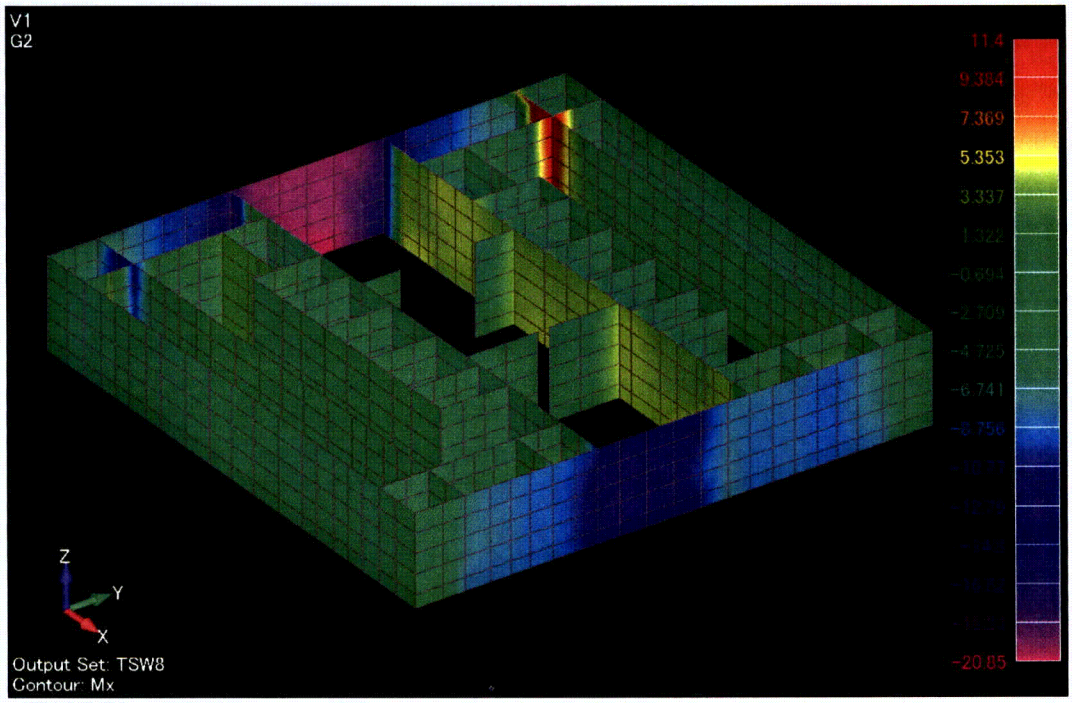

DCD Revision 5 FE Model

[Bending Moment: Mx]

Figure 3.8-41(87) Comparison of Element Force Distribution on Pool Girder and Wall (Thermal)

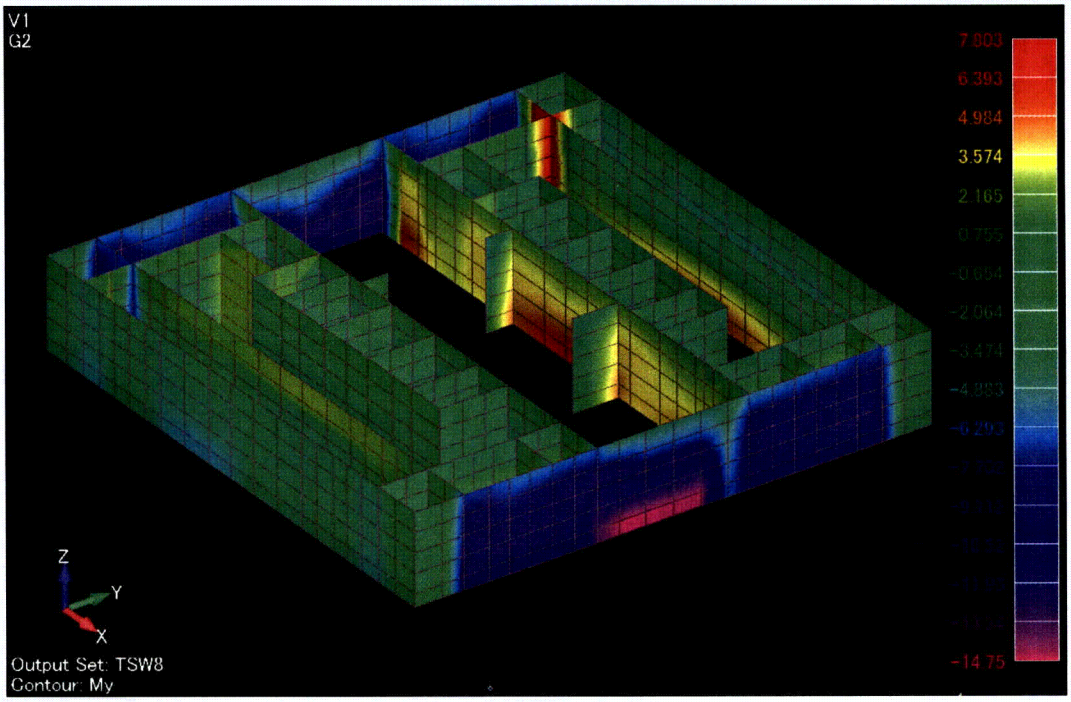

Updated FE Model

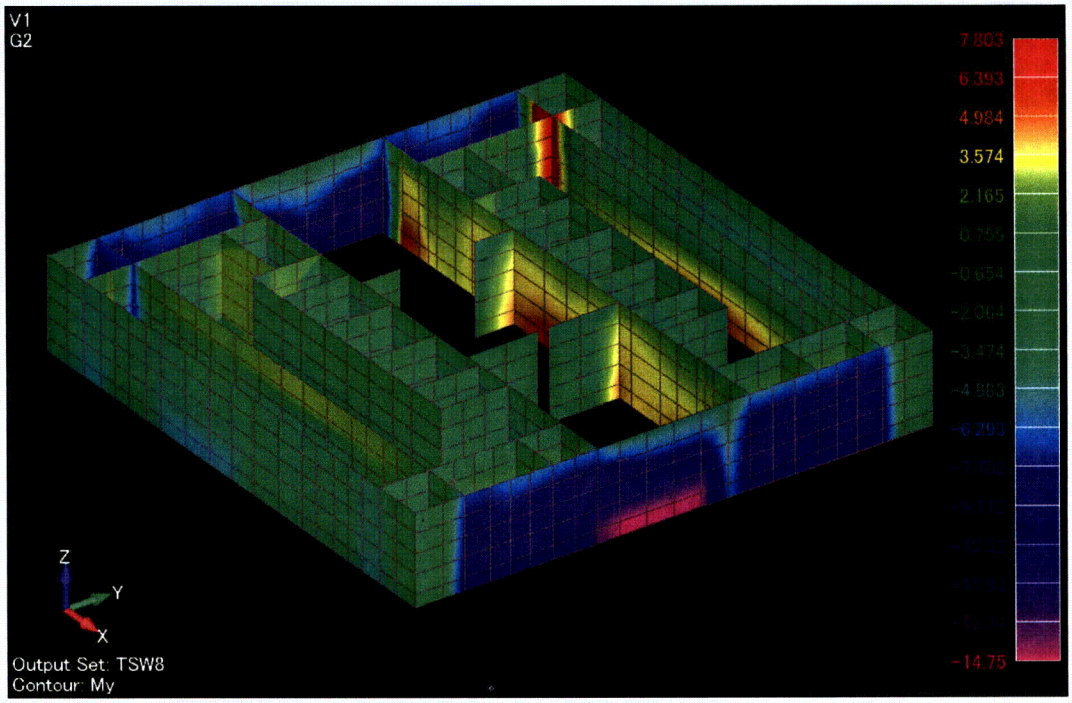

DCD Revision 5 FE Model

[Bending Moment: My]

Figure 3.8-41(88) Comparison of Element Force Distribution on Pool Girder and Wall (Thermal)

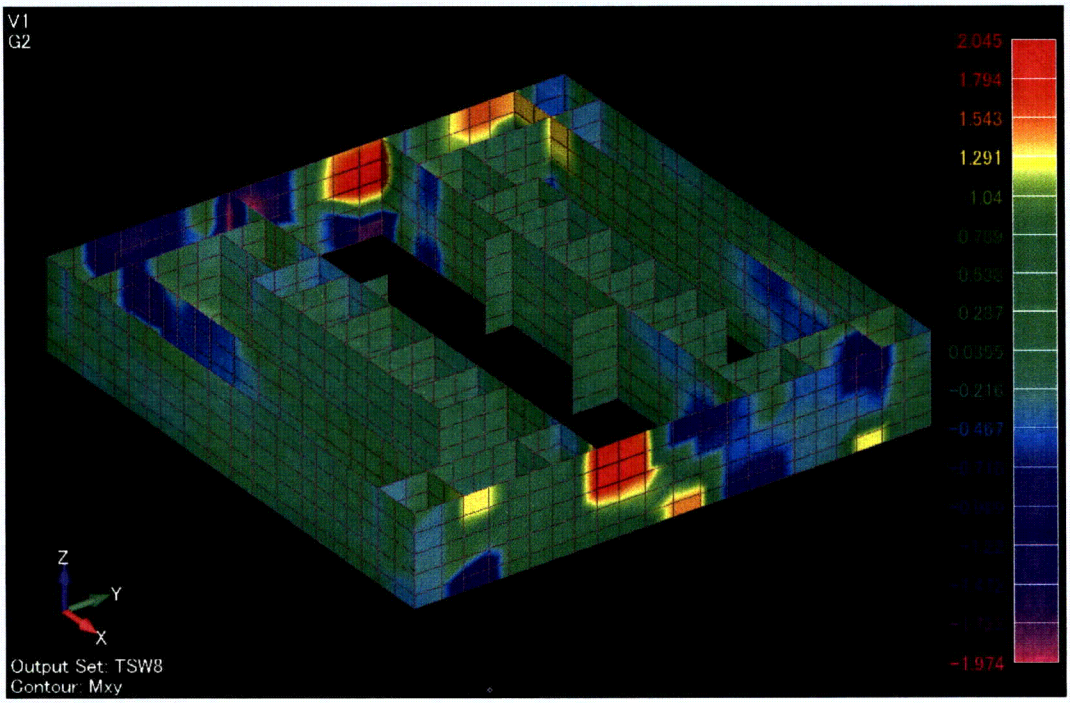

Updated FE Model

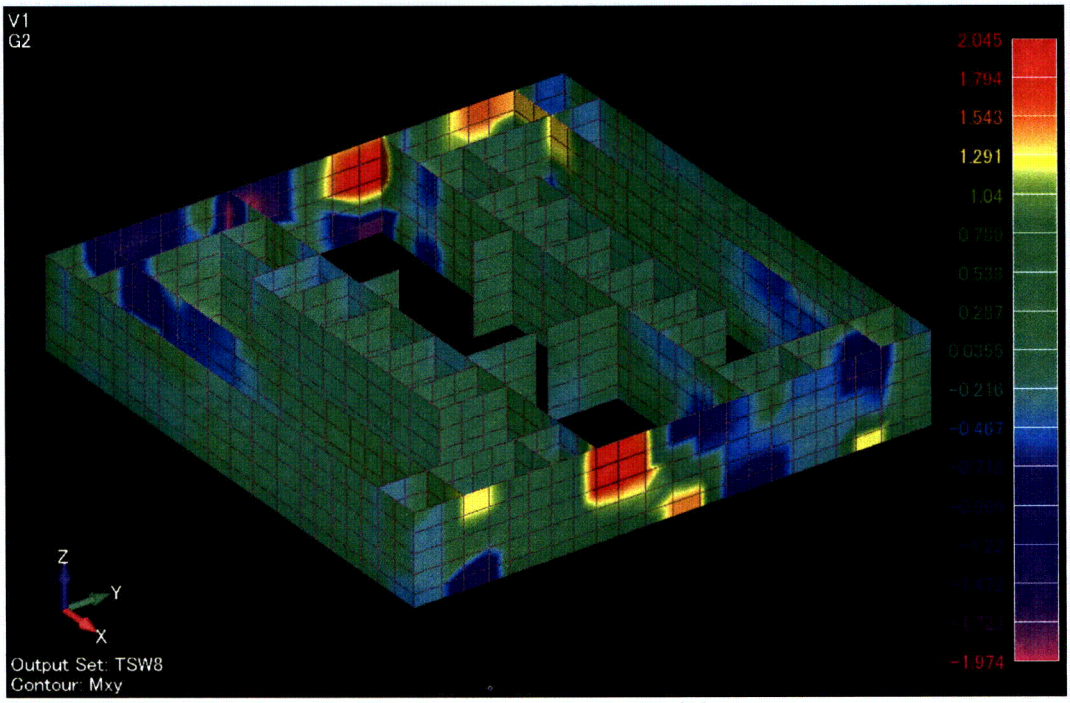

DCD Revision 5 FE Model

[Bending Moment: Mxy]

Figure 3.8-41(89) Comparison of Element Force Distribution on Pool Girder and Wall (Thermal)

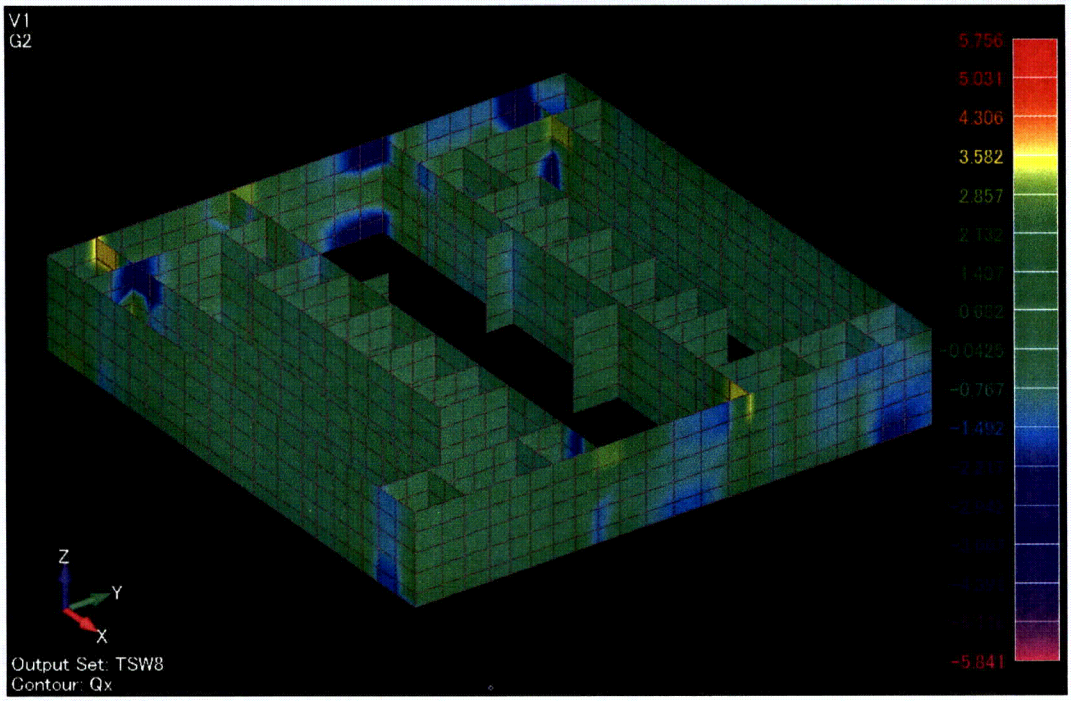

Updated FE Model

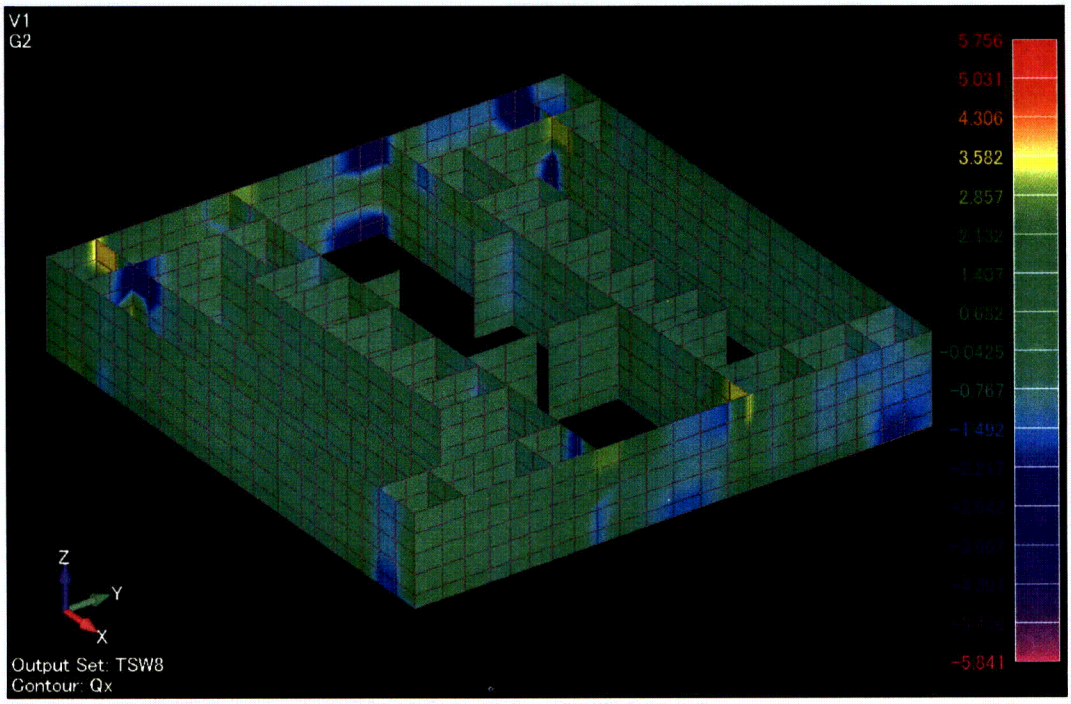

DCD Revision 5 FE Model

[Transverse Shear: Qx]

Figure 3.8-41(90) Comparison of Element Force Distribution on Pool Girder and Wall (Thermal)

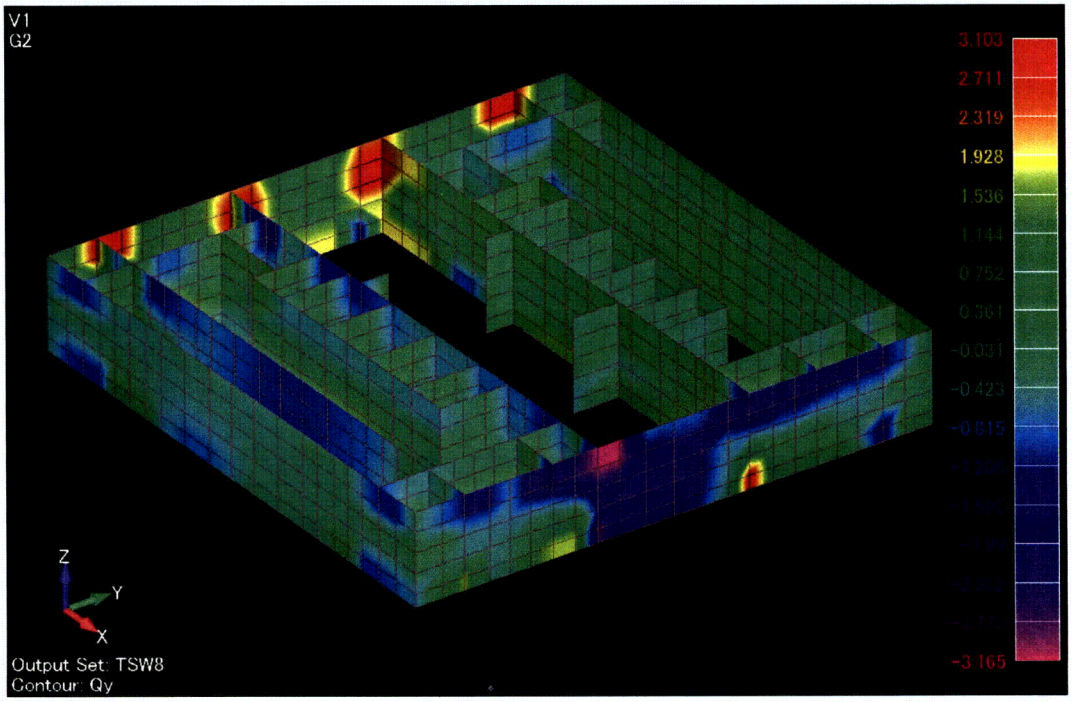

Updated FE Model

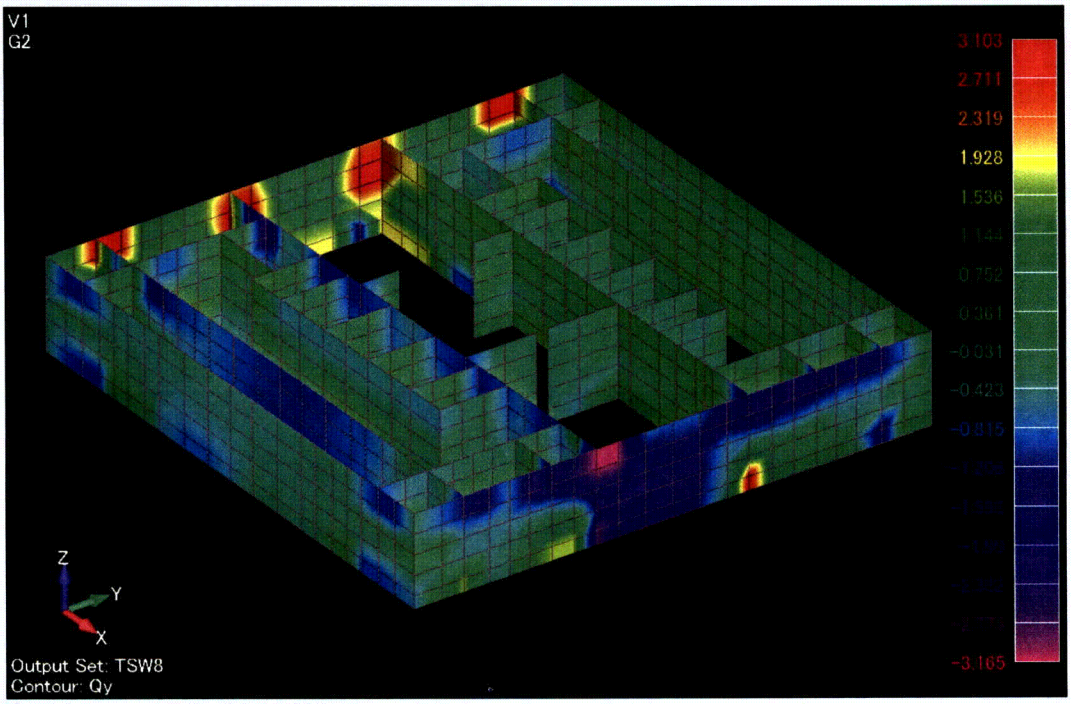

DCD Revision 5 FE Model

[Transverse Shear: Qy]

Figure 3.8-41(91) Comparison of Element Force Distribution on Pool Girder and Wall (Thermal)

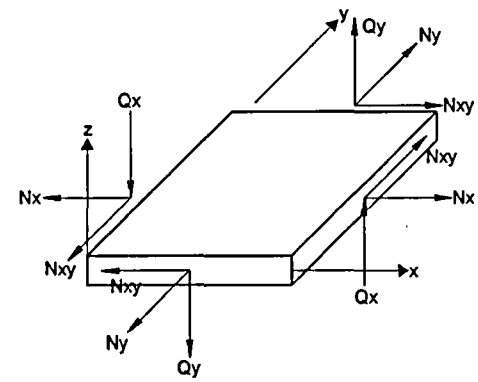

Membrane and Shear Forces

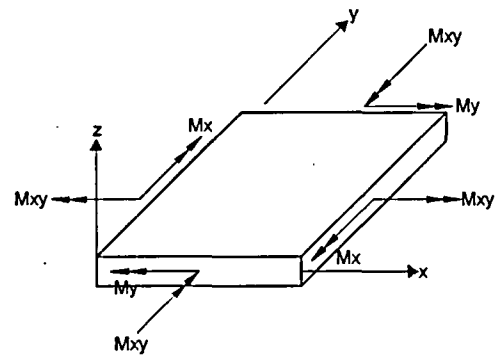

Moments

Structure	Direction (Global Coordinate System)	Element Coordinate System		
		x	y	z
RCCV Top Slab	-	toward X (South)	toward Y (West)	toward Z (Downward)
Pool Girder	N-S (X)	Horizontal	Vertical	Toward Y (West)
External Wall	-	Horizontal	Vertical	Outward
Other Wall	N-S (X)	Horizontal	Vertical	Toward Y (West)
	E-W (Y)	Horizontal	Vertical	Toward X (South)

Figure 3.8-41(92) Force and Moment in Shell Element)

DCD Impact

DCD Tier 1 Table 2.16.5-1 and Figure 2.16.5-8 and DCD Tier 2 Section 3G, Subsection 3G.1.4.1, Table 3G.1-4, Figures 3G.1-4 through 3G.1-6, 3G.1-44 and 3G.1-46 will be revised in Revision 6 as noted in the attached markups.

3G. DESIGN DETAILS AND EVALUATION RESULTS OF SEISMIC CATEGORY I STRUCTURES

This appendix presents the structural design and analysis for the Reactor Building (RB), Control Building (CB), Fuel Building (FB) and Firewater Service Complex (FWSC) of the ESBWR Standard Plant. It addresses all applicable items included in Appendix C to United States Nuclear Regulatory Commision (NRC) Standard Review Plan, NUREG-0800, Subsection 3.8.4. Drawings depicted in the Design Control Document (DCD) are not used for construction. Construction drawings meet the technical licensing commitments made in the DCD but are issued under different contractual/industrial rules than the DCD drawings and reflect detailed design configuration. The final design details~~, and hence final component stresses may be different from those reported here but they~~ will meet the structural acceptance criteria presented in Section 3.8 and in ~~accordance with~~ Tier 1 ITAACs in Tables 2.16.5-2, 2.16.6-2, and 2.16.7-2.

3G.1 REACTOR BUILDING

The RB encloses the concrete containment and its internal systems, structures, and components. Located above the concrete containment in the RB are the Isolation Condenser/Passive Containment Cooling System (IC/PCCS) pools (including expansion pools), the buffer pool, which is also used to store the dryer, and the equipment storage pool, which is also used to store the chimney partitions and the separator.

3G.1.1 Objective and Scope

The objective of this subsection is to document the structural design details, inputs and analytical results from the analysis of the ESBWR main building structures encased in the RB. The scope includes the design and analysis of the structure for normal, severe environmental, extreme environmental, and abnormal loads.

3G.1.2 Conclusions

The following are the major summary conclusions on the design and analysis of the RB, the concrete containment and the containment internal structures.

- Based on the results of finite element analyses performed in accordance with the design conditions identified in Subsections 3G.1.3 and 3G.1.5, stresses and/or strains in concrete, reinforcement, liner and containment internal structures are less than the allowable stresses and/or strains per the applicable regulations, codes or standards listed in Section 3.8.
- The factors of safety against floatation, sliding, and overturning of the structure under various loading combinations are higher than the required minimum.
- The thickness of the roof slabs and exterior walls are more than the minimum required to preclude penetration, perforation or spalling resulting from impact of design basis tornado missiles.

3G.1.3.1.3 Reactor Building Structure/Containment Structure Connections

The RCCV and the RB structure are integrated by the IC/PCCS pool girders at the top of the containment and by floor slabs at elevations that are defined as part of the RB structure and the basemat. The IC/PCCS pool girders are deep reinforced concrete girders, and they are integrated with the containment top slab and with RB walls.

3G.1.3.1.4 Containment Internal Structures

The containment internal structures consist of the diaphragm floor slab, vent wall, GDCS pool walls, reactor shield wall (RSW), and the RPV support bracket. These structures are shown in the general arrangement drawings in this appendix.

The diaphragm floor slab acts as a barrier between the drywell and the wetwell. The diaphragm floor slab is supported on the reinforced concrete containment wall at its outer periphery and on the vent wall at its inner periphery. The diaphragm floor slab is a concrete-filled steel structure. The space between the floor slab top and bottom plates is filled with concrete. The slab is supported by a system of radial beams spaced evenly all around and spanning between the vent wall structure and the reinforced concrete containment wall.

The vent wall structure is also a concrete–filled steel design consisting of two concentric carbon steel cylinders connected together by vertical web plates evenly spaced all around. The vent wall structure is anchored at the bottom into the RPV pedestal and is restrained at the top by the diaphragm floor slab. The cylindrical annulus carries 12 vent pipes and 12 safety relief valve (SRV) downcomer pipes with sleeves, from the drywell into the suppression pool. The space in the cylindrical annulus is filled with concrete.

There are three GDCS pools supported on top of the diaphragm floor slab. The pools on one side are contained by the reinforced concrete containment wall and on the other side by structural steel walls.

The RSW is a thick steel cylindrical structure that surrounds the RPV. It is supported by the RPV support brackets and the reactor pedestal. The function of the RSW is to attenuate radiation emanating from the RPV. In addition, the RSW provides structural support for the RPV stabilizer, the RPV insulation and miscellaneous equipment, piping and commodities. Openings are provided in the RSW to permit the routing of necessary piping to the RPV and to permit in-service inspection of the RPV and piping.

3G.1.4 Analytical Models

3G.1.4.1 Structural Models

The RB and the RCCV including its internal structures are analyzed as one integrated structure utilizing the finite element computer program NASTRAN. The finite element model consists of quadrilateral, triangular, and beam elements. The quadrilateral and triangular elements are used to represent the slabs and walls. Beam elements are used to represent columns and beams. The model is shown in Figures 3G.1-8 to 3G.1-18. The buffer pool gate wall modeled in Figure 3G.1-8 is wider than the current configuration. It is updated in a separate analysis for the most critical loadings of accident pressure and accident temperature. The resulting stresses are taken into account in the design of the RCCV top slab and the pool gate walls.

Table 3G.1-4

Equipment and Hydrostatic Loads in RB Pools

Description	Weight	Remarks
Reactor Well		
a. Water (H=6.7m)	66 kN/m^2	
b. Wall Liner	1.0 kN/m^2	
c. Floor Liner	1.6 kN/m^2	
Equipment Storage Pool		
a. Water (H=6.7m)	66 kN/m^2	
b. Wall Liner	1.0 kN/m^2	
c. Floor Liner	1.6 kN/m^2	
d. Steam Dryer, Steam Separator	66 kN/m^2	During refueling
Fuel Buffer Pool		
a. Water (H=6.7m)	66 kN/m^2	
b. Wall Liner	1.0 kN/m^2	
c. Floor Liner	1.6 kN/m^2	
d. Fuel Storage Racks	153 kN/m^2	During refueling
IC/PCCS Pools		
a. Water (H=4.8m)	47 kN/m^2	
b. Wall Liner	1.0 kN/m^2	
c. Floor Liner	1.6 kN/m^2	
d. IC heat exchanger	333 kN/unit	
e. PCCS heat exchanger	233 kN/unit	
Inclined Fuel Transfer Tube Pool		
a. Water (H=11.64m)	114 kN/m^2	
b. Wall Liner	1.0 kN/m^2	
c. Floor Liner	1.6 kN/m^2	
IC/PCCS Expansion Pools		
a. Water (H=4.8m)	47 kN/m^2	
b. Wall Liner	1.0 kN/m^2	
c. Floor Liner	1.6 kN/m^2	
Equipment Storage Pool Gate	300 kN	
Buffer Pool Gate	~~50~~ 300 kN	The actual value considered in the building stress analysis is 50 kN. The increased pool gate weight is negligibly small as compared to the weight of the RCCV top slab which supports the pool gates.(1)
Inclined Fuel Transfer Tube Pool Gate	50 kN	

(1) RCCV top slab weight (w) = $\prod[(R_o)^2-(R_i)^2](t)(\rho)$; where R_o=18 m, R_i=5.25 m, t=2.4 m, ρ=0.0235 MN/m^2. Then, w=52500kN or 175 times the 300 kN pool gate weight.

{{{Security-Related Information - Withheld Under 10 CFR 2.390}}}

Figure 3G.1-4. RB and FB Concrete Outline Plan at EL 27000

{{{Security-Related Information - Withheld Under 10 CFR 2.390}}}

{{{Security-Related Information - Withheld Under 10 CFR 2.390}}}

Figure 3G.1-5. RB Concrete Outline Plan at EL 34000

{{{Security-Related Information - Withheld Under 10 CFR 2.390}}}

Figure 3G.1-6. RB and FB Concrete Outline N-S Section

{{{Security-Related Information - Withheld Under 10 CFR 2.390}}}

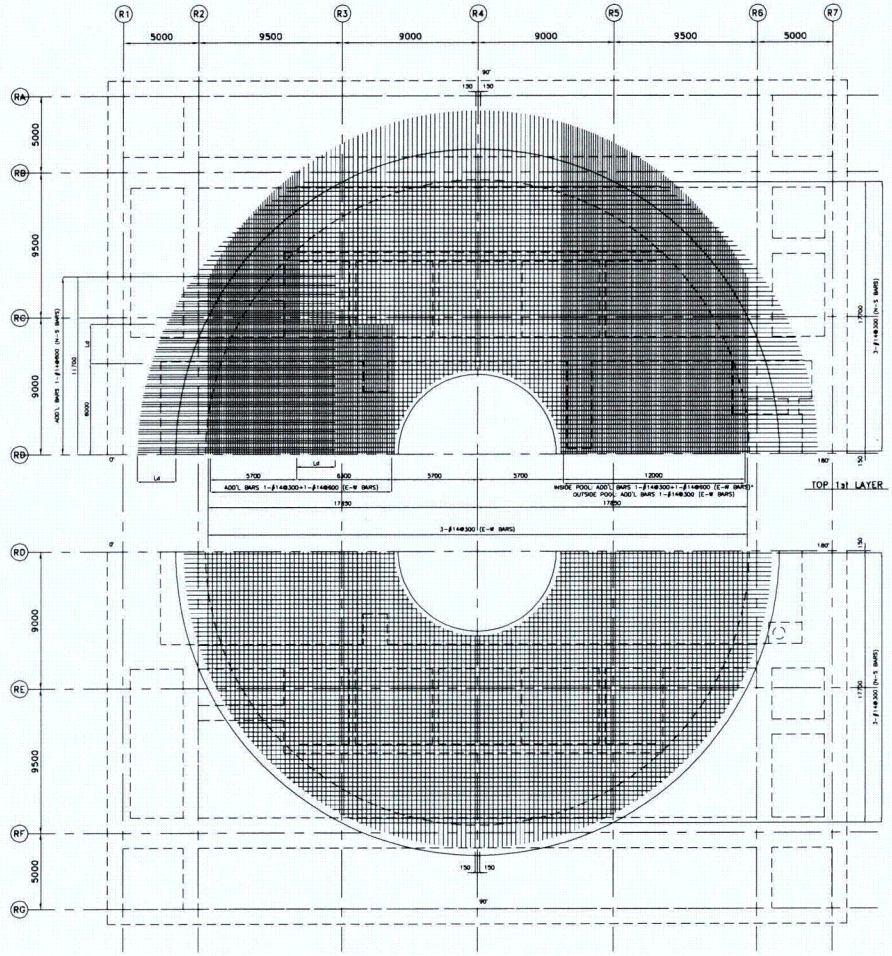

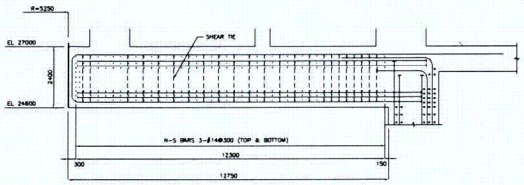

SECTION AT 90°

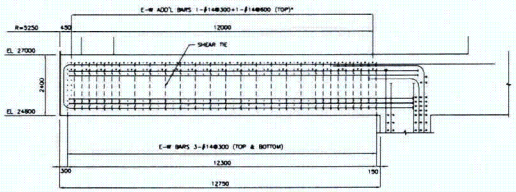

SECTION AT 180°

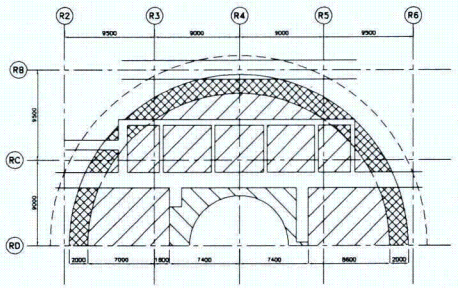

SYMBOLS	SHEAR TIES	SYMBOLS	SHEAR TIES
	β@600×600		β@300×300
	β@300×600		

SHEAR TIES

*:BECAUSE OF WIDENING OF BUFFER POOL GATE, ADDITIONAL REBAR WILL BE ADDED LOCALLY.

LEGEND

(1) TIP END OF REBAR

: W/ TERMINATOR

(2) Ld : DEVELOPMENT LENGTH

NOTE:

1. POSITIONS OF REBARS MAY BE ADJUSTED LOCALLY AS NECESSARY TO AVOID INTERFERENCES WITH EMBEDMENTS.

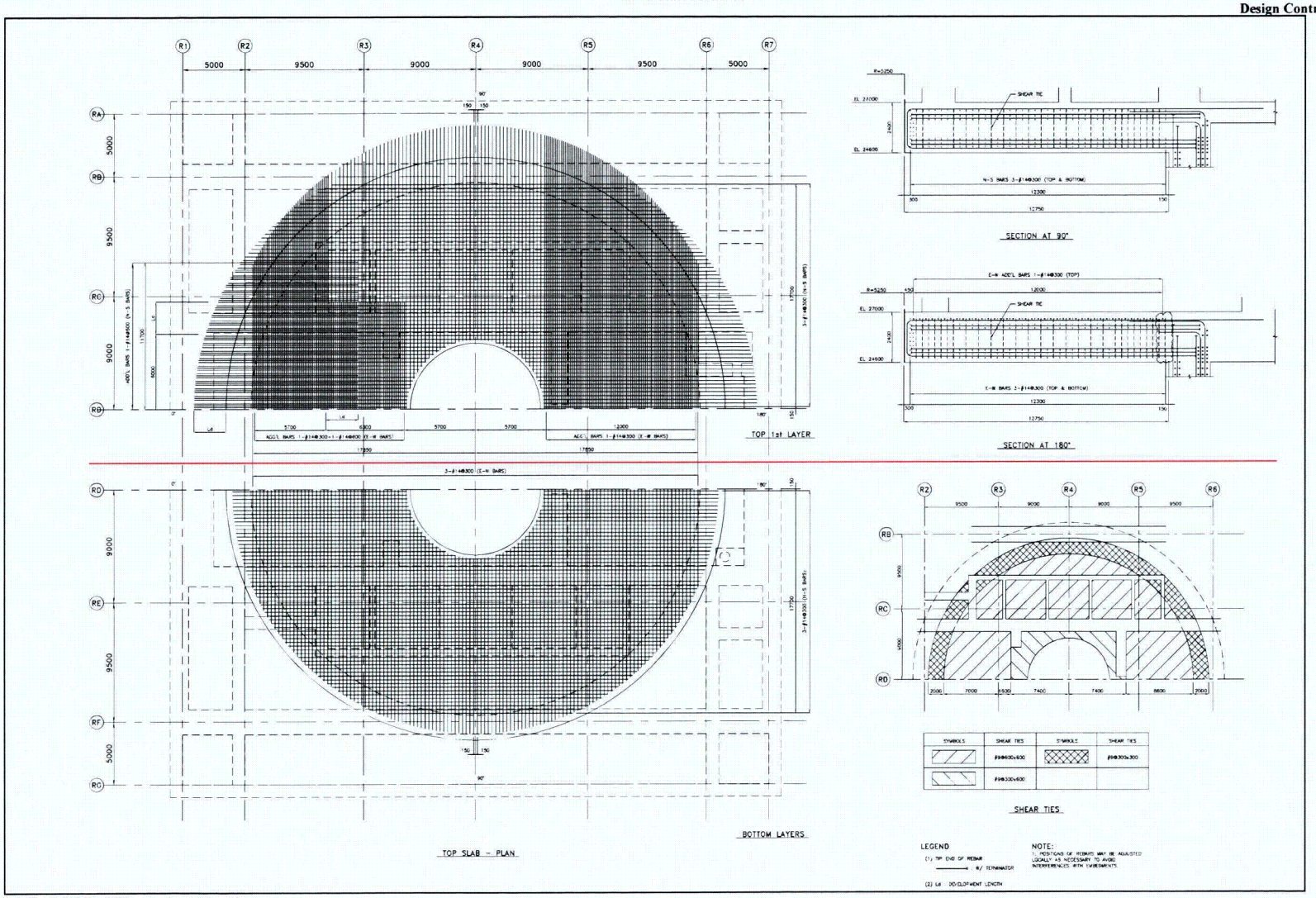

Figure 3G.1-44. Reinforcing Steel of Top Slab

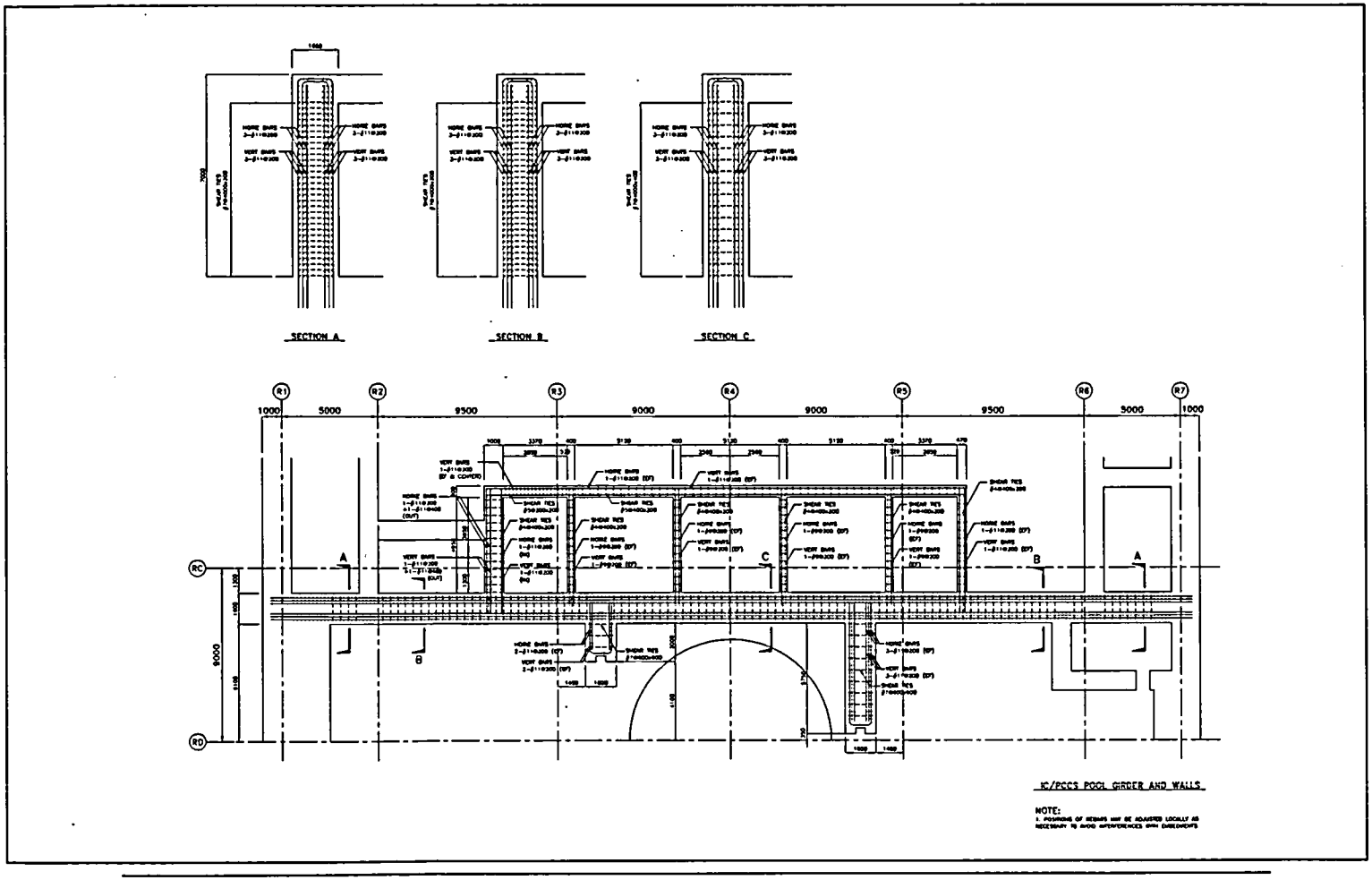
SECTION A
SECTION B
SECTION C
R1
R2
R3
R4
R5
R6
R7
RC
RD
1000
5000
9500
9000
9000
9500
5000
1000
9000
A
B
C
IC/PCCS POOL GIRDER AND WALLS
NOTE:

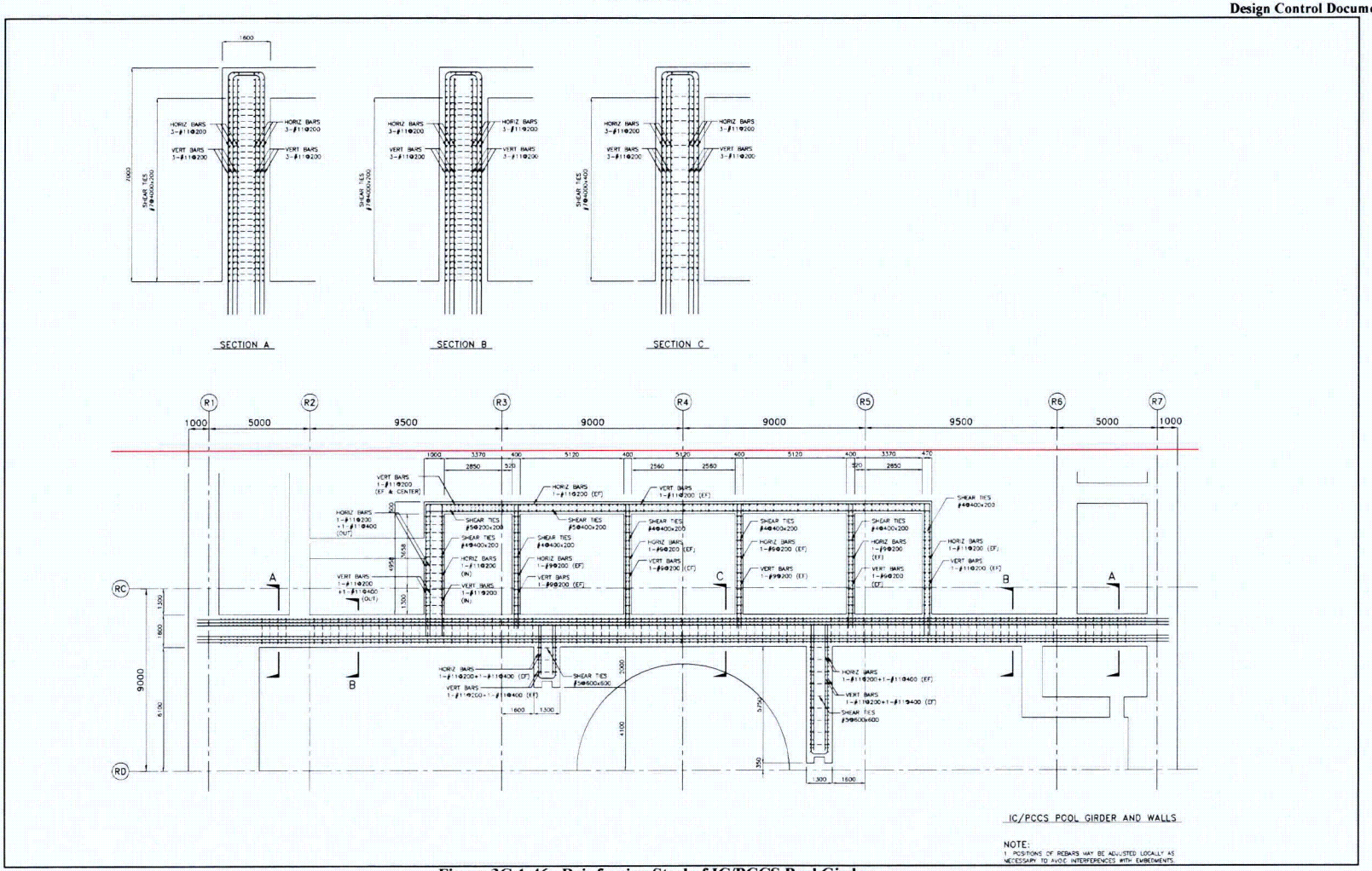

Figure 3G.1-46. Reinforcing Steel of IC/PCCS Pool Girder

Note: Subsection 1.1.2.4 applies to this figure.

Figure 2.16.5-8. RB Concrete Outline Plan at EL 27000

{{{Security-Related Information – Withheld Under 10 CFR 2.390}}}

Table 2.16.5-1

Critical Dimensions of Reactor Building – Part 1

Label	Wall or Section Description	Column Line or Region	Floor Elevation or Elevation Range (EL: mm)	Concrete Thickness (mm) (ft/in)	Tolerance (mm) (in)
				(5'-3")	(+1"/- ¾")
44	Wall between Column Lines RE and RF	From R6 to R7	From 27000 to 33000	1000 (3'-3 ⅜")	+25/-20 (+1"/- ¾")
45	Wall at Column Line RF	From R1 to R7	From 27000 to 33000	2000 (6'-6 ¾")	+25/-20 (+1"/- ¾")
46	Wall at Column Line RG	From R1 to R7	From 27000 to 33000	1000 (3'-3 ⅜")	+25/-20 (+1"/- ¾")
47	Reactor Cavity Wall (Northeast side)	From RC to between RC and RD	From 27000 to 34000	~~1300~~1600 (5'-3")	+25/-20 (+1"/- ¾")
48	Reactor Cavity Wall (Northwest side)	From between RD and RE to RE	From 27000 to 34000	~~1300~~1600 (5'-3")	+25/-20 (+1"/- ¾")
49	Reactor Cavity Wall (Southeast side)	From RC to between RC and RD	From 27000 to 34000	~~1300~~1600 (5'-3")	+25/-20 (+1"/- ¾")
50	Not used				
51	IC/PCCS Pool Wall between Column Lines R2 and R3	From between RB and RC to RC	From 27000 to 33000	1000 (3'-3 ⅜")	+25/-20 (+1"/- ¾")
52	IC/PCCS Pool Wall between Column Lines R2 and R3	From RE to between RE and RF	From 27000 to 33000	1000 (3'-3 ⅜")	+25/-20 (+1"/- ¾")
53	IC/PCCS Pool Wall at Column Line R3	From between RB and RC to RC	From 27000 to 33000	400 (1'-3¾")	+15/-10 (+ ½"/-⅜")
54	IC/PCCS Pool Wall at Column Line R3	From RE to between RE and RF	From 27000 to 33000	400 (1'-3¾")	+15/-10 (+ ½"/-⅜")
55	IC/PCCS Pool Wall between Column Lines R3 and R4	From between RB and RC to RC	From 27000 to 33000	400 (1'-3¾")	+15/-10 (+ ½"/-⅜")
56	IC/PCCS Pool Wall between Column Lines R3 and R4	From RE to between RE and RF	From 27000 to 33000	400	+15/-10